Abstract

The MSSM is often augmented by heavy singlets, in order to account for neutrino masses via the seesaw mechanism. However, these singlets can significantly impact predictions for neutralino relic density via RG effects on the SUSY mass spectrum and the concomitant changes to annihilation and detection rates. We study the interplay between these RG-mediated neutrino sector effects on relic density and constraints from lepton flavor violation, in CMSSM/mSUGRA-like models using several different GUT-inspired schemes for choosing neutrino sector parameters and mixings.

We find that these effects can be very important for predictions of LFV rates; proper consideration of the changes to relic density bounds alters the predicted LFV rates by factors from a few up to two orders of magnitude, depending on the location in parameter space. Surprisingly, our results indicate that a large neutrino Yukawa unification parameter $R_{\nu u} = 3$ is not ruled out by current LFV bounds as was commonly thought. We also discuss our code Isajet-M, a modification and extension of standard Isajet, which we used to solve the RGEs. Isajet-M handles both the neutrino and quark sectors in complex matrix form, integrates out all particles at their individual scales, and calculates the sparticle spectrum, neutrino masses and mixings, rates for LFV processes, contributions to $(g-2)_\mu$, and neutralino relic density and cross-sections.

SUPERSYMMETRIC DARK MATTER AND LEPTON FLAVOR VIOLATION

BY

Ali Soleimani

Submitted to the graduate degree program in Physics
and the Graduate Faculty of the University of Kansas
in partial fulfillment of the requirements for the degree of
Doctor of Philosophy.

_____
Chairperson

Committee members: _____

_____

_____

_____

Date defended:_____

The Dissertation Committee for Ali Soleimani certifies
that this is the approved version of the following dissertation:

SUPERSYMMETRIC DARK MATTER AND LEPTON FLAVOR VIOLATION

Committee:

_____
Chairperson

_____

_____

_____

_____

Date approved:_____

Contents

1 Introduction **1**
- 1.1 The Standard Model . . . 1
- 1.2 Standard Model Difficulties . . . 3
- 1.3 Supersymmetry . . . 4
  - 1.3.1 Superfield formalism . . . 7
  - 1.3.2 Chiral superfields . . . 8
  - 1.3.3 Vector superfields . . . 10
  - 1.3.4 Constructing a SUSY Lagrangian . . . 12
  - 1.3.5 SUSY breaking . . . 14
  - 1.3.6 MSSM . . . 18
  - 1.3.7 mSUGRA . . . 28
- 1.4 Neutrinos . . . 29
  - 1.4.1 Neutrino mass . . . 29
  - 1.4.2 Seesaw mechanism . . . 32
- 1.5 Notation and Conventions . . . 34
- 1.6 Flavor violation . . . 40
  - 1.6.1 Quark sector flavor-violation . . . 40
  - 1.6.2 Lepton flavor-violation . . . 43
  - 1.6.3 LFV rates in SUSY-seesaw models . . . 44

2 SUSY dark matter constraints and LFV rates **47**
- 2.1 $SO(10)$ GUTs . . . 49
- 2.2 Procedure . . . 53
- 2.3 Code description . . . 54
- 2.4 Results . . . 61
  - 2.4.1 Large mixing . . . 61
  - 2.4.2 Small mixing . . . 72
- 2.5 Discussion . . . 78
- 2.6 Conclusions . . . 80

Appendices **82**

A Yukawa RGEs **83**

B Detailed code description **85**
B.1 Common blocks 85
B.2 Functions 91
B.2.1 Main program routines 91
B.2.2 General RGE routines 95
B.2.3 Neutrino sector routines 98
B.2.4 Mass and LFV calculation routines 103
B.2.5 Mathematical and utility routines 105

Chapter 1

Introduction

1.1 The Standard Model

The Standard Model (SM) of particle physics is perhaps the most successful theory of fundamental physics to date. It is a quantum field theory describing all observed physical particles and their fundamental interactions via the strong, weak and electromagnetic interactions. It is a non-Abelian gauge theory with the gauge group $SU(3)_c \times SU(2)_L \times U(1)_Y$, with $SU(3)_c$ the color gauge group, $SU(2)_L$ the weak isospin gauge group, and $U(1)_Y$ the hypercharge gauge group. Part of this gauge symmetry is spontaneously broken via the Higgs mechanism, in which the Higgs field ϕ acquires a nonzero vacuum expectation value, breaking $SU(2)_L \times U(1)_Y$ down to $U(1)_{em}$.

The field content of the Standard Model (pre-symmetry breaking) consists of spin-1 gauge bosons, three generations of spin-$1/2$ quarks and leptons, and one doublet of Higgs scalar fields and is summarized in Table 1.1.

The Standard Model Lagrangian is given by

$$\mathcal{L} = \mathcal{L}_{\text{gauge}} + \mathcal{L}_{\text{matter}} + \mathcal{L}_{\text{Higgs}} + \mathcal{L}_{\text{Yukawa}}, \tag{1.1}$$

where

$$\mathcal{L}_{\text{gauge}} = -\frac{1}{4} G_{A\mu\nu} G_A^{\mu\nu} - \frac{1}{4} W_{A\mu\nu} W_A^{\mu\nu} - \frac{1}{4} B_{\mu\nu} B^{\mu\nu}, \tag{1.2}$$

Field			$SU(3)_c$	$SU(2)_L$	$U(1)_Y$
G^a_μ, a=1…8			**8**	**1**	0
W^k_μ, k=1…3			**1**	**3**	0
B_μ			**1**	**1**	0
$Q_1 = \begin{pmatrix} u \\ d \end{pmatrix}_L$	$Q_2 = \begin{pmatrix} c \\ s \end{pmatrix}_L$	$Q_3 = \begin{pmatrix} t \\ b \end{pmatrix}_L$	**3**	**2**	$1/3$
u^c_R	c^c_R	t^c_R	$\mathbf{3}^*$	**1**	$4/3$
d^c_R	s^c_R	b^c_R	$\mathbf{3}^*$	**1**	$-2/3$
$L_1 = \begin{pmatrix} \nu_e \\ e \end{pmatrix}_L$	$L_2 = \begin{pmatrix} \nu_\mu \\ \mu \end{pmatrix}_L$	$L_3 = \begin{pmatrix} \nu_\tau \\ \tau \end{pmatrix}_L$	**1**	**2**	-1
e^c_R	μ^c_R	τ^c_R	**1**	**1**	-2
$\phi = \begin{pmatrix} \phi^+ \\ \phi^0 \end{pmatrix}$			**1**	**2**	1

Table 1.1: The field content of the Standard Model along with the gauge quantum numbers.

$$\mathcal{L}_{\text{matter}} = \sum_{\text{generations}} \left[i\bar{L}\, \not{D} L + i\bar{Q}\, \not{D} Q + i\bar{u}_R\, \not{D} u_R + i\bar{d}_R\, \not{D} d_R + i\bar{e}_R\, \not{D} e_R \right], \tag{1.3}$$

$$\mathcal{L}_{\text{Higgs}} = |D_\mu \phi|^2 + \mu^2 \phi^\dagger \phi - \lambda (\phi^\dagger \phi)^2, \tag{1.4}$$

and

$$\mathcal{L}_{\text{Yukawa}} = \sum_{\text{generations}} \left[-\mathbf{f}_e \bar{L} \cdot \phi e_R - \mathbf{f}_d \bar{Q} \cdot \phi d_R - \mathbf{f}_u \epsilon^{ab} \bar{Q}_a \phi^\dagger_b u_R + \text{h.c.} \right]. \tag{1.5}$$

Here, $G^{\mu\nu}_A$, $W^{\mu\nu}_A$, $B^{\mu\nu}$ are the color, weak isospin and hypercharge field tensors respectively, with the D's being the covariant derivatives for the matter multiplets under these gauge groups. ϵ^{ab} is the usual completely antisymmetric tensor here in $SU(2)$ space, with the convention $\epsilon^{12} = 1$.

For the quark fields, their weak interaction eigentstates Q_i are not identical to their mass eigenstates. Instead, they are mixed through the Cabibbo-Kobayashi-Maskawa (CKM) matrix. There are therefore four additional parameters in the SM, three mixing angles and one imaginary Dirac phase. In the Standard Model proper, the lepton mass eigenstates are the same as their weak interaction eigenstates. (This is altered when neutrino masses are included; see below.)

Ordinary mass terms in the Lagrangian are prohibited by gauge symmetries ($SU(2)_L$ and

$U(1)_Y$) and also break renormalizability. Therefore, these masses are generated by electroweak symmetry breaking via the Higgs mechanism. This provides effective mass terms via the Yukawa couplings when the Higgs field is expanded around its vev; hence SM particle masses are all proportional to the Higgs vev v and are each proportional to their Yukawa couplings f.

As a result of the Higgs mechanism, the weak boson fields W_i, B are mixed into the physical fields

$$W_\mu^\pm = \frac{W_{1\mu} \mp iW_{2\mu}}{\sqrt{2}} \qquad Z_\mu^0 = -\cos\theta_W W_{3\mu} + \sin\theta_W B_\mu \tag{1.6}$$

with masses

$$m_W = \frac{1}{\sqrt{2}} gv \qquad m_Z = \frac{m_W}{\cos\theta_W}. \tag{1.7}$$

The remaining linear combination of these gives the massless photon field

$$A_\mu = \sin\theta_W W_{3\mu} + \cos\theta_W B_\mu. \tag{1.8}$$

The Z_μ and the $W_\mu^\pm$ obtain their extra degrees of freedom from components of the Higgs field ("eating" them), leaving a single uncharged massive Higgs scalar h as a physical particle.

1.2 Standard Model Difficulties

The Standard Model of particle physics is the result of immense efforts in experimental and theoeretical particle physics, and it has been astonishingly successful. The SM provides a simple model which explains nearly all observed particle physics data. All of its particles have now been observed except for the Higgs boson. Nevertheless, there are a number of shortcomings in the SM, particularly some unsatisfactory theoretical aspects:

- The Higgs mass in the SM is quadratically divergent, requiring fine-tuning of perhaps 17 orders of magnitude to match the expected mass – the *hierarchy problem*,
- There is no unification of electroweak and strong interactions,

- Electroweak symmetry breaking must be imposed by hand via the selection of an arbitrary Higgs potential,
- Dark energy is not clearly explicable in the SM,
- There is no satisfactory mechanism to generate matter-antimatter asymmetry in the SM, and
- Gravity is not included in the SM.

There are also experimental issues with the Standard Model, namely

- Neutrinos in the SM are massless, contrary to observation, and
- There is no candidate for dark matter in the SM.

These considerations together are often taken to imply that the SM is an effective field theory up to some energy scale large compared with the weak scale. In order to provide a natural solution to the hierarchy problem, this scale should be $\sim$1 TeV. Above that scale, it is likely that some new physics will appear to ameliorate these issues. There have been many suggestions for such new physics theories beyond this scale. Here we will focus on one of the most popular possibilities, which seems to be favored by current data: supersymmetric Grand Unified Theories (GUTs.)

1.3 Supersymmetry

Supersymmetry has been one of the most promising and popular ideas for physics beyond the Standard Model in recent decades[1, 2]. Supersymmetry (SUSY) postulates a new symmetry of nature which associates a fermion of identical mass and charge with every boson (and vice versa.) It is a *spacetime* symmetry; that is, its generators do not commute with the generators of generalized Lorentz transformations. SUSY is appealing for a number of reasons. First, it is interesting on purely theoretical grounds, since by the Haag-Lopuszanski-Sohnius

theorem[3] it is the largest possible spacetime symmetry that could exist in a Lorentz-invariant quantum field theory meeting certain reasonable technical conditions.

SUSY also solves the hierarchy problem. In quantum field theories, renormalization effects cause particle masses to be shifted from their "bare" values by quantum corrections arising from loop diagrams. For nearly all particles in the Standard Model, symmetries of one sort or another "protect" their masses from receiving overly-large corrections. (That is, the symmetries ensure that cancellations occur so that such corrections are at most logarithmic in the renormalization scale Q and so will be comparable to the bare mass for reasonable Q, e.g. $Q \approx M_{\text{GUT}},\ M_{\text{Planck}}$.) However, no such symmetry protects fundamental scalars such as the Higgs boson. A straightforward calculation shows that the Higgs should pick up corrections to its mass comparable to the scale at which the Standard Model is replaced by new physics – presumably the GUT scale or the Planck scale. This implies a miraculous cancellation of many orders of magnitude between the Higgs bare mass and its loop corrections to result in the expected mass of $\sim 10^2$ GeV. Supersymmetry solves this problem very elegantly. The quadratically-divergent part of each loop diagram contributing to the divergence in the Higgs mass is exactly cancelled by a matching diagram with particles in the loops replaced by their superpartners. This cancellation can be shown to hold to all orders in perturbation theory[4].

There are several other considerations beyond these theoretical ones that make supersymmetry especially appealing. First, it naturally provides a candidate for weakly-interacting dark matter (in models with R-parity.) The lightest supersymmetric particle (LSP) is both stable and weakly-interacting in most models. Second, it leads to gauge coupling unification, consistent with the existence of a GUT. If the gauge groups of the Standard Model are subgroups of a larger gauge group spontaneously broken at the GUT scale, then their coupling constants must unify at that scale. As can be seen from Fig. (1.1), in the Standard Model, extrapolating the runnings of the three coupling constants up to high energies shows that they nearly, but not quite, meet at a scale around $M_{\text{GUT}} \approx 10^{16}$ GeV. In the minimal supersymmetric standard model, or MSSM, the coupling constants do meet within a range explainable by GUT threshold corrections[5].

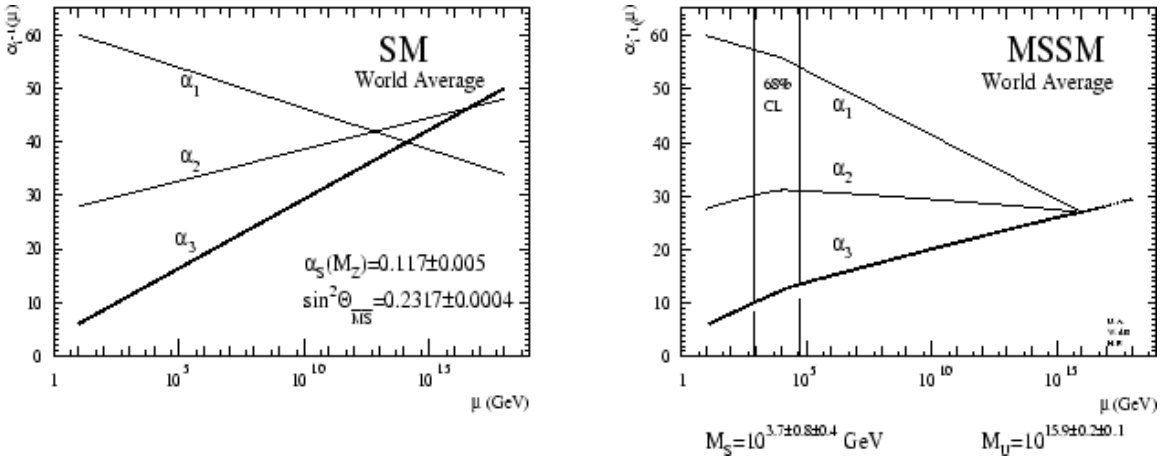

Figure 1.1: Running of couplings in the SM and MSSM. Figure is from CERN.

The fundamental idea of supersymmetry is to extend the usual Poincaré algebra of space-time

$$[P_\mu, P_\nu] = 0, \tag{1.9}$$

$$[M_{\mu\nu}, P_\lambda] = i(g_{\nu\lambda}P_\mu - g_{\mu\lambda}P_\nu), \tag{1.10}$$

$$[M_{\mu\nu}, M_{\rho\sigma}] = -i(g_{\mu\rho}M_{\nu\sigma} - g_{\mu\sigma}M_{\nu\rho} - g_{\nu\rho}M_{\mu\sigma} + g_{\nu\sigma}M_{\mu\rho}), \tag{1.11}$$

by introducing anti-commuting 'spinorial' charges Q_a $(a = 1 \ldots N)$:

$$[P_\mu, Q_a] = 0, \tag{1.12}$$

$$[M_{\mu\nu}, Q_a] = -(\sigma_{\mu\nu})_{ab}Q_b, \tag{1.13}$$

$$\{Q_a, \bar{Q}_b\} = 2(\gamma^\mu)_{ab}P_\mu \tag{1.14}$$

$$\{Q_a, Q_b\} = -2(\gamma^\mu C)_{ab}P_\mu, \tag{1.15}$$

$$\{\bar{Q}_a, \bar{Q}_b\} = 2(C^{-1}\gamma^\mu)_{ab}P_\mu, \tag{1.16}$$

where $A, B \equiv AB + BA$. The resulting algebra is not a Lie algebra, since it involves generators which anti-commute as well as commuting ones. It is instead known as a *graded* Lie algebra. This is how SUSY evades the Coleman-Mandula theorem, the Lie group version of the HLS

theorem mentioned above, showing that the largest Lie symmetry group for a reasonable quantum field theory is the direct product of the Poincaré group and purely "internal" symmetries. This algebra defines an extension of the Poincaré group known as the super-Poincaré group.

By the SUSY generators Q being spinorial, we mean that

$$\begin{aligned} Q|\text{boson}\rangle &= |\text{fermion}\rangle \\ Q|\text{fermion}\rangle &= |\text{boson}\rangle, \end{aligned} \tag{1.17}$$

i.e. Q takes fermions into bosons and vice versa. Therefore representations of the super-Poincaré group (*supermultiplets*) necessarily include both bosons and fermions. The fermions and bosons sharing a supermultiplet are known as each other's *superpartners*.

Superpartners necessarily have spins differing by a half-integer. The SUSY generators Q_a commute with the generators of purely internal degrees of freedom, such as gauge transformations, just as the generators of ordinary spacetime transformations do. So superpartners live in the same gauge representation, and necessarily share such quantum numbers such as electric charge, hypercharge, color, etc..

1.3.1 Superfield formalism

A convenient way to formulate SUSY is in terms of *superfields*. A superfield is an object containing all the members of a supermultiplet. To develop the superfield formalism, we begin by extending spacetime by four 'fermionic' coordinates θ_a $(a = 1 \dots 4)$; these along with the ordinary spacetime coordinates x_a $(a = 1 \dots 4)$ form *superspace*. The θ_a are anticommuting Grassmann numbers:

$$\{\theta_a, \theta_b\} = 0, \quad \theta_a^2 = 0. \tag{1.18}$$

Taken together, these four components can be viewed as the four components of a Majorana spinor θ.

Superfields are then taken to be fields over superspace, i.e. over both spatial coordinates x^μ and superspace coordinates θ_a. Given any such analytic superfield $\hat{\Phi}(x, \theta)$, we can Taylor

expand it around the coordinates θ. Because of the Grassmann nature of the superspace variables, $\theta_a^2 = -\theta_a^2 = 0$, and so this expansion will necessarily terminate after a few terms. It is therefore an exact expansion, not an approximation.

1.3.2 Chiral superfields

If we require that the θ-independent term be a Lorentz scalar, the Taylor expansion contains exactly 16 independent terms since the θ's anticommute: 1 θ-independent term, 4 terms θ_a, 6 terms $\theta_a\theta_b$, 4 terms $\theta_a\theta_b\theta_c$, and 1 term $\theta_1\theta_2\theta_3\theta_4$. It is convenient to arrange these terms as follows:

$$\begin{aligned}\hat{\Phi}(x,\theta) &= \mathcal{S} - i\sqrt{2}\bar{\theta}\gamma_5\psi - \frac{i}{2}(\bar{\theta}\gamma_5\theta)\mathcal{M} + \frac{1}{2}(\bar{\theta}\theta)\mathcal{N} + \frac{1}{2}(\bar{\theta}\gamma_5\gamma_\mu\theta)V^\mu \\ &+ i(\bar{\theta}\gamma_5\theta)\left[\bar{\theta}\left(\lambda + \frac{i}{\sqrt{2}}\partial\psi\right)\right] - \frac{1}{4}(\bar{\theta}\gamma_5\theta)^2\left[\mathcal{D} - \frac{1}{2}\Box\mathcal{S}\right]. \end{aligned} \tag{1.19}$$

We have arranged the expansion terms into a vector field V_μ, two spinors ψ and λ, and four scalars $\mathcal{S}, \mathcal{M}, \mathcal{N}, \mathcal{D}$. A superfield in which $\hat{\Phi}^\dagger = \hat{\Phi}$ is called *real* and contains real bosons and Majorana fermions.

Under an infinitesimal SUSY transformation α:

$$\hat{\Phi} \to \hat{\Phi} + \delta\hat{\Phi} \quad \text{with} \quad \delta\hat{\Phi} = i\left[\bar{\alpha}Q, \hat{\Phi}\right] = \left(-\bar{\alpha}\frac{\partial}{\partial\bar{\theta}} - i\bar{\alpha}\partial\theta\right)\hat{\Phi}, \tag{1.20}$$

the component fields transform as

$$\begin{aligned}
\delta\mathcal{S} &= i\sqrt{2}\bar{\alpha}\gamma_5\psi, && (1.21)\\
\delta\psi &= -\frac{\alpha\mathcal{M}}{\sqrt{2}} - i\frac{\gamma_5\alpha\mathcal{N}}{\sqrt{2}} - i\frac{\gamma_\mu\alpha V^\mu}{\sqrt{2}} - \frac{\gamma_5\partial\!\!\!/\mathcal{S}\alpha}{\sqrt{2}}, && (1.22)\\
\delta\mathcal{M} &= \bar{\alpha}\left(\lambda + i\sqrt{2}\partial\!\!\!/\psi\right), && (1.23)\\
\delta\mathcal{N} &= i\bar{\alpha}\gamma_5\left(\lambda + i\sqrt{2}\partial\!\!\!/\psi\right), && (1.24)\\
\delta V^\mu &= -i\bar{\alpha}\gamma^\mu\lambda + \sqrt{2}\bar{\alpha}\partial^\mu\psi, && (1.25)\\
\delta\lambda &= -i\gamma_5\alpha\mathcal{D} - \frac{1}{2}[\partial\!\!\!/, \gamma_\mu]V^\mu\alpha, && (1.26)\\
\delta\mathcal{D} &= \bar{\alpha}\partial\!\!\!/\gamma_5\lambda. && (1.27)
\end{aligned}$$

(The reader is referreed to Refs. ([1, 2]) for a full development of the machinery of Grassman variables and superspace used here.)

However, this representation of the super-Poincaré group on superspace is not irreducible. We can find a simpler representation by imposing the condition

$$\psi_R = 0,\ V^\mu = -i\partial^\mu\mathcal{S},\ \mathcal{N} = -i\mathcal{M} \equiv \mathcal{F}. \tag{1.28}$$

This is known as a *left chiral superfield*

$$\hat{\mathcal{S}}_L = \mathcal{S} + i\sqrt{2}\bar{\theta}\psi_L + i\bar{\theta}\theta_L\mathcal{F} + \frac{i}{2}(\bar{\theta}\gamma_5\gamma_\mu\theta)\partial^\mu\mathcal{S} - \frac{1}{\sqrt{2}}\bar{\theta}\gamma_5\theta\cdot\bar{\theta}\partial\!\!\!/\psi_L + \frac{1}{8}(\bar{\theta}\gamma_5\theta)^2\Box\mathcal{S}, \tag{1.29}$$

consisting just of a Majorana spinor ψ_L and complex scalars $\mathcal{F}$ and $\mathcal{S}$. It transforms as

$$\begin{aligned}
\delta\mathcal{S} &= -i\sqrt{2}\bar{\alpha}\psi_L, && (1.30)\\
\delta\psi_L &= -\sqrt{2}\mathcal{F}\alpha_L + \sqrt{2}\partial\!\!\!/\mathcal{S}\alpha_R, && (1.31)\\
\delta\mathcal{F} &= i\sqrt{2}\bar{\alpha}\partial\!\!\!/\psi_L. && (1.32)
\end{aligned}$$

One can similarly form a *right chiral superfield*

$$\hat{\mathcal{S}}_R = \mathcal{S} - i\sqrt{2}\bar{\theta}\psi_R - i\bar{\theta}\theta_R\mathcal{F} - \frac{i}{2}(\bar{\theta}\gamma_5\gamma_\mu\theta)\partial^\mu\mathcal{S} - \frac{1}{\sqrt{2}}\bar{\theta}\gamma_5\theta\cdot\bar{\theta}\partial\psi_R + \frac{1}{8}(\bar{\theta}\gamma_5\theta)^2\Box\mathcal{S}. \quad (1.33)$$

satisfying the condition

$$\psi_L = 0,\ V^\mu = i\partial^\mu\mathcal{S},\ \mathcal{N} = i\mathcal{M} \equiv i\mathcal{F}. \quad (1.34)$$

We can simplify the notation somewhat by changing to a new variable $\hat{x}_\mu = x_\mu + \frac{i}{2}\bar{\theta}\gamma_5\gamma_\mu\theta$. Left and right chiral superfields then take the form

$$\hat{\mathcal{S}}_L(x,\theta) = \mathcal{S}(\hat{x}) + i\sqrt{2}\bar{\theta}\psi_L(\hat{x}) + i\bar{\theta}\theta_L\mathcal{F}(\hat{x}), \quad (1.35)$$

$$\hat{\mathcal{S}}_R(x,\theta) = \mathcal{S}(\hat{x}^\dagger) - i\sqrt{2}\bar{\theta}\psi_R(\hat{x}^\dagger) - i\bar{\theta}\theta_R\mathcal{F}(\hat{x}^\dagger). \quad (1.36)$$

By the use of some superspace identities, it can be shown that a conjugated left chiral superfield $\hat{\mathcal{S}}_L^\dagger(x,\theta)$ transforms as a right chiral superfield. Thus we can build a general chiral theory out of left chiral superfields. It can also straightforwardly be shown that the product of left (right) chiral superfields yields another left (right) chiral superfield.

1.3.3 Vector superfields

Chiral superfields can accomodate scalar bosons and spin-1/2 fermions. To handle SM gauge bosons, however, we need an additional type of superfield, known as a *vector* or *curl* superfield. A vector superfield $\hat{V} = \hat{V}^\dagger$ is purely real, and so contains real bosons and Majorana fermions. If we define the usual field-strength tensor $F^{\mu\nu} \equiv \partial^\mu V^\nu - \partial^\nu V^\mu$, the SUSY transformation laws for $F^{\mu\nu}$, λ, $\mathcal{D}$ are

$$\delta F^{\mu\nu} = -i\bar{\alpha}\left(\gamma_\nu\partial^\mu - \gamma_\mu\partial^\nu\right)\lambda, \quad (1.37)$$

$$\delta\lambda = -i\gamma_5\alpha\mathcal{D} + \frac{1}{4}[\gamma_\nu,\gamma_\mu]F^{\mu\nu}\alpha, \quad (1.38)$$

$$\delta\mathcal{D} = \bar{\alpha}\partial\gamma_5\lambda, \quad (1.39)$$

indicating that these components transform among themselves. Unfortunately, the remaining components $\mathcal{S}, \mathcal{M}, \mathcal{N}, \psi$ do not transform into one another, so they cannot be set to zero and remain so under general SUSY transformations. We will use these vector superfields as gauge potential superfields in SUSY gauge theories, however, where the action is invariant under a SUSY extended gauge transformation parameterized by a left chiral parameter superfield $\hat{\Omega}$:

$$\hat{\mathcal{S}}_L \longrightarrow e^{igt_A\hat{\Omega}}\hat{\mathcal{S}}_L, \tag{1.40}$$

$$\hat{\mathcal{S}}_R \longrightarrow \hat{\mathcal{S}}_R e^{-igt_A\hat{\Omega}^\dagger}, \tag{1.41}$$

$$e^{-2gt_A\hat{V}_A} \longrightarrow e^{igt_P\hat{\Omega}_P^\dagger}e^{-2gt_B\hat{V}_B}e^{-igt_Q\hat{\Omega}_Q}. \tag{1.42}$$

It can be shown that any vector superfield can be put into a form where $\mathcal{S} = \mathcal{M} = \mathcal{N} = \psi = 0$ by means of such an extended gauge transformation. While a SUSY transformation will re-introduce these components, we can always make another extended gauge transformation back to the gauge where they are zero. This is called the *Wess-Zumino* gauge, and we will work in it from now on. Choosing the Wess-Zumino gauge does not eliminate all the degrees of freedom in the SUSY extended gauge transformation $\hat{\Omega}$; those that remain are exactly the ordinary gauge degrees of freedom from the underlying non-supersymmetric theory.

It is useful to construct a field-strength superfield $\hat{W}_A$ from the vector superfield $\hat{V}$. We define it by

$$gt_A\hat{W}_A \equiv -\frac{i}{8}\hat{D}D_R\left[e^{2gt_C\hat{\Phi}_C}D_L e^{-2gt_B\hat{\Phi}_B}\right], \tag{1.43}$$

and it can be shown to transform according to

$$t_A\hat{W}_A \longrightarrow e^{igt_P\hat{\Omega}_P}t_B\hat{W}_B e^{-igt_Q\hat{\Omega}_Q}. \tag{1.44}$$

$\hat{W}_A$ is a left chiral superfield, with a leading component that is spinorial. Its mass dimension is therefore $3/2$. It includes the field-strength tensor $F_{\mu\nu}$ as its corresponding vector gauge field. The product $\bar{\hat{W}}_A^c\hat{W}_A$ is gauge-invariant and Lorentz-invariant, and a product of left-chiral superfields so therefore a left-chiral superfield itself. This is useful for providing gauge kinetic

terms in the Lagrnagian.

1.3.4 Constructing a SUSY Lagrangian

Having introduced superfields which hold all the fields in a supermultiplet together in convenient form, we now need to construct a supersymmetric Lagrangian density involving these fields. One of the chief benefits of the superfield formalism is that it allows us to straightforwardly write down possible supersymmetric Langrangians in a systematic manner.

We seek a Lagrangian density which changes by at most a total derivative under SUSY transformations. We can immediately see from Eq. (1.27) that the coefficient of $(\bar{\theta}\gamma_5\theta)^2$ of any superfield, called the *D-term* of that superfield, is a candidate for the Lagrangian density. Similarly from Eq. (1.32) the coefficient of $\bar{\theta}\theta_L$, or *F-term*, of any *chiral* superfield also transforms properly. We will denote the D-term and F-term of a superfield $\hat{\mathcal{S}}$ by $[\hat{\mathcal{S}}]_D$ and $[\hat{\mathcal{S}}]_F$ respectively. Thus we can write a general SUSY Lagrangian as

$$\begin{aligned}\mathcal{L} = & - \left[K\left(\hat{\mathcal{S}}^\dagger e^{-2gt_A\hat{\Phi}_A}, \hat{\mathcal{S}}\right)\right]_D - \left[\hat{f}(\hat{\mathcal{S}}) + \text{h.c.}\right]_F \\ & - \left[f_{AB}(\hat{\mathcal{S}})\overline{\hat{W}_A^c}\hat{W}_B\right]_F . \end{aligned} \tag{1.45}$$

Alternatively we can write this in terms of superspace integrals which pick out the D- and F-terms:

$$\begin{aligned}\mathcal{L} = & - \frac{1}{4}\int d^4\theta K\left(\hat{\mathcal{S}}^\dagger e^{-2gt_A\hat{\Phi}_A}, \hat{\mathcal{S}}\right) - \frac{1}{2}\int d^2\theta_L\left(\hat{f}(\hat{\mathcal{S}}) + \text{h.c.}\right) \\ & - \frac{1}{4}\int d^2\theta_L f_{AB}(\hat{\mathcal{S}})\overline{\hat{W}_A^c}\hat{W}_B . \end{aligned} \tag{1.46}$$

The two are equivalent.

$\hat{f}(\hat{\mathcal{S}})$ is a general function of left chiral superfields $\hat{\mathcal{S}}_{Li}$ and is called the *superpotential*; K is a function of general superfields and is called the *Kähler potential*. The last term supplies kinetic terms for the gauge fields and contains f_{AB}, a dimensionless function of left chiral superfields known as the *gauge kinetic function*. (f_{AB} must also transform as a representation contained

in the symmetric product of two adjoints.) We did not include the D-term of the superpotential $[\hat{f}(\hat{\mathcal{S}})]_D$ since from Eq. (1.19) this is itself a total derivative. So far, these functions are almost completely general.

Renormalizability, however, strongly constrains the forms of the Kähler potential, superpotential, and gauge kinetic term f_{AB}. From Eqs. (1.14) and (1.20) we can show that $[\theta] = [\bar{\theta}] = -1/2$ and hence $[(\bar{\theta}\gamma_5\theta)^2] = -2$, so by Eq. (1.19) [D-term of K] $- 2 = [K]$. For the theory to be renormalizable, the dimension of the D-term must be less than or equal to 4, meaning the Kähler potential has dimension at most 2. Therefore it is restricted to being at most quadratic in the fields $\hat{\mathcal{S}}_i$ as $[\hat{\mathcal{S}}] = 1$. Similarly one finds that the dimension of the underlying superfield whose F-term appears in the Lagrangian can be at most 3. So the superpotential can be at most a cubic function of the $\hat{\mathcal{S}}_i$'s, and the gauge kinetic function f_{AB} must be dimensionless, i.e. a constant.

By choosing the appropriate basis and normalizing our superfields appropriately, we can restrict the Kähler potential and gauge kinetic function to be

$$K[\hat{\mathcal{S}}^\dagger, \hat{\mathcal{S}}] = \sum_{i=1}^{N} \hat{\mathcal{S}}_i^\dagger \hat{\mathcal{S}}_i, \tag{1.47}$$

$$f_{AB} = \delta_{AB}. \tag{1.48}$$

So the general form of the Lagrangian density in a supersymmetric theory, sometimes called the *master Lagrangian*, is:

$$
\begin{aligned}
\mathcal{L} &= \sum_i (D_\mu \mathcal{S}_i)^\dagger (D^\mu \mathcal{S}_i) + \frac{i}{2}\sum_i \bar{\psi}_i \not{D}\psi_i + \sum_{\alpha,A}\left[\frac{i}{2}\bar{\lambda}_{\alpha A}(\not{D}\lambda)_{\alpha A} - \frac{1}{4}F_{\mu\nu\alpha A}F^{\mu\nu}_{\alpha A}\right] \\
&- \sqrt{2}\sum_{i,\alpha,A}\left(\mathcal{S}_i^\dagger g_\alpha t_{\alpha A}\bar{\lambda}_{\alpha A}\frac{1-\gamma_5}{2}\psi_i + \text{h.c.}\right) \\
&- \frac{1}{2}\sum_{\alpha,A}\left[\sum_i \mathcal{S}_i^\dagger g_\alpha t_{\alpha A}\mathcal{S}_i + \xi_{\alpha A}\right]^2 - \sum_i \left|\frac{\partial \hat{f}}{\partial \hat{\mathcal{S}}_i}\right|^2_{\hat{\mathcal{S}}=\mathcal{S}} \\
&- \frac{1}{2}\sum_{i,j}\bar{\psi}_i\left[\left(\frac{\partial^2 \hat{f}}{\partial\hat{\mathcal{S}}_i\partial\hat{\mathcal{S}}_j}\right)_{\hat{\mathcal{S}}=\mathcal{S}}\frac{1-\gamma_5}{2} + \left(\frac{\partial^2 \hat{f}}{\partial\hat{\mathcal{S}}_i\partial\hat{\mathcal{S}}_j}\right)^\dagger_{\hat{\mathcal{S}}=\mathcal{S}}\frac{1+\gamma_5}{2}\right]\psi_j,
\end{aligned}
\tag{1.49}
$$

The gauge covariant derivatives are explicitly given by,

$$
D_\mu \mathcal{S} = \partial_\mu \mathcal{S} + i\sum_{\alpha,A} g_\alpha t_{\alpha A} V_{\mu\alpha A}\mathcal{S}, \tag{1.50}
$$

$$
\begin{aligned}
D_\mu \psi &= \partial_\mu \psi + i\sum_{\alpha,A} g_\alpha (t_{\alpha A}V_{\mu\alpha A})\psi_L \\
&\quad -i\sum_{\alpha,A} g_\alpha (t^*_{\alpha A}V_{\mu\alpha A})\psi_R,
\end{aligned}
\tag{1.51}
$$

$$
(\not{D}\lambda)_{\alpha A} = \partial\lambda_{\alpha A} + ig_\alpha \left(t^{adj}_{\alpha B}\ \not{V}_{\alpha B}\right)_{AC}\lambda_{\alpha C}, \tag{1.52}
$$

$$
F_{\mu\nu\alpha A} = \partial_\mu V_{\nu\alpha A} - \partial_\nu V_{\mu\alpha A} - g_\alpha f_{\alpha ABC}V_{\mu\alpha B}V_{\nu\alpha C}, \tag{1.53}
$$

where α is an index parameterizing the different gauge groups in the theory.

1.3.5 SUSY breaking

We must say a brief word about supersymmetry breaking. Since the SUSY generators Q_a commute with the 4-momentum operator P_μ (and hence the mass operator P^2), in a supersymmetric theory all members of a supermultiplet must possess the same mass. We can see this by observing for a bosonic eigenstate of energy and momentum $|\mathcal{B}\rangle$

$$
P^2\, Q\,|\mathcal{B}\rangle = QP^2\,|\mathcal{B}\rangle = m_B Q\,|\mathcal{B}\rangle\,,
$$

so that the fermionic state $Q|\mathcal{B}\rangle$ must also have mass m_B. This is obviously not the case, since we have not detected the superpartners of any SM particles yet. Therefore supersymmetry must be *broken* somehow, as electroweak symmetry is broken.

At first glance, breaking SUSY would seem to eliminate the whole purpose of introducing it in the first place — particularly, the cancellation of quadratic divergences. Importantly, however, SUSY can be broken without endangering the cancellation of quadratic divergences. An explicit scalar mass term (differing from the corresponding fermion mass), for example, creates no additional quadratic divergences to any order in perturbation theory. Terms in the Lagrangian with this feature of preserving the cancellation of quadratic divergences are known as *soft* supersymmetry-breaking terms, in contrast to *hard* terms which do introduce such divergences. From here on, we will assume supersymmetry is softly broken.

It seems plausible that supersymmetry, like the electroweak symmetry, might be spontaneously broken by some field acquiring a vacuum expectation value. We can classify the different possibilities as follows. For SUSY to be remain unbroken, there must not be multiple ground states related by a SUSY transformation:

$$\begin{aligned} e^{i\alpha Q}|0\rangle &= |0\rangle\,, \text{ so} \\ Q|0\rangle &= |0\rangle \\ \langle 0|[\bar{\alpha}Q, \mathcal{O}]|0\rangle &= 0 \\ \langle 0|\delta\mathcal{O}|0\rangle &= 0. \end{aligned} \tag{1.54}$$

Hence if any field operator $\mathcal{O}$ has a nonzero variation in the ground state, supersymmetry is spontaneously broken. In order for Lorentz invariance to be preserved, $\delta\mathcal{O}$ has to be a scalar and so $\mathcal{O}$ must be spinorial.

We found the variation of the spinor components of chiral and vector superfields in Eqs. (1.31)

and (1.38) above,

$$\begin{aligned}\delta\psi_L &= -\sqrt{2}\mathcal{F}\alpha_L + \sqrt{2}\partial\mathcal{S}\alpha_R, \\ \delta\lambda &= -i\gamma_5\alpha\mathcal{D} + \frac{1}{4}[\gamma_\nu, \gamma_\mu]F^{\mu\nu}\alpha.\end{aligned}$$

Since $\partial_\mu\mathcal{S}$ and $F^{\mu\nu}$ cannot develop a vev without breaking Lorentz invariance, we see that the condition for spontaneously broken SUSY is

$$\langle 0 \,|\, \mathcal{F}_i \,|\, 0\rangle \neq 0 \quad \text{or} \quad \langle 0 \,|\, \mathcal{D}_A \,|\, 0\rangle \neq 0. \tag{1.55}$$

These possibilities are referred to as F-type and D-type SUSY breaking respectively. Naturally, the field developing a vev needs to be uncharged under electromagnetism and colorless. By selecting a superpotential (or Kähler potential) under which the F-term or D-term of a candidate superfield develops a vev, one can construct a model which spontaneously breaks supersymmetry, and does so softly.

Unfortunately, serious difficulties arise with these types of simple models. One stems from the *supertrace sum rule*, a robust restriction on particle masses in supersymmetric theories, even those where SUSY is spontaneously broken. The supertrace is defined as a weighted sum over particles,

$$\mathrm{STr}\,\mathcal{M}^2 = \sum_{\text{particles}} (-1)^{2J}(2J+1)m_J^2, \tag{1.56}$$

where the sum is over all particles, with J a particle's spin and m_J its mass. For a theory with chiral superfields, a lengthy but straightforward calculation reveals that at tree-level,

$$\mathrm{STr}\,\mathcal{M}^2 = 2\sum_A \mathcal{D}_A \,\mathrm{Tr}(g t_A)\,, \tag{1.57}$$

where $\mathcal{D}_A \equiv \sum_i \mathcal{S}_i^\dagger g t_A \mathcal{S}_i + \xi_A$, and the trace is taken over complex fields in the chiral supermultiplets.

The difficulty at hand arises because the Standard Model, and hence normal supersym-

metric extensions of it, have a U(1) hypercharge symmetry and are anomaly-free. That is, in order to prevent anomalies, the representations of the particles in the theory are chosen so that the sum over $U(1)_Y$ charges is 0. Therefore the right-hand side of Eq. (1.57), and thus the supertrace itself, vanishes. The sum of squared masses over fermion degrees of freedom then must equal that over bosons. But in realistic models, most of the chiral fermions (the SM particles) are relatively light, whereas their bosonic superpartners must be much heavier, making this rule extremely difficult to satisfy. Worse, when flavor symmetries are taken into account, more restrictive sum rules can be derived which apply to each sector individually. For example, in the limit where lepton flavor is conserved, the selectrons cannot mix with any other particles (assuming no new multiplets with electron flavor), and their part of the sum rule "decouples":

$$m_{\tilde{e}_1}^2 + m_{\tilde{e}_2}^2 = 2m_e^2 \,, \tag{1.58}$$

which is obviously not the case.

The supertrace sum rule is remarkably robust and poses a serious challenge for simple models of spontaneously-broken supersymmetry. As a result, most current efforts at model-building take a more complex approach that avoids these pitfalls. They introduce new sectors into the theory: a *hidden sector* containing new fields nearly decoupled from the SM, including one which develops a vev and breaks supersymmetry. There is also a *messenger sector* which couples these new fields to the SM fields, but does so weakly enough to preserve the experimental success of the SM. There are several popular classes of such models, including gravity-mediated SUSY breaking (supergravity), gauge-mediated SUSY breaking, and anomaly mediated SUSY breaking. These avoid the supertrace sum rule either by promoting SUSY to a local symmetry (which modifies the sum rule, as we will see below), or by giving sparticles their masses only at the loop level. We will discuss the first of these classes of models, gravity-mediated SUSY breaking, in detail later.

An alternative approach to model-building is to parameterize the effects of SUSY breaking by writing out all possible soft SUSY breaking terms consistent with the symmetries of our

theory. In essence, by choosing to work with the most general SUSY-breaking Lagrangian, we are parameterizing our ignorance of the mechanism of SUSY breaking. Each particular mechanism will then give a specific prediction for these parameters in terms of a (hopefully) much smaller number of more fundamental parameters.

It can be shown [6] that the following terms break supersymmetry softly:

1. Linear, bilinear, and trilinear self-interactions of scalar fields,
2. Scalar mass terms,
3. Gaugino mass terms,
4. Mixing (mass) terms between gauginos and and fermion members of chiral supermultiplets, and
5. Trilinear scalar interactions of the form $\mathcal{S}_i\mathcal{S}_j\mathcal{S}_k^*$.

The last two exist only in models without gauge singlet superfields.

So the soft SUSY-breaking (SSB) Lagrangian can be written as

$$\begin{aligned}\mathcal{L}_{\text{soft}} = &\sum_i C_i\mathcal{S}_i + \sum_{i,j} B_{ij}\mu_{ij}\mathcal{S}_i\mathcal{S}_j + \sum_{i,j,k} A_{ijk}f_{ijk}\mathcal{S}_i\mathcal{S}_j\mathcal{S}_k + \sum_{i,j,k} C_{ijk}f_{ijk}\mathcal{S}_i\mathcal{S}_j\mathcal{S}_k^* + \text{ h.c.} \\ &- \sum_{i,j}\mathcal{S}_i^\dagger m_{ij}^2\mathcal{S}_j - \frac{1}{2}\sum_{A,\alpha} M_{A\alpha}\bar{\lambda}_{A\alpha}\lambda A\alpha - \frac{i}{2}\sum_{A,\alpha} M'_{A\alpha}\bar{\lambda}_{A\alpha}\gamma_5\lambda A\alpha - \frac{1}{2}\sum_{A,\alpha,i} M''_{iA\alpha}\bar{\psi}_i\lambda A\alpha,\end{aligned} \tag{1.59}$$

where α runs over the different factors of the gauge group. Note that we have chosen to write some of the coefficients as products; in the MSSM, below, μ_{ij} and f_{ijk} are coefficients in the superpotential and it is standard to factor them out of the SSB terms.

1.3.6 MSSM

The minimal supersymmetric standard model, or MSSM, is the supersymmetric extension of the Standard Model which contains the minimal necessary field content and the most general set of soft supersymmetry breaking terms consistent with the symmetries of the SM. It contains

the smallest set of fields and new interactions possible while remaining compatible with SM constraints at low energies and accomodating arbitrary mechanism for SUSY-breaking.

The construction of the MSSM is fairly straightforward:

- The gauge symmetry group is $SU(3)_{\mathsf{C}} \times SU(2)_{\mathsf{L}} \times U(1)_{\mathsf{Y}}$, just as in the SM. This determines the theory's gauge interactions and leads to the introduction of gauge superfields, corresponding to the gauge fields of the SM:

$$B_\mu \longrightarrow \hat{B} \ni (\lambda_0, B_\mu, \mathcal{D}_B), \tag{1.60}$$

$$W_{A\mu} \longrightarrow \hat{W}_A \ni (\lambda_A, W_{A\mu}, \mathcal{D}_{WA}), \qquad A = 1, 2, 3, \text{ and} \tag{1.61}$$

$$g_{A\mu} \longrightarrow \hat{g}_A \ni (\tilde{g}, G_{A\mu}, \mathcal{D}_{gA}), \qquad A = 1, \ldots, 8. \tag{1.62}$$

- To obtain the matter content of the theory, we promote SM matter fields to chiral superfields. Since only left chiral superfields can appear in the superpotential, we do not introduce right-handed fields such as $\hat{e}_R$ themselves, but instead their (left-handed) charge-conjugate fields $(\hat{E}^c)_L \equiv (\hat{e}_R)^c$. For example, while the left-handed electron is contained in the superfield

$$\hat{e} = \tilde{e}_L(\hat{x}) + i\sqrt{2}\bar{\theta}\psi_{eL}(\hat{x}) + i\bar{\theta}\theta_L\mathcal{F}_e(\hat{x}), \tag{1.63}$$

  the right-handed field electron is in

$$\hat{E}^c = \tilde{e}_R^\dagger(\hat{x}) + i\sqrt{2}\bar{\theta}\psi_{E^cL}(\hat{x}) + i\bar{\theta}\theta_L\mathcal{F}_{E^c}(\hat{x}). \tag{1.64}$$

  The four-component Dirac electron field is given by the usual combination of the two-component Majorana fields,

$$e = P_L\psi_e + P_R\psi_{E^c}.$$

- The Higgs field of the MSSM must be handled specially. In the Standard Model, the Higgs

is introduced as an $SU(2)$ doublet $\begin{pmatrix}\phi^+\\ \phi^0\end{pmatrix}$ with hypercharge $Y=1$. It acquires a vev and thereby provides masses to the $Y=-1$ SM fermions via Yukawa interactions of the form $(\bar{\psi_u}\phi)\psi_{U^c}$. A similar term using the $Y=-1$ field $\phi^c = i\sigma_2\phi^*$ provides the masses for the $Y=1$ fermions. In the MSSM, however, ϕ^c is part of a *right* chiral supermultiplet $\hat{h}_u^{0\dagger}$, and so cannot appear in the superpotential. Since fermion mass terms are not soft SUSY-breaking, this means we cannot use the Higgs superfield $\hat{H}_u = \begin{pmatrix}\hat{h}_u^+\\ \hat{h}_u^0\end{pmatrix}$ to provide masses to the $Y=1$ fermions. Instead, we must introduce a separate doublet of Higgs superfields,

$$\hat{H}_d = \begin{pmatrix}\hat{h}_d^-\\ \hat{h}_d^0\end{pmatrix}, \tag{1.65}$$

transforming under the $\mathbf{2}^*$ representation of $SU(2)$ with hypercharge $Y=-1$. The scalar component $\hat{h}_d^0$ of $\hat{H}_d$ develops a vev and provides the masses for down-type quarks and charged leptons, while $\hat{h}_u^0$ does the same for up-type quarks. (This second Higgs doublet also fortuitously ensures cancellation of the anomalies introduced by adding the extra fermions $\psi_{h_u^+}$ and $\psi_{h_u^0}$ to the theory.)

It can be seen that the particle content of the MSSM is comprised of all SM fermions plus their scalar superpartners (*sfermions*), the SM gauge bosons along with their spin-$1/2$ superpartners (*gauginos*), and the two Higgs doublets with their spin-$1/2$ superpartners (*Higgsinos*). The physical particle content is slightly different, however, thanks to electroweak and SUSY symmetry breaking and the resulting mixing among the sparticles.

First, as can be seen from the MSSM interaction terms below, there are generally quadratic interactions mixing field pairs such as $\tilde{\tau}_L$, $\tilde{\tau}_R^\dagger$, the scalar superpartners of the left- and right-handed components of the τ lepton. Thus the physical particles are superpositions of these, labelled $\tilde{\tau}_1$ and $\tilde{\tau}_2$. While there can be mixing in any pair of squarks or sleptons of the same generation, it is typically only significant in the third generation pairs with their large Yukawa couplings.

Second, the Higgs mechanism causes some of the components of the two Higgs fields to be “eaten” by the gauge bosons. There are 8 real degrees of freedom in the two MSSM

Higgs doublets: 4 neutral, 2 postively charged, and 2 negatively charged. Of these, 3 are eaten by the W^+, W^-, and Z, leaving 2 charged and 3 neutral degrees of freedom. The resulting physical particles are the charged Higgses $H^\pm$, the CP-odd neutral Higgs A, and the light and heavy neutral Higgses h and H. Finally, there is also mixing among scalar Higgsinos and electroweak gauginos. As they share identical quantum numbers, the charged Higgsino components $\psi_{h_u^\pm}$ can (and in general do) mix with the charged winos $\tilde{W}^\pm$ to form two *charginos* $\tilde{W}_1$, $\tilde{W}_2$. Similarly, the neutral Higgsinos $\psi_{h_u^0}$, $\psi_{h_d^0}$ mix with the bino $\tilde{B}$ and the neutral wino $\tilde{W}^0$ to form four *neutralinos* $\tilde{Z}_1$, $\tilde{Z}_2$, $\tilde{Z}_3$, $\tilde{Z}_4$.

Now that we have specified the matter content (summarized in Table 1.2) and gauge interactions of the theory, we must select any further interaction terms. These come in two classes: SUSY preserving terms (from the superpotential) and SUSY breaking terms (which must be soft.)

- If we require our theory to be renormalizable, this constraint along with gauge invariance sharply limits the possible terms in the superpotential. The most general superpotential is

$$\hat{f}(\hat{\mathcal{S}}) \ni \mu \hat{H}_u^a \hat{H}_{da} + \sum_{i,j} \left[(\mathbf{f}_u)_{ij} \epsilon_{ab} \hat{Q}_i^a \hat{H}_u^b \hat{U}_j^c + (\mathbf{f}_d)_{ij} \hat{Q}_i^a \hat{H}_{da} \hat{D}_j^c + (\mathbf{f}_e)_{ij} \hat{L}_i^a \hat{H}_{da} \hat{E}_j^c \right] + \sum_{i,j,k} \left[\lambda_{ijk} \epsilon_{ab} \hat{L}_i^a \hat{L}_j^b \hat{E}_k^c + \lambda'_{ijk} \epsilon_{ab} \hat{L}_i^a \hat{Q}_j^b \hat{D}_k^c + \lambda''_{ijk} \hat{U}_i^c \hat{D}_j^c \hat{D}_k^c \right] + \sum_i \mu'_i \epsilon_{ab} \hat{L}_i^a \hat{H}_u^b. \quad (1.66)$$

  Some of these terms are problematic. Within the SM, baryon and lepton number are "accidental" symmetries: there are no renormalizable gauge-invariant interactions violating them. In the MSSM, this is not the case; all the terms on the second line of Eq. (1.66) violate either lepton or baryon number. We will set them to zero. There are several motivations for this: first, there are extremely strong experimental constraints on such processes, so any such terms would have to be highly suppressed if they existed at all. Second, all such terms can be eliminated by imposing symmetries known as *matter parity* or *R-parity*. The matter parity of all quark and lepton superfields is odd, while that

of gauge and Higgs superfields is even; or in other words, superfields containing SM fermions are odd and all others are even. It can be shown that in the MSSM conservation of matter parity is equivalent to conservation of R-parity

$$R = (-1)^{3B-L+2s}, \tag{1.67}$$

where s is the spin of the field: so all Standard Model particles are R-even whereas their superpartners are R-odd. R-parity has important phenomenological implications; in particular, since (heavy) superpartners cannot decay into only SM particles, the lightest supersymmetric particle is stable, providing a natural candidate for cold dark matter. Note that while we will assume here R-parity is conserved, it does not need to be; there are many interesting R-parity violating models.

- We choose include the most general set of soft SUSY breaking terms consistent with renormalizability and gauge invariance. Following Eq. 1.59, these are

$$\begin{aligned}
\mathcal{L}_{\text{soft}} = &- \left[\tilde{Q}_i^\dagger \mathbf{m}^{\mathbf{2}}_{\mathbf{Q}_{ij}} \tilde{Q}_j + \tilde{d}_{Ri}^\dagger \mathbf{m}^{\mathbf{2}}_{\mathbf{D}ij} \tilde{d}_{Rj} + \tilde{u}_{Ri}^\dagger \mathbf{m}^{\mathbf{2}}_{\mathbf{U}ij} \tilde{u}_{Rj}\right. \\
&\left. + \tilde{L}_i^\dagger \mathbf{m}^{\mathbf{2}}_{\mathbf{L}ij} \tilde{L}_j + \tilde{e}_{Ri}^\dagger \mathbf{m}^{\mathbf{2}}_{\mathbf{E}ij} \tilde{e}_{Rj} + m_{H_u}^2 |H_u|^2 + m_{H_d}^2 |H_d|^2\right] \\
&- \tfrac{1}{2}\left[M_1 \bar{\lambda}_0 \lambda_0 + M_2 \bar{\lambda}_A \lambda_A + M_3 \bar{\tilde{g}}_B \tilde{g}_B\right] \\
&- \tfrac{i}{2}\left[M_1' \bar{\lambda}_0 \gamma_5 \lambda_0 + M_2' \bar{\lambda}_A \gamma_5 \lambda_A + M_3' \bar{\tilde{g}}_B \gamma_5 \tilde{g}_B\right] \\
&+ \left[(\mathbf{a_u})_{ij} \epsilon_{ab} \tilde{Q}_i^a H_u^b \tilde{u}_{Rj}^\dagger + (\mathbf{a_d})_{ij} \tilde{Q}_i^a H_{da} \tilde{d}_{Rj}^\dagger + (\mathbf{a_e})_{ij} \tilde{L}_i^a H_{da} \tilde{e}_{Rj}^\dagger + \text{ + h.c.}\right] \\
&+ \left[(\mathbf{c_u})_{ij} \epsilon_{ab} \tilde{Q}_i^a H^{*b}_d \tilde{u}_{Rj}^\dagger + (\mathbf{c_d})_{ij} \tilde{Q}_i^a H_{ua}^* \tilde{d}_{Rj}^\dagger + (\mathbf{c_e})_{ij} \tilde{L}_i^a H_{ua}^* \tilde{e}_{Rj}^\dagger + \text{ h.c.}\right] \\
&+ \left[b H_u^a H_{da} + \text{ h.c.}\right].
\end{aligned} \tag{1.68}$$

This fully specifies the MSSM. The particle content and interactions of the theory are fixed, but there are many free parameters. Counting, in the gauge sector we have the SM parameters g_1, g_2, g_3 and θ_{QCD}, as well as the six real gaugino masses M_i, M_i'. One of the M_i', chosen to be M_3', can be eliminated by a rotation of the gaugino field, leaving 9 real parameters. In the Higgs sector we have the two Higgs mass terms, plus the complex μ and b terms; since

the phase for b can be absorbed by a redefinition of one of the Higgs fields, we have 5 real parameters. In the matter sector, we nine complex 3x3 matrices (18 parameters each): three Yukawas, three a's, and three c's, giving 162 parameters. We also have five soft SUSY breaking Hermitian mass matrices (9 parameters each), yielding another 45 parameters, for a total of 207 real parameters in this sector. However, another 43 of these parameters can be absorbed by redefinitions of the matter superfields. So, taken all together, the MSSM has 178 arbitrary real parameters.

As alluded to above, certain of the MSSM parameters are typically expressed in a different form; namely, the trilinear coupling matrices $\mathbf{a}_{ij}$ are specified by A_{ij}, where $\mathbf{a}_{ij} \equiv A_{ij}\mathbf{f}_{ij}$, and the the bilinear Higgs coupling b becomes B, where $b \equiv B\mu$. While this is not always even possible in the general MSSM (since e.g. one can have $\mathbf{f}_{ij} = 0$ and $\mathbf{a}_{ij} \neq 0$), it is motivated by gravity-mediated models in which it is a helpful choice.

The excessive number of free parameters in the MSSM should not be surprising, since we explicitly constructed it to parameterize our ignorance of the mechanism of SUSY breaking. So while it is quite general, it can be very unwieldly to work with. There are different strategies for making phenomological analyses of the MSSM more tractable. One can reduce the parameter space somewhat by eliminating or simplifying many of the parameters; for example, it is common to set the c parameters (which are highly suppressed in many models), the CP-violating SUSY parameters, and the off-diagonal (in the fermion mass basis) elements of the sfermion mass and a matrices (which induce flavor violation) to zero. Alternatively, one can select a particular model of SUSY breaking, which will specify all of the MSSM parameters in terms of a smaller number of more fundamental parameters. We will follow the latter approach here.

One of the most popular such frameworks for SUSY breaking in the context of the MSSM is that of *minimal supergravity*, or mSUGRA. Minimal supergravity avoids the consequences of the supertrace sum rule by not breaking *global* supersymmetry. SUSY is instead extended to a local symmetry, which is then broken. This extension of SUSY, a spacetime symmetry (recall Eq. (1.14)), necessarily leads to the inclusion of gravity, hence the name "supergravity." Supergravity is a large and complex topic in its own right[7], and we will only cover the aspects

Name		scalar	spinor	vector	$SU(3)_C$	$SU(2)_L$	$U(1)_Y$
left [s]quarks	$\hat{Q} = \begin{pmatrix} \hat{u}_L \\ \hat{d}_L \end{pmatrix}$	$\begin{pmatrix} \tilde{u}_L \\ \tilde{d}_L \end{pmatrix}$	$\begin{pmatrix} uL \\ dL \end{pmatrix}$		$\mathbf{3}$	$\mathbf{2}$	$\frac{1}{3}$
right up [s]quarks	$\hat{U}^c$	$\tilde{u}_R^*$	$\psi_{U^c R}$		$\bar{\mathbf{3}}$	$\mathbf{1}$	$-\frac{4}{3}$
right down [s]quarks	$\hat{D}^c$	$\tilde{d}_R^*$	$\psi_{D^c R}$		$\bar{\mathbf{3}}$	$\mathbf{1}$	$\frac{2}{3}$
left [s]leptons	$\hat{L} = \begin{pmatrix} \hat{\nu}_{eL} \\ \hat{e}_L \end{pmatrix}$	$\begin{pmatrix} \tilde{\nu}_{eL} \\ \tilde{e}_L \end{pmatrix}$	$\begin{pmatrix} \psi_{\nu L} \\ \psi_{eL} \end{pmatrix}$		$\mathbf{1}$	$\mathbf{2}$	-1
right [s]leptons	$\hat{E}^c$	$\tilde{e}_R^\dagger$	$\psi_{E^c L}$		$\mathbf{1}$	$\mathbf{1}$	2
gluon, gluino	$\hat{g}_A$		$\tilde{g}_A$	$G_{A\mu}$	$\mathbf{8}$	$\mathbf{1}$	0
W, wino	$\hat{W}_A$		λ_A	$W_{A\mu}$	$\mathbf{1}$	$\mathbf{3}$	0
B, bino	$\hat{B}$		λ_0	B_μ	$\mathbf{1}$	$\mathbf{1}$	0
Higgs, Higgsinos	$\hat{H}_u = \begin{pmatrix} \hat{h}_u^+ \\ \hat{h}_u^0 \end{pmatrix}$	$\begin{pmatrix} h_u^+ \\ h_u^0 \end{pmatrix}$	$\begin{pmatrix} \psi_{h_u^+} \\ \psi_{h_u^0} \end{pmatrix}$		$\mathbf{1}$	$\mathbf{2}$	$+1$
Higgs, Higgsinos	$\hat{H}_d = \begin{pmatrix} \hat{h}_d^- \\ \hat{h}_d^0 \end{pmatrix}$	$\begin{pmatrix} h_d^0 \\ h_d^- \end{pmatrix}$	$\begin{pmatrix} \psi_{h_d^0} \\ \psi_{h_d^-} \end{pmatrix}$		$\mathbf{1}$	$\mathbf{2}$	-1

Table 1.2: The MSSM particle content, showing each supermultiplet along with its component fields and gauge group representation. Generations are not shown.

necessary for familiarity with the mSUGRA framework.

Supergravity

The procedure for extending SUSY to a local symmetry parallels the procedure for extending gauge symmetries in the construction of gauge theories. We begin with a theory invariant under local SUSY – for illustration, we will use the simple case of the massless non-interacting Wess-Zumino model:

$$\mathcal{L} = \mathcal{L}_{\text{kin}} = \frac{1}{2}(\partial_\mu A)^2 + \frac{1}{2}(\partial_\mu B)^2 + \frac{i}{2}\bar{\psi}\partial\!\!\!/\psi, \tag{1.69}$$

invariant under the transformations

$$\delta A = i\bar{\alpha}\gamma_5\psi, \tag{1.70}$$

$$\delta B = -\bar{\alpha}\psi, \tag{1.71}$$

$$\delta\psi = -i\alpha\partial\!\!\!/(-B + i\gamma_5 A). \tag{1.72}$$

We then extend the transformation α to a spacetime-dependent transformation $\alpha(x)$. It can easily be verified that the Lagrangian density transforms under SUSY as

$$\delta\mathcal{L}_{\text{kin}} = \partial^\mu \left(\frac{1}{2}\bar{\alpha}\gamma_\mu \partial(-B + i\gamma_5 A)\psi \right) + (\partial^\mu \bar{\alpha})(\partial\gamma_\mu(-B + i\gamma_5 A))\psi. \tag{1.73}$$

The first term is just a total derivative, and the second can be cancelled by adding a new term,

$$\mathcal{L}_1 = -\kappa\bar{\psi}_\mu \partial_\nu(-B + i\gamma_5 A)\gamma^\nu\gamma^\mu\psi, \tag{1.74}$$

to the Lagrangian, where ψ_μ is a spin $\frac{3}{2}$ Rarita-Schwinger field (spinor index suppressed) chosen to transform as

$$\delta\bar{\psi}_\mu = \tfrac{1}{\kappa}\partial_\mu\bar{\alpha}. \tag{1.75}$$

κ is a constant with mass dimension -1 necessary to make the term dimension 4.

$\mathcal{L}_1$, however, generates additional terms under local SUSY transformations,

$$\delta(\mathcal{L}_{\text{kin}} + \mathcal{L}_1) = -2i\kappa\bar{\psi}_\mu\gamma_\nu T^{\mu\nu}\alpha + \cdots, \tag{1.76}$$

where

$$T^{\mu\nu} = (\partial^\mu A)(\partial^\nu A) + (\partial^\mu B)(\partial^\nu B) - \frac{1}{2}\eta^{\mu\nu}\left[(\partial_\mu A)^2 + (\partial_\mu B)^2\right] + \frac{i}{2}\bar{\psi}\gamma^\mu\partial^\nu\psi \tag{1.77}$$

is the canonical energy-momentum tensor. To cancel this term, we must add another piece to the Lagrangian density,

$$\mathcal{L}_2 = -g_{\mu\nu}T^{\mu\nu}, \tag{1.78}$$

where $g_{\mu\nu}$ transforms as

$$\delta g_{\mu\nu} = -i\kappa\bar{\alpha}(\gamma_\nu\psi_\mu + \gamma_\mu\psi_\nu). \tag{1.79}$$

Thus we have been forced to introduce a massless spin-2 field coupling to the energy-momentum tensor, just as in general relativity (GR.) Somewhat surprisingly, the adoption of local super-

symmetry has turned out to imply gravity; hence the term *supergravity*.

While the Lagrangian we have written is locally supersymmetric, it is not the complete Lagrangian for even the simple non-interacting, massless, on-shell Wess-Zumino model. To obtain that, we must also add in the kinetic terms for the gravitino ψ_μ and graviton $g_{\mu\nu}$ fields, as well as making all derivates covariant with respect to general coordinate transformations. The complete derivation and results are rather complex and can be found in Ref. [8].

In principle, by beginning with the most general globally supersymmetric Lagrangian, Eq. (1.46), this procedure can be used to obtain a complete general supergravity Lagrangian, analagous to our global SUSY master formula Eq. (1.50). In practice, more advanced techniques are used to obtain this result more efficiently. The full Lagrangian contains very many terms and we will not give it here; it can be found in Ref. [9].

We will, however, briefly discuss the choice of starting global SUSY Lagrangian for a supergravity theory. Note that we were forced above to introduce a nonrenormalizable term, $\mathcal{L}_1$, with a coefficient $-\kappa$ of mass dimension -1. This is unavoidable in supergravity; indeed the Einstein Lagrangian for GR can itself be shown to be nonrenormalizable. While nonrenormalizability may appear to disqualify these as truly "fundamental" theories, it does not render them useless. Just like Fermi's nonrenormalizable theory of β-decay, supergravity can be fruitfully used as a low-energy effective theory representing the limit of some as-yet-unknown more fundamental theory.

The necessary introduction of nonrenormalizable terms leads us to relax our requirements that the superpotential, Kähler potential, and gauge kinetic terms themselves be nonrenormalizable. So the potential global SUSY Lagrangian for supegravity becomes,

$$\begin{aligned}\mathcal{L} = & - \frac{1}{4}\int d^4\theta K\left(\hat{\mathcal{S}}^\dagger e^{-2gt_A\hat{\Phi}_A}, \hat{\mathcal{S}}\right) - \frac{1}{2}\int d^2\theta_L\left(\hat{f}(\hat{\mathcal{S}}) + \text{h.c.}\right) \\ & - \frac{1}{4}\int d^2\theta_L f_{AB}(\hat{\mathcal{S}})\overline{\hat{W}_A^c}\hat{W}_B \ . \end{aligned} \tag{1.80}$$

The Kähler potential $K(\hat{\mathcal{S}}^\dagger, \hat{\mathcal{S}})$, the superpotential $\hat{f}(\hat{\mathcal{S}})$, and the gauge kinetic function $f_{AB}(\hat{\mathcal{S}})$ are all now general functions of chiral superfields, save that the Kähler potential and superpo-

tential must be invariant under global gauge transformations, the gauge kinetic function must transform as the symmetric product of two adjoints of the gauge group, and the superpotential and gauge kinetic function must both be analytic functions. This is the most general form for a locally supersymmetric theory.

Thus there is a great deal of freedom in the construction of supergravity theories. A common choice is to restrict the Kähler potential and gauge kinetic functions to their values in renormalizable theories,

$$K = \sum_i \hat{\mathcal{S}}^{i\dagger} \hat{\mathcal{S}}_i \tag{1.81}$$

$$f_{AB}(\hat{\mathcal{S}}) = \delta_{AB}, \tag{1.82}$$

sometimes called the *minimal* or *flat* choice for these functions. Such a choice leads to canonical kinetic terms for scalar, fermion, and gaugino fields.

Local supersymmetry can be broken in the same manner as global supersymmetry, with a spinor field operator developing a nonzero variation in the ground state. In addition to the usual F- and D-term breaking, local supersymmetry can also be broken if (non-SM) interactions become strong and cause gauginos or chiral fermions to condense. Regardless of how it is broken, there is a "super-Higgs" mechanism by which the goldstino degrees of freedom are eaten by the gravitino, giving it a mass $m_{3/2}^2 = e^{G_0} M_P^2$, where G_0 is the vev of $G \equiv K + \log|\hat{f}|^2$ and M_P is the Planck scale at which supergravity is broken.

The supertrace sum rule is modified in the presence of local supersymmetry to

$$\mathrm{STr}\, \mathcal{M}^2 = 2 \sum_A \mathcal{D}_A \,\mathrm{Tr}(g t_A) + (N-1) \left(2 m_{3/2}^2 - \frac{\mathcal{D}_A \mathcal{D}_A}{M_P^2} \right) . \tag{1.83}$$

The second term is new and allows us to avoid the difficult requirement of a vanishing supertrace. Supergravity models can thereby accomodate superpartners that are all heavier than SM particles, consistent with experiment.

1.3.7 mSUGRA

Minimal supergravity, or mSUGRA, is a simple and popular supergravity model, often used in phenomenological analyses. Its conceptual simplicity is appealing, and its small number of parameters makes detailed prospective phenomenological analysis tractable. In this work we will adopt mSUGRA boundary conditions and the mSUGRA parameter set.

mSUGRA is motivated by the appeal of supergravity as a mechanism for transmitting SUSY breaking, by the apparent success of gauge coupling unification within the MSSM (cf. Fig. 1.1), and by the tight constraints on SUSY flavor-changing processes (Sec. 1.6). Together, these can be taken to suggest the adoption of *universality* at the GUT scale $M_{GUT} \approx 10^{16}$ GeV, in which not only the gauge couplings but also the scalar masses, gaugino masses, and trilinear A couplings are all taken to be diagonal and equal at the GUT scale:

$$g_{\text{GUT}} \equiv g_1 = g_2 = g_3 \tag{1.84}$$

$$m_{\frac{1}{2}} \equiv M_1 = M_2 = M_3 \tag{1.85}$$

$$m_0^2 \equiv m_{Q_i}^2 = m_{U_i}^2 = m_{D_i}^2 = m_{L_i}^2 = m_{E_i}^2 = m_{H_u}^2 = m_{H_d}^2 \tag{1.86}$$

$$A_0 \equiv A_t = A_b = A_\tau. \tag{1.87}$$

Adopting the simplifying assumptions from Sec. 1.3.6, there are only a handful of parameters of the MSSM still unspecified. From the superpotential, we have the fermion Yukawa couplings $\mathbf{f}_u, \mathbf{f}_d, \mathbf{f}_e, \mathbf{f}_\nu$ and the SUSY analog of the quadratic Higgs coupling, μ; from the soft SUSY-breaking terms, we have only the parameter B coupling up-type and down-type Higgs. The fermion Yukawas are set by the known fermion masses.[1] μ and B are often exchanged for more convenient parameters by using constraints from electroweak symmetry breaking. A straightforward calculation of the Higgs scalar potential (after rotating away the charged com-

[1] Except for the neutrino Yukawa, on which see the discussion in Sec. 2.1.

ponents) yields

$$V_{\text{scalar}} = (m_{H_u}^2 + \mu^2)|h_u^0|^2 + (m_{H_d}^2 + \mu^2)|h_d^0|^2 - B\mu(h_u^0 h_d^0 + \text{h.c.}) + \frac{1}{8}(g^2 + g'^2)(|h_u^0|^2 + |h_d^0|^2)^2. \tag{1.88}$$

It is then simple to show that when there is a nontrivial minima of the potential, it will occur at

$$B\mu = \frac{(m_{H_u}^2 + m_{H_d}^2 + 2\mu^2)\sin 2\beta}{2}, \tag{1.89}$$

$$\mu^2 = \frac{m_{H_d}^2 - m_{H_u}^2 \tan^2\beta}{\tan^2\beta - 1} - \frac{M_Z^2}{2}, \tag{1.90}$$

where β is defined by

$$\tan\beta \equiv \frac{v_u}{v_d}, \tag{1.91}$$

and the Z mass at the tree-level in the MSSM is $M_Z^2 = \frac{g^2+g'^2}{2}(v_u^2 + v_d^2)$. Using these relations, we can exchange the parameters B and μ for $\tan\beta$ and $\text{sgn}(\mu)$ by choosing $\tan\beta$ to reproduce $B\mu$, and then using the observed Z mass to fix $|\mu|$.

This leaves us with the final set of parameters determining an mSUGRA model:

$$(m_0, m_{1/2}, A_0, \text{sgn}\,\mu, \tan\beta) \tag{1.92}$$

where we have not included g_{GUT} as it will be fixed by the value of the couplings at low energies.

1.4 Neutrinos

1.4.1 Neutrino mass

In the Standard Model, as well as in most treatments of the MSSM, the neutrinos are massless fermions ν_L which transform as SU(2) doublets along with the left-handed charged leptons e_L. There are three generations of neutrinos just as there are three generations of charged leptons. As neutrinos are uncharged under the electromagnetic and strong interactions (see Table 1.1) they interact only weakly and are difficult to detect. Indeed, they were originally discovered

only as consistently missing energy and momentum in certain weak decays[10], and were not directly detected until many years later[11].

One of the most striking aspects of the weak force is that it is maximally parity-violating. All the other known forces forces respect parity symmetry, that is, they are invariant under the transformation $\mathbf{x} \to -\mathbf{x}$. Until parity violation in the weak force was discovered, this was widely thought to be a universal symmetry applicable to all fundamental physical theories. The weak interaction, however, does not respect this symmetry. Not only does it violate parity, but it only couples to left-handed particles (and right-handed antiparticles), which indicate not only that neutrinos thus making it a maximally parity-violating interaction. Its current has the so-called *V-A* form:

$$\mathcal{L} \ni \frac{G_F}{\sqrt{2}} J^{(ab)\mu} J^{(cd)\dagger}_{\mu}, \qquad J^{(ab)\mu} = \bar{\psi}^{(a)} \gamma^{\mu} (1 - \gamma_5) \psi^{(b)}. \tag{1.93}$$

Early experiments put stringent bounds on neutrino masses, much lower than any of the masses of other known SM particles. These limits, combined with the maximally parity-violating nature of the weak interaction — which leaves right-handed neutrinos sterile, without any nongravitational interactions at all — led to the natural assumption that neutrinos were perfectly massless. In that case right-handed neutrinos would not only be sterile but would simply not exist.

Over the past decade or so, however, this picture has been completely overturned. Direct experiments have not yet measured absolute neutrino masses (bounds are now near $\sum_i m_{\nu_i} \lesssim 0.5$ eV-2 eV [12]), but there is now definitive evidence in the form of neutrino oscillations, which indicates not only that neutrinos are massive but that they also mix with one another.[13] That is, the neutrino mass matrix, like the quark mass matrix, is not diagonal in the flavor basis, and so the neutrino mass eigenstates ν_1, ν_2, ν_3 differ from the flavor eigenstates ν_e, ν_μ, ν_τ. The two bases are related by the Maki-Nakagawa-Sakata (MNS) mixing matrix V_{MNS}: $(\nu_e \ \nu_\mu \ \nu_\tau)^{\mathrm{T}} = V_{\text{MNS}} \, (\nu_1 \ \nu_2 \ \nu_3)^{\mathrm{T}}$.

Just as CKM mixing allows for flavor-changing charged-current interactions among quarks, MNS mixing allows for flavor oscillation among neutrinos. This can be easily understood qualitatively by considering the evolution of a neutrino produced in a flavor eigenstate. As long as

the relevant portion of the MNS matrix is not diagonal, this flavor eigenstate corresponds to a mix of mass eigenstates. And as long as these masses differ from one another, each mass eigenstates will propagate independently, with different wavelengths. Therefore the neutrino will consist of different mixtures of the mass eigenstates at different distances from the point of production, i.e. it will show spatial *oscillation* among two or more different flavors. It is the observation of these oscillations, between various pairs of neutrino flavors and over various distance scales, which experimentally established the existence of neutrino masses.

The MNS mixing matrix $\mathbf{V}_{\text{MNS}}$ is commonly parameterized as:

$$V_{\text{MNS}}^{\text{T}} m_\nu \mathbf{V}_{\text{MNS}} = \text{diag}(m_1, m_2, m_3)$$

$$\mathbf{V}_{\text{MNS}} = \begin{pmatrix} c_{12}c_{13} & s_{12}c_{13} & s_{13}e^{-i\delta} \\ -c_{23}s_{12} - s_{23}s_{13}c_{12}e^{i\delta} & c_{23}c_{12} - s_{23}s_{13}s_{12}e^{i\delta} & s_{23}c_{13} \\ s_{23}s_{12} - c_{23}s_{13}c_{12}e^{i\delta} & -s_{23}c_{12} - c_{23}s_{13}s_{12}e^{i\delta} & c_{23}c_{13} \end{pmatrix} \times \text{diag}(e^{i\frac{\phi_1}{2}}, e^{i\frac{\phi_2}{2}}, 1)$$

$$\text{with } c_{ij} = \cos\theta_{ij}, s_{ij} = \sin\theta_{ij}. \tag{1.94}$$

θ_{ij} are the mixing angles and $\delta,\ \phi_{1,2} \in [0, 2\pi]$ are the Dirac and Majorana CP-violating phases.

There are three mixing angles describing the mixings between the flavor states; because of the hiererachical nature of the mass splittings and the smallness of the mixing angle θ_{13}, two of these angles correspond to a particular experimental mixing situation. θ_{12} is known as the solar mixing angle θ_{sol}, and dominates the mixing of neutrinos produced in the sun and observed on Earth. θ_{23}, known as the atmospheric mixing angle θ_{atm}, dominates the mixing in the case of "atmospheric" neutrinos, those created in the Earth's atmosphere from cosmic ray interactions. The third mixing angle θ_{13} is very small and may be zero. There is also the CP-violating Dirac phase δ, and two Majorana phases φ_1, φ_2. One may note that a 3×3 complex unitary matrix should be parameterized by $3^2 = 9$ real parameters. The remaining three phases, $\delta_e, \delta_\mu, \delta_\tau$, are unphysical and can be eliminated by field rotations.

In addition to the parameters of the MNS matrix, there are the three masses of the diagonalized neutrino mass matrix, m_1, m_2, m_3. Since the absolute scale of neutrino masses is not

yet known, these are typically expressed as two mass-squared differences,

$$\Delta m^2_{21} \equiv \Delta m^2_{\rm sol} \equiv m_2^2 - m_1^2 \tag{1.95}$$

$$|\Delta m^2_{32}| \equiv \Delta m^2_{\rm atm} \equiv |m_3^2 - m_2^2|. \tag{1.96}$$

A global fit to current data from neutrino oscillation experiments [14] gives the current 3σ bounds on the mixing parameters and the splittings of the eigenvalues of m_ν (in the "standard parametrization" Eq.(1.94)):

$$\begin{aligned}
\sin^2(2\theta_{12}) &= 0.86 \pm 0.04 \\
\sin^2(2\theta_{23}) &> 0.92 \\
\sin^2(2\theta_{13}) &< 0.19 \\
\Delta m^2_{21} &= (8.0 \pm 0.3) \times 10^{-5}\ \ \text{eV}^2 \\
|\Delta m^2_{32}| &= (2.5 \pm 0.6) \times 10^{-3}\ \ \text{eV}^2.
\end{aligned} \tag{1.97}$$

(There are currently no bounds on the Majorana phases φ_1, φ_2, which have no effect on oscillations, nor on the Dirac phase δ.) These provide additional experimental constraints for models to satisfy, and calculating their RG evolution in order to explore the impact of these constraints was a major impetus behind Isajet-M.

$$\begin{aligned}
\sin^2\theta_{12} &= 0.304^{+0.066}_{-0.054}\,, & \Delta m^2_{21} &= (7.65^{+0.69}_{-0.60}) \times 10^{-5}\text{eV}^2, \\
\sin^2\theta_{23} &= 0.50^{+0.17}_{-0.14}\,, & |\Delta m^2_{31}| &= (2.40^{+0.35}_{-0.33}) \times 10^{-3}\text{eV}^2, \\
\sin^2\theta_{13} &< 0.056\,.
\end{aligned} \tag{1.98}$$

1.4.2 Seesaw mechanism

It is an interesting question why neutrino masses are so much smaller (6–11 orders of magnitude) than other fermion masses. An elegant and general solution to the problem is given by the (type-I) *seesaw mechanism*[15]. We assume the existence of three heavy SU(2) gauge

singlet fields N_j along with the ordinary neutrino fields ν_j in the lepton SU(2) doublet L_j, and consider a Lagrangian containing

$$\mathcal{L} \supset -\frac{1}{2}\bar{N}_i \mathbf{M}_{Nij} N_j^{\mathsf{C}} - \mathbf{f}_{\nu ij}^{\mathrm{T}} \epsilon_{ab} \bar{L}_i^a H_u{}^b N_j^{\mathsf{c}} + \text{h.c.} \quad . \tag{1.99}$$

In this Lagrangian, the heavy singlets have a Majorana mass matrix M_{Nij}, with eigenvalues of the order of the *seesaw scale*, $M_{\text{Maj}} \approx 10^{12}$ GeV $\lesssim M_{\text{GUT}}$. This can be generated for example by interactions of the heavy singlets with singlet scalar fields in a GUT. After electroweak symmetry breaking, there will be Dirac mass terms coupling the neutrinos and heavy singlets as well; the Yukawa couplings should presumably be comparable to those of the other fermions.

Now, as the ordinary neutrinos and heavy SU(2) singlets possess identical quantum numbers, they will mix, resulting in an effective mass matrix

$$\begin{pmatrix} 0 & \mathbf{f}_\nu^{\mathrm{T}} v_u \\ \mathbf{f}_\nu v_u & M_N \end{pmatrix},$$

where v_u is the vacuum expectation value of the neutral component h_u^0 of the up-type Higgs doublet H_u. By diagonalizing this 6x6 mass matrix we find the masses of the physical particles. Assuming $\mathbf{f}_\nu v_u \ll M_N$, the heavy ("right-handed") neutrinos will have a mass matrix $M_{\nu_R} \approx \mathbf{M}_N$, while physical light neutrinos have a mass matrix given by the seesaw formula[15],

$$M_\nu(\mu) = -v_u^2 \mathbf{f}_\nu(\mu) \mathbf{M}_N^{-1}(\mu) \mathbf{f}_\nu^{\mathrm{T}}(\mu) \quad . \tag{1.100}$$

The eigenvalues of this matrix will be of order $m_{\text{lepton}}^2 / M_{\text{Maj}}$, which gives neutrino masses in the allowed range for $M_{\text{Maj}} \lesssim M_{\text{GUT}}$ given above. Thus the seesaw mechanism provides a mechanism for naturally generating small neutrino masses. In the context of SUSY, this mechanism has additional attractions: SUSY both stabilizes the seesaw mechanism [16] and ameliorates the hierarchy problem appearing from the presence of the very high scale M_{Maj} [17].

Neutrino masses and mixings have several important impacts on SUSY model-building.

First, of course, they provide additional experimental constraints on models. Second, the existence of nonzero neutrino Yukawas and right-handed singlets can affect model predictions outside the neutrino sector as well, through RGE effects. For example, neutrino RGE effects have been shown to change predicted neutralino relic density by up to several orders of magnitude in some cases[18]. These changes can significantly alter which types of models, and which regions of parameter space, can remain experimentally viable. Such effects, in particular neutrino sector RGE effects on relic density constraints and predicted LFV rates, are the focus of the remainder of this work.

1.5 Notation and Conventions

Putting together all the above, we arrive at our formalism, a generic SUSY GUT augmented with heavy singlets, the right-handed neutrinos $\hat{N}_i^c$. We will outline our setup here; further details and derivations can be found in Ref. [1] whose notation and conventions we follow.

The superpotential is given by

$$\hat{f} = \hat{f}_{MSSM} + (\mathbf{f}_\nu)_{ij}\epsilon_{ab}\hat{L}_i^a\hat{H}_u^b\hat{N}_j^c + \frac{1}{2}(\mathbf{M}_N)_{ij}\hat{N}_i^c\hat{N}_j^c\,, \tag{1.101}$$

where $\hat{L}$ and $\hat{H}_u$ are respectively the lepton doublet and up Higgs superfields, and $\mathbf{M}_N$ is the Majorana mass matrix for the (heavy) right-handed neutrinos. $\hat{N}_i^c$ are the gauge singlet superfields whose fermionic component is the left-handed anti-neutrino and scalar component is $\tilde{\nu}_{Ri}^\dagger$. This choice of RHN superpotential yields a Lagrangian containing the seesaw terms above, so that above the scale M_{Maj} the light neutrino mass matrix is given by the usual seesaw formula Eq. (1.100).

At low energies, however, the heavy singlets decouple, and the theory is governed by the effective superpotential

$$\hat{f}_{\text{eff}} = \hat{f}_{MSSM} + \frac{1}{2}\kappa_{ij}\epsilon_{ab}\hat{L}_i^a\hat{H}_u^b\epsilon_{df}\hat{L}_j^d\hat{H}_u^f\,. \tag{1.102}$$

Here, κ is a 3×3 complex symmetric coupling matrix that breaks lepton number explicitly. Its value is defined by matching conditions at RHN thresholds

$$(\kappa)_{ij}|_{M^-_{N_k}} = (\kappa)_{ij}|_{M^+_{N_k}} + (\mathbf{f}_\nu)_{ik}\frac{1}{M_{N_k}}(\mathbf{f}_\nu^T)_{ik}\Big|_{M^+_{N_k}} \tag{1.103}$$

where $M^+_{N_k}(M^-_{N_k})$ denotes the upper (lower) limit approaching the scale of decoupling of the k-th generation RHN, M_{N_k}. At intermediate scales, with some singlets decoupled and some not, the theory contains both the effective operator κ and the singlet terms from Eq. (1.101) for those singlets not yet decoupled.

$\hat{f}_{MSSM}$ above is the standard MSSM superpotential

$$\hat{f} = \mu \hat{H}^a_u \hat{H}_{da} + \sum_{i,j=1,3}\left[(\mathbf{f}_u)_{ij}\epsilon_{ab}\hat{Q}^a_i \hat{H}^b_u \hat{U}^c_j + (\mathbf{f}_d)_{ij}\hat{Q}^a_i \hat{H}_{da}\hat{D}^c_j + (\mathbf{f}_e)_{ij}\hat{L}^a_i \hat{H}_{da}\hat{E}^c_j\right], \tag{1.104}$$

where $a,\ b$ are $SU(2)_L$ doublet indices, i, j are generation indices, ϵ_{ab} is the totally antisymmetric tensor with $\epsilon_{12} = 1$, and the superscript c denotes charge conjugation.

The soft SUSY breaking part of the Lagrangian can be written as

$$\mathcal{L} = \mathcal{L}_{MSSM} - \tilde{\nu}^\dagger_{Ri}(\mathbf{m}^2_{\tilde{\nu}_R})_{ij}\tilde{\nu}_{Rj} + \left[(\mathbf{a}_\nu)_{ij}\epsilon_{ab}\tilde{L}^a_i \tilde{H}^b_u \tilde{\nu}^\dagger_{Rj} + \frac{1}{2}(\mathbf{b}_\nu)_{ij}\tilde{\nu}_{Ri}\tilde{\nu}_{Rj} + \text{h.c.}\right], \tag{1.105}$$

where the MSSM soft SUSY-breaking Lagrangian $\mathcal{L}_{MSSM}$ is given by

$$\begin{aligned}
\mathcal{L}_{\text{soft}} \;=\; & -\Big[\tilde{Q}^\dagger_i(\mathbf{m}^{\mathbf{2}}_{\mathbf{Q}})_{ij}\tilde{Q}_j + \tilde{d}^\dagger_{Ri}(\mathbf{m}^{\mathbf{2}}_{\mathbf{D}})_{ij}\tilde{d}_{Rj} + \tilde{u}^\dagger_{Ri}(\mathbf{m}^{\mathbf{2}}_{\mathbf{U}})_{ij}\tilde{u}_{Rj} \\
& + \tilde{L}^\dagger_i(\mathbf{m}^{\mathbf{2}}_{\mathbf{L}})_{ij}\tilde{L}_j + \tilde{e}^\dagger_{Ri}(\mathbf{m}^{\mathbf{2}}_{\mathbf{E}})_{ij}\tilde{e}_{Rj} + m^2_{H_u}|H_u|^2 + m^2_{H_d}|H_d|^2\Big] \\
& -\frac{1}{2}\left[M_1\bar{\lambda}_0\lambda_0 + M_2\bar{\lambda}_A\lambda_A + M_3\bar{\tilde{g}}_B\tilde{g}_B\right] \\
& + \Big[(\mathbf{a_u})_{ij}\epsilon_{ab}\tilde{Q}^a_i H^b_u \tilde{u}^\dagger_{Rj} + (\mathbf{a_d})_{ij}\tilde{Q}^a_i H_{da}\tilde{d}^\dagger_{Rj} + (\mathbf{a_e})_{ij}\tilde{L}^a_i H_{da}\tilde{e}^\dagger_{Rj} + \text{h.c.}\Big] \\
& + \left[bH^a_u H_{da} + \text{h.c.}\right].
\end{aligned} \tag{1.106}$$

The eigenvalues of matrices $\mathbf{a}_\nu$ and $\mathbf{b}_\nu$ as well as the square roots of the eigenvalues of $\mathbf{m}^2_{\tilde{\nu}_R}$ are all assumed to be of the order of the weak scale M_{weak}. The gaugino fields $\tilde{g}_B$ $(B =$

$1\ldots8)$, λ_A $(A=1\ldots3)$, and λ_0 transform according to the adjoint representations of $SU(3)_c$, $SU(2)_L$, and $U(1)_Y$ respectively.

We use the RL convention for the fermion mass term, $\mathcal{L}_{mass} = -(\bar{\psi}^i_R m_{ij} \psi^j_L + \text{h.c.})$, in which lepton and quark physical (*i.e.*, real diagonal) mass matrices read

$$\mathbf{m}_u = v_u \mathbf{V_{u_R}} \mathbf{f}_u^T \mathbf{V}^\dagger_{\mathbf{u_L}}, \qquad \mathbf{m}_d = v_d \mathbf{V_{d_R}} \mathbf{f}_d^T \mathbf{V}^\dagger_{\mathbf{d_L}}, \qquad \mathbf{m}_e = v_d \mathbf{V_{e_R}} \mathbf{f}_e^T \mathbf{V}^\dagger_{\mathbf{e_L}}, \tag{1.107}$$

where v_u, v_d are up- and down-higgs VEVs, $v = \sqrt{v_u^2 + v_d^2} \simeq 174$ GeV. Unitary rotation matrices $\mathbf{V^u_L}$, $\mathbf{V^u_R}$, $\mathbf{V^d_R}$ transform gauge eigenstates (unprimed) to mass eigenstates (primed) as

$$\begin{aligned}
u'_{Li} &= (\mathbf{V_{u_L}})_{ij}\, u_{Lj}\,, & u'_{Ri} &= (\mathbf{V_{u_R}})_{ij}\, u_{Rj}\,, \\
d'_{Li} &= (\mathbf{V_{d_L}})_{ij}\, d_{Lj}\,, & d'_{Ri} &= (\mathbf{V_{d_R}})_{ij}\, d_{Rj}\,, \\
e'_{Li} &= (\mathbf{V_{e_L}})_{ij}\, e_{Lj}\,, & e'_{Ri} &= (\mathbf{V_{e_R}})_{ij}\, e_{Rj}\,.
\end{aligned} \tag{1.108}$$

The Cabibo-Kobayashi-Maskawa matrix is $\mathbf{V}_{CKM} = \mathbf{V_{u_L}} \mathbf{V}^\dagger_{\mathbf{d_L}}$. Due to different matrix diagonalization conventions, our rotation matrices $\mathbf{V_\bullet}$ are hermitian conjugates of those in Refs. [19, 20].

We work in the Super-CKM (SCKM) basis [21] where gluino vertices remain diagonal. Here, the diagonalization of sfermion mass matrices proceed in two steps. First, the squarks and sleptons are rotated "in parallel" to their fermionic superpartners

$$\begin{aligned}
\tilde{u}'_{Li} &= (\mathbf{V_{u_L}})_{ij}\, \tilde{u}_{Lj}\,, & \tilde{u}'_{Ri} &= (\mathbf{V_{u_R}})_{ij}\, \tilde{u}_{Rj}\,, \\
\tilde{d}'_{Li} &= (\mathbf{V_{d_L}})_{ij}\, \tilde{d}_{Lj}\,, & \tilde{d}'_{Ri} &= (\mathbf{V_{d_R}})_{ij}\, \tilde{d}_{Rj}\,, \\
\tilde{e}'_{Li} &= (\mathbf{V_{e_L}})_{ij}\, \tilde{e}_{Lj}\,, & \tilde{e}'_{Ri} &= (\mathbf{V_{e_R}})_{ij}\, \tilde{e}_{Rj}\,, \\
\tilde{\nu}'_{Li} &= (\mathbf{V_{e_L}})_{ij}\, \tilde{\nu}_{Lj}\,.
\end{aligned} \tag{1.109}$$

where the SCKM scalar fields (primed) form supermultiplets with corresponding fermion mass

eigenstates, *i.e.* the SCKM basis preserves the superfield structure after diagonalization of the fermions. Next, for all sfermions save the sneutrino, 6×6 sfermion mass squared matrices in the SCKM basis are constructed:

$$\begin{aligned}
\mathcal{M}^{\mathbf{2}}_{\tilde{\mathbf{u}}} &= \begin{pmatrix} \mathbf{M}^2_{\tilde{u}LL} + \mathbf{m}^2_u + D(\tilde{u}_L)\mathbb{1} & -\mathbf{M}^2_{\tilde{u}LR} + \mu \cot\beta\, \mathbf{m}_u \\ -\mathbf{M}^{2\dagger}_{\tilde{u}LR} + \mu^* \cot\beta\, \mathbf{m}_u & \mathbf{M}^2_{\tilde{u}RR} + \mathbf{m}^2_u + D(\tilde{u}_R)\mathbb{1} \end{pmatrix}, \\
\mathcal{M}^2_{\tilde{d}} &= \begin{pmatrix} \mathbf{M}^2_{\tilde{d}LL} + \mathbf{m}^2_d + D(\tilde{d}_L)\mathbb{1} & -\mathbf{M}^2_{\tilde{d}LR} + \mu \tan\beta\, \mathbf{m}_d \\ -\mathbf{M}^{2\dagger}_{\tilde{d}LR} + \mu^* \tan\beta\, \mathbf{m}_d & \mathbf{M}^2_{\tilde{d}RR} + \mathbf{m}^2_d + D(\tilde{d}_R)\mathbb{1} \end{pmatrix}, \\
\mathcal{M}^2_{\tilde{e}} &= \begin{pmatrix} \mathbf{M}^2_{\tilde{e}LL} + \mathbf{m}^2_e + D(\tilde{e}_L)\mathbb{1} & -\mathbf{M}^2_{\tilde{e}LR} + \mu \tan\beta\, \mathbf{m}_e \\ -\mathbf{M}^{2\dagger}_{\tilde{e}LR} + \mu^* \tan\beta\, \mathbf{m}_e & \mathbf{M}^2_{\tilde{e}RR} + \mathbf{m}^2_e + D(\tilde{d}_R)\mathbb{1} \end{pmatrix},
\end{aligned} \tag{1.110}$$

where the $D(\tilde{f})$ stand for hypercharge $D-$term contributions to corresponding sfermions, $\mathbb{1}$ is the 3×3 unit matrix, $\mathbf{m}_f$ are diagonal fermion mass matrices given in Eq.(1.109), and the flavor-changing entries are contained in rotated SSB matrices

$$\begin{aligned}
\mathbf{M}^2_{\tilde{u}LL} &= \mathbf{V}_{\mathbf{u_L}} \mathbf{m}^{\mathbf{2}}_{\mathbf{Q}} \mathbf{V}^\dagger_{\mathbf{u_L}} & \mathbf{M}^2_{\tilde{u}RR} &= \mathbf{V}_{\mathbf{u_R}} \mathbf{m}^{\mathbf{2}}_{\mathbf{U}} \mathbf{V}^\dagger_{\mathbf{u_R}} & \mathbf{M}^2_{\tilde{u}LR} &= \mathbf{V}_{\mathbf{u_L}} \mathbf{a}^*_{\mathbf{u}} \mathbf{V}^\dagger_{\mathbf{u_R}} \\
\mathbf{M}^2_{\tilde{d}LL} &= \mathbf{V}_{\mathbf{d_L}} \mathbf{m}^{\mathbf{2}}_{\mathbf{Q}} \mathbf{V}^\dagger_{\mathbf{d_L}} & \mathbf{M}^2_{\tilde{d}RR} &= \mathbf{V}_{\mathbf{d_R}} \mathbf{m}^{\mathbf{2}}_{\mathbf{D}} \mathbf{V}^\dagger_{\mathbf{d_R}} & \mathbf{M}^2_{\tilde{d}LR} &= \mathbf{V}_{\mathbf{d_L}} \mathbf{a}^*_{\mathbf{d}} \mathbf{V}^\dagger_{\mathbf{d_R}} \\
\mathbf{M}^2_{\tilde{e}LL} &= \mathbf{V}_{\mathbf{e_L}} \mathbf{m}^{\mathbf{2}}_{\mathbf{L}} \mathbf{V}^\dagger_{\mathbf{e_L}} & \mathbf{M}^2_{\tilde{e}RR} &= \mathbf{V}_{\mathbf{e_R}} \mathbf{m}^{\mathbf{2}}_{\mathbf{E}} \mathbf{V}^\dagger_{\mathbf{e_R}} & \mathbf{M}^2_{\tilde{e}LR} &= \mathbf{V}_{\mathbf{e_L}} \mathbf{a}^*_{\mathbf{e}} \mathbf{V}^\dagger_{\mathbf{e_R}}.
\end{aligned} \tag{1.111}$$

Note that the squark doublet mass-squared SSB matrix $\mathbf{m}^{\mathbf{2}}_{\mathbf{Q}}$ is rotated differently for $\mathcal{M}^2_{\tilde{u}}$ and $\mathcal{M}^2_{\tilde{d}}$. Finally, the mass squared matrices (1.110) are diagonalized to obtain sfermion mass eigenstates. These mass eigenstates are labelled in ascending mass order.

The sneutrinos are handled similarly. In the MSSM itself, the absence of right-handed neutrinos means that the sneutrino mass-squared matrix is only a 3×3 matrix of the form

$$\mathcal{M}^2_{\tilde{\nu}} = \mathbf{V}_{\mathbf{e_L}} \mathbf{m}^{\mathbf{2}}_{\mathbf{L}} \mathbf{V}^\dagger_{\mathbf{e_L}} + D(\tilde{\nu}_L)\mathbb{1}. \tag{1.112}$$

However, the addition of the $\hat{N}^c_i$ superfields leads to an expansion of the sneutrino mass-

squared matrix; it becomes a 12×12 matrix, so that the relevant part of Lagrangian is

$$\mathcal{L} \ni -\frac{1}{2}\tilde{n}^\dagger \begin{pmatrix} \boldsymbol{\mathcal{M}}^2_{L^\dagger L} & \mathbf{0} & \boldsymbol{\mathcal{M}}^2_{L^\dagger R} & v_u \mathbf{f}^*_\nu \mathbf{M}^T_{\mathbf{N}} \\ \mathbf{0} & (\boldsymbol{\mathcal{M}}^2_{L^\dagger L})^T & v_u \mathbf{f}_\nu \mathbf{M}^\dagger_{\mathbf{N}} & (\boldsymbol{\mathcal{M}}^2_{L^\dagger R})^* \\ (\boldsymbol{\mathcal{M}}^2_{L^\dagger R})^\dagger & v_u \mathbf{M}_{\mathbf{N}} \mathbf{f}^\dagger_\nu & \boldsymbol{\mathcal{M}}^2_{R^\dagger R} & -\mathbf{b}^\dagger_\nu \\ v_u \mathbf{M}^*_{\mathbf{N}} \mathbf{f}^T_\nu & (\boldsymbol{\mathcal{M}}^2_{L^\dagger R})^T & -\mathbf{b}_\nu & (\boldsymbol{\mathcal{M}}^2_{R^\dagger R})^T \end{pmatrix} \tilde{n} \tag{1.113}$$

where $\tilde{n}^T \equiv (\tilde{\nu}^T_L, \tilde{\nu}^\dagger_L, \tilde{\nu}^T_R, \tilde{\nu}^\dagger_R)$, $\mathbf{0}$ is the 3×3 null matrix and

$$\begin{aligned} \boldsymbol{\mathcal{M}}^2_{L^\dagger L} &= \mathbf{m}^{\mathbf{2}}_{\mathbf{L}} + v_u^2 \mathbf{f}^*_\nu \mathbf{f}^T_\nu + D(\tilde{\nu}_L)\mathbb{1} \\ \boldsymbol{\mathcal{M}}^2_{R^\dagger R} &= \mathbf{m}^2_{\tilde{\nu}_R} + v_u^2 \mathbf{f}^T_\nu \mathbf{f}^*_\nu + \mathbf{M}_{\mathbf{N}} \mathbf{M}^\dagger_{\mathbf{N}} \\ \boldsymbol{\mathcal{M}}^2_{L^\dagger R} &= -v_u \mathbf{a}^*_\nu + \mu v_d \mathbf{f}^*_\nu \end{aligned} \tag{1.114}$$

From this structure we see that there is sneutrino-antisneutrino mixing for right-handed states introduced by $\mathbf{b}_\nu$ with no corresponding terms in the left-handed sector. The Majorana mass matrix $\mathbf{M}_{\mathbf{N}}$ contributes to the mass of the right-handed states and also results in the mixing of right-handed anti-sneutrino states with left-handed sneutrinos. Since $\mathbf{M}_{\mathbf{N}}$ eigenvalues are much heavier than the rest of SSB parameters the matrix exhibits a seesaw type behavior, similar to the one for neutrinos: the 6×6 L-L block is of $\mathcal{O}(M^2_{\text{weak}})$, while R-L blocks are of $\mathcal{O}(M_{\text{weak}} M_{\text{Maj}})$ and the R-R block is $\mathcal{O}(M^2_{\text{Maj}})$. Therefore the right-handed sneutrinos decouple and the phenomenologically relevant left-handed sneutrinos have a mass-squared matrix of the familiar MSSM form (1.112). Diagonalization of this matrix then yields the sneutrino mass eigenstates, just as with the other sfermions.

In the neutrino sector, the neutrino Yukawa and Majorana mass matrices are diagonalized in analogy with Eq.(1.109) by unitary matrices $\mathbf{V}_{\nu_{\mathbf{L}}}, \mathbf{V}_{\nu_{\mathbf{R}}}, \mathbf{V}_{\mathbf{N}}$ according to

$$\boldsymbol{m}_D = v_u \mathbf{V}_{\nu_{\mathbf{R}}} \mathbf{f}^T_\nu \mathbf{V}^\dagger_{\nu_{\mathbf{L}}}, \qquad \mathbf{V}_{\mathbf{N}} \mathbf{M}_{\mathbf{N}} \mathbf{V}^T_{\mathbf{N}} = \text{diag}(M_{N_1}, M_{N_2}, M_{N_3}), \tag{1.115}$$

where $\boldsymbol{m}_D$ is the Dirac neutrino mass matrix.

After electroweak symmetry breaking, the Majorana mass matrix $\mathcal{M}_\nu$ for the light left-handed neutrinos is generated either by the seesaw formula, Eq. (1.100), above the RHN decoupling scales; or, below the RHN decoupling scales, by the effective mass operator κ:

$$\mathcal{M}_\nu = \begin{cases} -\mathbf{f}_\nu \mathbf{M}_N^{-1} \mathbf{f}_\nu^T v_u^2 & \text{above } M_{Ni}, \\ -\kappa v_u^2 & \text{below } M_{Ni}\,, \end{cases} \tag{1.116}$$

where v_u is the vacuum expectation value of the neutral component h_u^0 of the up-type Higgs doublet H_u. At intermediate scales, where both κ and non-decoupled singlets exist, the mass matrix is given by the combination of both these terms.

This symmetric 3×3 matrix, $\mathcal{M}_\nu$, is diagonalized as

$$\mathbf{U}_\nu \mathcal{M}_\nu \mathbf{U}_\nu^{\mathrm{T}} = \mathbf{m}_\nu \equiv \mathrm{diag}(m_1, m_2, m_3), \tag{1.117}$$

where $\mathbf{U}_\nu$ is a unitary matrix, and m_i are the physical neutrino masses. In labeling the (real non-negative) mass eigenstates we follow the usual conventions that 1 and 2 denote states with the smallest mass-squared difference and that $m_1 < m_2$.

Then the Maki-Nakagava-Sakata mixing matrix of physical neutrinos [22] is $\mathbf{V}_{MNS} = \mathbf{V}_{\mathbf{e_L}} \mathbf{U}_\nu^\dagger$. Note that because of the seesaw mechanism, this is different from the neutrino Yukawa diagonalization matrix $\mathbf{V}_{\nu_\mathbf{L}}$ defined in Eq. (1.115). We use the usual parameterization of $\mathbf{V}_{\text{MNS}}$ given above in Eq. (1.94),

$$\mathbf{V}_{\text{MNS}} = \begin{pmatrix} c_{12}c_{13} & s_{12}c_{13} & s_{13}e^{-i\delta} \\ -c_{23}s_{12} - s_{23}s_{13}c_{12}e^{i\delta} & c_{23}c_{12} - s_{23}s_{13}s_{12}e^{i\delta} & s_{23}c_{13} \\ s_{23}s_{12} - c_{23}s_{13}c_{12}e^{i\delta} & -s_{23}c_{12} - c_{23}s_{13}s_{12}e^{i\delta} & c_{23}c_{13} \end{pmatrix} \times \mathrm{diag}(e^{i\frac{\phi_1}{2}}, e^{i\frac{\phi_2}{2}}, 1).$$

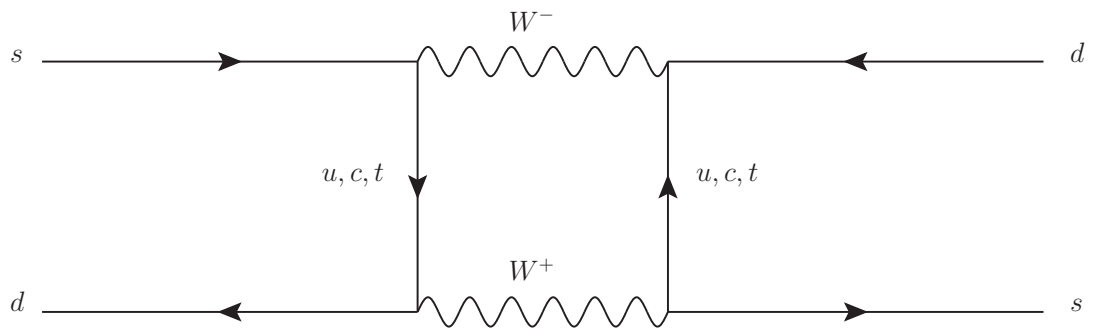

Figure 1.2: A SM box diagram contributing to the $K_L - K_S$ mass difference.

1.6 Flavor violation

1.6.1 Quark sector flavor-violation

Although flavor is not exactly conserved in the Standard Model, flavor-violating processes are strictly limited. Flavor symmetry is respected by all forces save the weak force. Within the quark sector, flavor violation stems from off-diagonal elements in the CKM matrix [23] relating quark mass eigenstates to their weak-interaction (flavor) eigenstates. However, not only does the CKM matrix have a hierarchical form with off-diagonal elements much smaller than diagonal ones, the GIM mechanism [24] operates to highly suppress flavor-changing neutral current (FCNC) processes. While FCNC processes do occur, they do so at very low rates because of GIM cancellations. For example, the neutral kaon mass difference $K_L - K_S$, which arises via box diagrams such as Fig. (1.2), is suppressed by a factor $\sim (m_c^2 - m_u^2)/m_W^2 \sim 10^-4$.

This suggests a potentially fruitful approach for constraining new physics models such as the MSSM. Such models will often introduce additional contributions to FCNC processes; without some analogous mechanism to suppress them, we might naturally suspect that these contributions may tend to be large compared to the SM contributions and hence exceed experimental bounds. This is indeed the case in the MSSM. For example, in the case of the $K_L - K_S$ mass splitting, the dominant additional contributions arise from box diagrams involving squarks and gluinos, such as the one in Fig. (1.3), as well as from chargino and neutralino loops. The mass

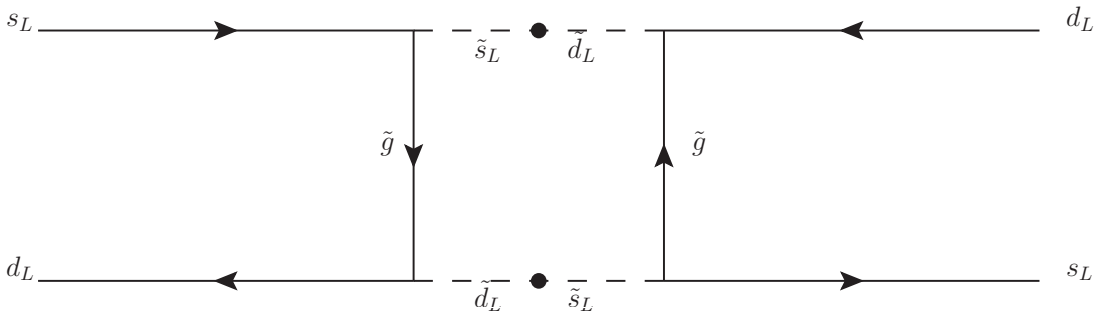

Figure 1.3: An MSSM diagram contributing to the $K_L - K_S$ mass difference.

insertion shown is proportional to an off-diagonal element in the squark mass matrix,

$$\tilde{d}_L^\dagger (\mathbf{m}_Q^2)_{12} \tilde{s}_L. \tag{1.118}$$

Generically we would expect this element to be comparable to the diagonal entries in the squark mass matrix, which in order to solve the hierarchy problem will be on the order of $100 - 1000$ GeV. But this leads to a contribution greatly exceeding experimental bounds.

This is an example of the *SUSY flavor problem.* It arises in this case because of the impact of additional weakly-interacting particles with significant masses, the squarks, which need not be diagonal in the same basis as the quarks. Flavor problems arise from the trilinear couplings as well, as these will generate flavor-mixing mass terms after electroweak symmetry breaking, e.g.,

$$\mathcal{L} \ni (\mathbf{a_d})_{ij} \tilde{Q}_i^a H_{da} \tilde{d}_{Rj}^\dagger \tag{1.119}$$

includes terms such as $(\mathbf{a_d})_{12} v_d \, \tilde{d}_L \, \tilde{s}_R^\dagger$, which contribute to the kaon mass splitting shown in Fig. 1.3.

Several possible solutions to the SUSY flavor problem in the quark sector immediately suggest themselves:

Alignment

A simple solution is to arrange the squark and quark mass matrices so that they *can* be diagonalized by the same transformation. They are then said to be “aligned”, and the

flavor problem obviously does not exist. Note that the effective mass terms generated by the trilinear couplings must either be aligned as well, or else these terms must be sufficiently small to avoid disturbing the alignment.

Irrelevancy

As with any loop diagram, the contribution from Fig. 1.3 is suppressed by the propagators of the heavy particles in the loop. If the masses of the sparticles (squarks for Fig. 1.3) are large enough, they will be suppressed at low energies enough so that their contributions to SM processes will be below the experimental bounds. Masses of ~ 40 TeV are generally necessary given the current bounds[1].

Universality

Alternatively, we can eliminate the flavor problem by assuming that the masses of the squarks are *universal* in flavor – that the squarks of the same flavor are (approximately) degenerate with one another. A detailed calculation shows that contributions such as those from Fig. (1.3) to Δm_K are proportional to sums like

$$\sum_{\alpha,\beta=\tilde{d}_L,\tilde{s}_L,\tilde{b}_L} (U\tilde{U}^\dagger)_{i\alpha}(U\tilde{U}^\dagger)^*_{j\alpha}(U\tilde{U}^\dagger)_{i\beta}(U\tilde{U}^\dagger)^*_{j\beta} f(m^2_\alpha, m^2_\beta). \tag{1.120}$$

If $m^2_\alpha \approx m^2_\beta$, unitarity causes the terms to cancel. This can be easily understood if we view the process in terms of oscillations of squarks. Squark flavor changing vertices, such as the $\tilde{d}_L$-$\tilde{s}_L$ vertices in Figure 1.3, correspond to a squark being produced in a flavor eigenstate, then oscillating not and interacting as a different flavor. Such oscillation occurs, just as in the case of neutrinos, because the squark flavor eigenstates correspond to mixtures of different mass eigenstates, which each propagate with their own wavelengths. If, though, the squark mass eigenstates all have identical masses, they will remain in-phase as they propagate, and no oscillation and flavor changee can occur.

A common solution to the SUSY flavor problem is to assume that at some scale (often the GUT scale) the sfermion SSB mass-squared matrices are diagonal and universal in flavor, and

the trilinear couplings are proportional to their corresponding fermion Yukawa couplings. It is essentially a combination of the alignment and universality solutions above, where the explicit SSB masses are chosen to be universal and the induced mass terms from the trilinear couplings to be aligned. This type of solution arises in many SUSY GUTs, and is the approach we adopt here.

In our framework of mSUGRA extended by right-handed neutrinos (mSUGRA-seesaw) these SSB boundary conditions at Grand Unification Scale M_{GUT} take a particularly simple form:

$$\begin{aligned} \mathbf{m^2_{Q,U,D,L,E,\tilde{\nu}_R}} &= m_0^2 \mathbb{1} \\ m^2_{H_u} = m^2_{H_d} &= m_0^2 \\ \mathbf{a}_{u,d,e,\nu} &= -A_0 \mathbf{f}_{u,d,e,\nu} \end{aligned} \tag{1.121}$$

1.6.2 Lepton flavor-violation

Flavor-violation in the lepton sector is especially interesting for constraining new physics processes. Lepton flavor-violating (LFV) processes do exist in the SM with massive neutrinos, since neutrinos mix. Such processes occur via diagrams with flavor-changing mass insertions in propagating neutrinos. These diagrams, however, will be proportional to powers of m_ν/m_W. Because of the smallness of neutrino masses, this leads to extremely tiny cross-sections and branching ratios for LFV processes (other than neutrino oscillations!) in the SM[25], generally far below present experimental sensitivities. On the other hand, just as in the case of quark sector FCNCs, relatively high rates for such processes can be generated through slepton loops in the MSSM with generic SSB mass matrices.

Since they effectively lack SM backgrounds, measurements of LFV processes are therefore of great phenomological interest as experimental probes for new physics effects, and provide a powerful source of constraints on SUSY models. Our work centers on these constraints, and how they are affected by the interplay between neutrino RG effects and dark matter relic-density

	Present	Future
BR($\mu \to e\gamma$)	1.2×10^{-11} [26]	10^{-13} [33]
BR($\tau \to \mu\gamma$)	4.5×10^{-8} [27]	10^{-9} [34]
BR($\tau \to e\gamma$)	1.1×10^{-7} [28]	10^{-9} [34]
BR($\mu \to eee$)	1.0×10^{-12} [29]	10^{-14} [35]
BR($\tau \to \mu\mu\mu$)	3.2×10^{-8} [30]	10^{-9} [34]
BR($\tau \to eee$)	3.6×10^{-8} [30]	10^{-9} [34]
CR(μ Ti $\to e$ Ti)	4.3×10^{-12} [31]	10^{-18} [36]
CR(μ Al $\to e$ Al)	-	10^{-16} [32]

Table 1.3: Present bounds and projected sensitivities for LFV processes.

constraints. The current bounds on the LFV processes we use, $l_i \to l_j\gamma$, $l_i \to 3l_j$m and $l_i \to l_j$ conversion in nuclei, along with projected sensitivities of future experiments, are summarized in Table 1.3.

1.6.3 LFV rates in SUSY-seesaw models

Our GUT-scale SSB boundary conditions (Eq. (1.121)) suppress both lepton and problematic quark-sector flavor violation, as discussed above. However, these boundary conditions apply at the GUT-scale, while the experimentally-constrained LFV processes we are interested in occur at low energies (i.e. the weak-scale.) Effects arising from renormalization group evolution must therefore be considered. Since $\mathbf{f}_e$ and $\mathbf{f}_\nu$ cannot be simultaneously diagonalized, RGE evolution will generate non-vanishing off-diagonal entries in the left-handed slepton mass matrix $\boldsymbol{m}_L^2$. With our universal boundary conditions, the off-diagonal elements in the leading-logarithmic approximation are

$$(\mathbf{m}_L^2)_{i\neq j} \simeq -\frac{1}{8\pi^2}(3m_0^2 + A_0)\sum_k (\mathbf{f}_\nu^T)_{ik}(\mathbf{f}_\nu^*)_{kj}\log\frac{M_{GUT}}{M_{N_k}} \tag{1.122}$$

where M_{N_k} are the scales of right-handed neutrino decoupling, which will be approximately equal to eigenvalues of the Majorana mass matrix $\mathbf{M}_N$.

These off-diagonal terms break lepton-sector universality and will induce low-energy LFV processes such as $l_i \to l_j\gamma$, $l_i \to 3l_j$ and $l_i \to l_j$ conversion in nuclei. We will examine each of

these processes in turn.

$l_i \to l_j \gamma$

The branching ratio for the flavor-violating radiative decay of a charged lepton is given by

$$BR(l_i \to l_j \gamma) = \frac{\alpha}{4\Gamma(l_i)} m_{l_i}^5 (|A_L|^2 + |A_R|^2) \tag{1.123}$$

Here α is the electromagnetic coupling constant, $\Gamma(l_i)$ is the total decay width of the initial lepton, and $A_{L,R}$ are form factors for left and right chiralities of the incoming lepton whose full expressions in SUSY were obtained in Ref. [37]. Because $m_{l_i} \gg m_{l_j}$ one has $A_R \gg A_L$ in the case of initial universality such as (1.121) [38, 39]. In the mass-insertion approximation, the branching ratio can be related to the corresponding off-diagonal element of the left-handed slepton mass matrix [38]

$$BR(l_i \to l_j \gamma) \simeq BR(l_i \to l_j \bar{\nu}_j \nu_i) \frac{\alpha^3}{G_F^2 m_s^8} \left| (\boldsymbol{m}_L^2)_{i \neq j} \right|^2 \tan^2 \beta \tag{1.124}$$

where G_F is the Fermi coupling constant and m_s is the characteristic mass scale of the SUSY particles in the loop. In the case of universal boundary conditions (1.121), this expression used in conjunction with the leading-log result (1.122) well approximates the full expression (1.123), if one sets [40]

$$m_s^8 \simeq 0.5 m_0^2 m_{1/2}^2 \left(m_0^2 + 0.6 m_{1/2}^2 \right)^2 \tag{1.125}$$

$l_i \to 3 l_j$

LFV $l_i \to 3l_j$ decays and $l_i \to l_j$ conversion occur via γ-, $Z-$ and Higgs-penguins as well as squark/slepton box diagrams [37]. Higgs-penguins dominate in the regime of large $\tan\beta \simeq 60$ and light H/A Higgs boson mass ~ 100 GeV, and enhance rates by up to a few orders of magnitude [41]. However, the latter condition cannot be realized in the universal scenario (1.121) [42]. It was shown in Ref. [43] that these LFV rates are well described in

the universal scanario by the same γ-penguins that contribute to the radiative decays. The branching ratio for trilepton decays is approximately given by

$$BR(l_i \to 3l_j) \simeq \frac{\alpha}{3\pi}\left(\log\frac{m_{l_i}^2}{m_{l_j}^2} - \frac{11}{4}\right) BR(l_i \to l_j\gamma) \tag{1.126}$$

$l_i \to l_j$ conversion

For $\mu \to e$ conversion a similar relation holds

$$CR(\mu\mathrm{N} \to e\mathrm{N}) \equiv \frac{\Gamma(\mu\mathrm{N} \to e\mathrm{N})}{\Gamma_{capt}} = \frac{16\alpha^4 Z}{\Gamma_{capt}} Z_{eff}^4 \left|F(q^2)\right|^2 BR(\mu \to e\gamma) \tag{1.127}$$

where Z is the proton number of the nucleus N, Z_{eff} is an effective atomic charge obtained by averaging the muon wave function over the nuclear density [44], $F(q^2)$ denotes the nuclear form factor at momentum transfer q [45] and Γ_{capt} is the measured total muon capture rate [46]. In this work we consider two target materials that will be used by future experiments. For $^{48}_{22}$Ti, which will be used by PRIME experiment at J-PARC [36], $Z_{eff} = 17.6$, $F(q^2 \simeq -m_\mu^2) \simeq 0.54$ and $\Gamma_{capt} = 2.590 \times 10^6\mathrm{sec}^{-1}$. For $^{27}_{13}$Al, the target material for the proposed Mu2e experiment at Fermilab [32], $Z_{eff} = 11.48$, $F(q^2 \simeq -m_\mu^2) \simeq 0.64$ and $\Gamma_{capt} = 7.054 \times 10^5\mathrm{sec}^{-1}$.

Chapter 2

SUSY dark matter constraints and LFV rates

As we have seen above, the simplest solution to the SUSY flavor problem is to assume SUSY breaking is mediated by a flavor-blind mechanism, which would generate flavor-universal SSB terms at some high scale. However, this does not mean that the SSB terms remain flavor-universal at the weak scale: flavor-violating terms are still be generated from Yukawa couplings during evolution from the high to the weak scale. As a consequence, there will be SUSY contributions to LFV processes suppressed by the characteristic mass scale of the SUSY particles $M_{SUSY} \sim 1$ TeV, which can be at an observable level. Many authors have studied these processes under various assumptions for SUSY models and seesaw parameters (see for example [47, 49, 50, 37, 38, 43, 40, 41, 39, 51]).

The prediction of LFV rates requires knowledge of the neutrino Yukawa coupling matrix. However, experimentally measured light neutrino masses and mixings do not provide sufficient information to determine it [39]. To address this difficulty, a top-down approach is frequently adopted in which the neutrino Yukawa matrix is set by a specific SUSY GUT model, with an $SO(10)$ gauge group being the favorite choice. Here the seesaw mechanism is often naturally present and the neutrino Yukawa coupling matrix is related to the up-quark one. The exact value of the Yukawa unification parameter $R_{\nu u}$ (defined in Eqs. (2.6,2.9) below) varies depending on the model. We take a general approach here, and consider two extreme cases of Yukawa unification parameters inspired by $SO(10)$ relations. For both of these cases we study two scenarios with small and large mixings in the neutrino Yukawa matrix.

Point	m_0	$m_{1/2}$	A_0	$\tan\beta$	Region
A	80	170	-250	10	bulk
B	100	500	0	10	$\tilde{\tau}$-coan.
C	150	300	-1095	5	$\tilde{t}$-coan.
D	500	450	0	51	A-funnel
E	1370	300	0	10	HB/FP
F	3143	1000	0	10	HB/FP
G	2000	130	-2000	10	h-funnel

Table 2.1: Input parameters for benchmark points and corresponding DM-allowed regions of mSUGRA. The dimensionful parameters m_0, $m_{1/2}$ and A_0 are in GeV units. For all points $\mu > 0$ and $m_t = 171$ GeV.

The existence of a massive, electrically and color neutral, stable weakly interacting particle that can serve as a Cold Dark Matter (CDM) candidate is perhaps the most compelling feature of the $R-$parity conserving MSSM. In most cases the CDM particle is the lightest neutralino, $\widetilde{Z}_1$ [52]. The mass density of CDM has been precisely determined by modern cosmological measurements: a combination of WMAP CMB data with the baryon acoustic oscillations in galaxy power spectra gives [53]

$$\Omega_{CDM}h^2 = 0.1120^{+0.0074}_{-0.0076} \qquad (2\sigma)\ , \tag{2.1}$$

where $\Omega \equiv \rho/\rho_c$ with ρ_c the critical mass density of the universe, and h the scaled Hubble parameter. Such a precise determination places severe constraints on new physics scenarios. In the simplest SUSY model with universal SSB values at high scale, mSUGRA (or CMSSM) [54], only a few regions of parameter space survive: the bulk region [55, 56], the stau [57, 71] or stop [58] coannihilation regions, the hyperbolic branch/focus point (HB/FP) region [59], and the A or h resonance annihilation (Higgs funnel) regions [56, 60, 61]. The benchmark values of the mSUGRA input parameters for these regions are listed in Table 2.1. We take these benchmark values as the starting points for our analysis of each region.

The inclusion of RHNs and their associated Yukawa couplings changes the predictions for some sparticle masses by introducing new contributions to the renormalization group equations. These imprints can be used to extract neutrino Yukawa couplings in collider experiments [62].

Previous work [18] by collaborators demonstrated that these neutrino-induced changes in the SUSY mass spectrum can significantly alter the Dark Matter (DM) (co)annihilation mechanisms with concomitant changes in $\Omega_{\widetilde{Z}_1}h^2$ and DM direct and indirect detection rates.

Our aim in this work was to study predictions for LFV rates, while correctly taking into account the aforementioned effect on neutralino relic density. We take a model-independent approach and only consider effects from RGE running below the unification scale M_{GUT}. These two important points distinguish this work from previous studies[63].

We find that proper consideration of the interplay between the neutrino and SUSY sectors can change the predictions for the LFV rates in WMAP-allowed regions by a factor up to about 5 compared with naive estimates. We performed a similar study for the case of the neutrino-up quark unification parameter equal to three. This case naturally appears in GUT models but is somewhat obscured by model builders. We find here that, contrary to common belief, such large neutrino Yukawa couplings are *not* ruled out by current LFV bounds. Moreover, the LFV rates are an order of magnitude smaller than in the commonly used case of a unification parameter equal to one, if mixing in the neutrino Yukawas is small. In case of the large mixing, the neutrino-neutralino interplay leads to LFV rates in WMAP-allowed regions up to about two orders of magnitude smaller than naively expected.

In the next sections, we motivate our ansatz for the neutrino parameters and give an overview of our code, Isajet-M, before presenting our results from numerical analysis in Section 2.4. We then discuss our findings in Section 2.5. Finally, our conclusions are summarized in section 2.6.

2.1 $SO(10)$ GUTs

As discussed earlier, LFV rates crucially depend on the neutrino Yukawa coupling matrix $\mathbf{f}_\nu$. However this matrix cannot be reconstructed from experimental data by inverting the seesaw formula (1.100): $\mathbf{f}_\nu$ and $\mathbf{M}_N$ together depend on 18 parameters, while $\mathcal{M}_\nu$ contains only 9 observables. A common solution is to turn to GUTs where $\mathbf{f}_\nu$ is related to the known Yukawa

matrices of SM fermions.

$SO(10)$ GUTs unify all SM fermions and the right-handed neutrino of each generation in a single **16**-dimensional spinor representation. The Higgs representation assignments are determined by the following decompositions of the direct products:

$$\mathbf{16} \otimes \mathbf{16} = \mathbf{10} \oplus \mathbf{120} \oplus \mathbf{126}, \tag{2.2}$$

$$\mathbf{16} \otimes \bar{\mathbf{16}} = \mathbf{1} \oplus \mathbf{45} \oplus \mathbf{210} \tag{2.3}$$

Many $SO(10)$ models exist in the literature with different choices of Higgs representations and, frequently, with additional flavor symmetries. These models can be divided into two general classes [64]. The first uses only low dimensional Higgs multiplets **10, 16, 45** with some non-renormalizable operators constructed from them. This necessarily leads to large $R-$parity violation, so that these models cannot provide a DM candidate. Models in the other class involve **10, 120** or **126** Higgs representations, have renormalizable couplings, preserve R-parity, and are often referred to as minimal Higgs models. The resulting set of sum-rules for the mass matrices are

$$\begin{aligned}
\mathbf{f}_u v_u &= \mathbf{f}_{10} v_u^{10} + \mathbf{f}_{126} v_u^{126} + \mathbf{f}_{120} v_u^{120} \\
\mathbf{f}_d v_d &= \mathbf{f}_{10} v_d^{10} + \mathbf{f}_{126} v_d^{126} + \mathbf{f}_{120} v_d^{120} \\
\mathbf{f}_e v_d &= \mathbf{f}_{10} v_d^{10} - 3\mathbf{f}_{126} v_d^{126} + \mathbf{f}_{120} v_d^{120} \\
M_{\nu,LR} \equiv \mathbf{f}_\nu v_u &= \mathbf{f}_{10} v_u^{10} - 3\mathbf{f}_{126} v_u^{126} + \mathbf{f}_{120} v_u^{120} \\
M_{\nu,RR} \equiv \mathbf{M}_N &= \mathbf{f}_{126} V_R \\
M_{\nu,LL} &= \mathbf{f}_{126} v_L
\end{aligned} \tag{2.4}$$

where $\mathbf{f}_\mathcal{R}$ are $SO(10)$ Yukawa coupling matrices, $v_{u,d}^\mathcal{R}$ are VEVs of the various $SU(2)_L$ doublets (with Higgs fields residing in $\mathcal{R} \equiv \mathbf{10},\ \mathbf{126},\ \mathbf{120}$), and v_L and V_R are the $B-L$ breaking VEVs of the $SU(2)_L$ triplet and singlet respectively. In the type-I seesaw, which we consider in this paper, $v_L = 0$ and SUSY prevents its reappearance via loop diagrams [16].

From Eq.(2.5), if Higgs superfields reside in $\mathbf{10}$, as they do in the simplest scenarios, then the neutrino Yukawa matrix will be identical to the up-quark Yukawa at M_{GUT}. If the Higgs superfields are in $\mathbf{126}$, then $\mathbf{f}_\nu = -3\mathbf{f}_u$. A dominant $\mathbf{120}$ Higgs would lead to at least a pair of degenerate heavy up-quarks [65] and is thus phenomenologically excluded. Motivated by the above, we introduce the *neutrino Yukawa unification parameter* as

$$(\mathbf{f}_\nu)_{ij} = R_{\nu u}(\mathbf{f}_u)_{ij} \tag{2.5}$$

and consider two cases,[1] $|R_{\nu u}| = 1$ and $|R_{\nu u}| = 3$. Note that $\mathbf{f}_\nu$ and $\mathbf{f}_u$ need not be aligned: the subdominant contributions from other Higgs multiplets and/or flavor group structure can lead to different diagonalization matrices. To keep our discussion as simple as possible, we consider two extreme cases of the mixing present in $\mathbf{f}_\nu$.

Case A: large mixing The measured values of the neutrino mixing angles (1.98) are consistent with the so-called tri-bimaximal pattern [66, 67], where $\sin^2\theta_{12} = \frac{1}{3}$, $\sin^2\theta_{23} = \frac{1}{2}$, $\sin^2\theta_{13} = 0$. Thus it is reasonable to postulate that mixing in the neutrino Yukawa matrix at the GUT scale also has a tri-bimaximal form. In other words, we assume that the observed MNS mixing matrix arises only from the left-handed rotation matrix only (*i.e.* we set $\mathbf{V}_{\nu_\mathbf{R}} = \mathbb{1}$). We take a neutrino Yukawa matrix of the form [2]

$$\mathbf{f}_\nu = R_{\nu u}\mathbf{V}_{\nu_\mathbf{L}}\mathbf{f}_u^{\text{diag}} \tag{2.6}$$

Here

$$\mathbf{V}_{\nu_\mathbf{L}}^\dagger = \mathbf{U}_\nu^\dagger = \begin{pmatrix} \sqrt{\frac{2}{3}}c_\chi c_\phi + i\sqrt{\frac{2}{3}}s_\chi s_\phi & \frac{1}{\sqrt{3}} & -\sqrt{\frac{2}{3}}c_\chi s_\phi - i\sqrt{\frac{2}{3}}s_\chi c_\phi \\ -\frac{c_\chi c_\phi + i s_\chi s_\phi}{\sqrt{6}} - \frac{c_\chi s_\phi - i s_\chi c_\phi}{\sqrt{2}} & \frac{1}{\sqrt{3}} & -\frac{c_\chi c_\phi - i s_\chi s_\phi}{\sqrt{2}} + \frac{c_\chi s_\phi + i s_\chi c_\phi}{\sqrt{6}} \\ -\frac{c_\chi c_\phi + i s_\chi s_\phi}{\sqrt{6}} + \frac{c_\chi s_\phi - i s_\chi c_\phi}{\sqrt{2}} & \frac{1}{\sqrt{3}} & \frac{c_\chi c_\phi - i s_\chi s_\phi}{\sqrt{2}} + \frac{c_\chi s_\phi + i s_\chi c_\phi}{\sqrt{6}} \end{pmatrix} \tag{2.7}$$

where $s_\chi = \sin\chi$, $c_\chi = \cos\chi$, $s_\phi = \sin\phi$, $c_\phi = \cos\phi$ and the parameters $\chi,\ \phi \in [0, 2\pi]$.

[1] Henceforth, we denote $|R_{\nu u}|$ by $R_{\nu u}$.

[2] This corresponds to trivial misalignment matrix $\mathbf{R} = \mathbb{1}$ in the Casas-Ibarra parametrization [39].

This is the simplest generalization of a tri-bimaximal mixing ($\chi = \phi = 0$) that allowes CP violation [67]. A fit to experimental values (1.98) reveals that the Harrison-Scott parameters χ and ϕ are restricted to the vicinity of $\chi + \phi \simeq n\pi$, with θ_{13} being the strongest constraint. Ignoring RGE effects, we invert the seesaw formula and obtain the approximate form for the Majorana mass matrix

$$\mathbf{M}_N \simeq diag\left(\frac{m_u^2}{m_{\nu_1}}, \frac{m_c^2}{m_{\nu_2}}, \frac{m_t^2}{m_{\nu_3}}\right) \times R_{\nu u}^2 \tag{2.8}$$

We will consider this case as representative for the large mixing scenario.

Case B: Small mixing For the small mixing scenario, we take the neutrino and up-quark Yukawa matrices to be exactly aligned with each other at the GUT scale,

$$\mathbf{f}_\nu = R_{\nu u}\mathbf{f}_u \tag{2.9}$$

so that neutrino mixing is given by the CKM matrix. Then, in the absence of significant RGE magnification effects, the Majorana mass matrix cannot be diagonal. Assuming tri-bimaximal mixing in $\mathcal{M}_\nu$ and neglecting the small mixing in $\mathbf{f}_\nu$ we can estimate eigenvalues $\mathbf{M}_N$ for the normal hierarchy of light neutrinos ($m_{\nu_1} \ll m_{\nu_2} \ll m_{\nu_3}$),

$$M_{N_1} \simeq \frac{3m_u^2}{m_{\nu_2}} R_{\nu u}^2,\ M_{N_2} \simeq \frac{2m_c^2}{m_{\nu_3}} R_{\nu u}^2,\ M_{N_3} \simeq \frac{m_t^2}{6m_{\nu_1}} R_{\nu u}^2. \tag{2.10}$$

For the inverted mass hierarchy ($m_{\nu_1} \simeq m_{\nu_2} \gg m_{\nu_3}$), a similar procedure yields

$$M_{N_1} \simeq \frac{3m_u^2}{m_{\nu_2}} R_{\nu u}^2,\ M_{N_2} \simeq \frac{2m_c^2}{3m_{\nu_1}} R_{\nu u}^2,\ M_{N_3} \simeq \frac{m_t^2}{2m_{\nu_3}} R_{\nu u}^2. \tag{2.11}$$

Notice that the largest RHN mass is controlled by the smallest light neutrino mass.

From Eqs. (2.8)-(2.11), we see that RHNs have a very strong mass hierarchy "quadratic" to the one in up-quark sector: $M_{N_1} : M_{N_2} : M_{N_3} \sim m_u^2 : m_c^2 : m_t^2$. For this reason, only the spectrum with normal hierarchy of light neutrinos is feasible. A quasi-degenerate spectrum ($m_{\nu_1} \simeq m_{\nu_2} \simeq m_{\nu_3}$) would require the lightest Majorana mass to be in the $10^2 - 10^3$ GeV range with significant L-R mixing in the sneutrino sector, which is in confict with our approximations

(see the discussion pertaining to Eq.(1.113)). Moreover, such light Majorana masses make successful thermal leptogenesis impossible. The inverse hierarchical case would require the heaviest Majorana mass to be of order 10^{17} GeV, which is well above the GUT scale. This type of spectrum also suffers instabilities under both very small changes to $\mathbf{M}_N$ and RGE evolution [68]. Therefore we will concentrate on the normal hierarchy case, which is also favored by GUT model building [69].

2.2 Procedure

We have extensively modified ISAJET[70] by including the neutrino sector and by implementing RGE evolution in matrix form to incorporate flavor effects in both the quark and lepton sectors. The resulting program, ISAJET-M, performs RGE evolution in the MSSM augmented with RHNs at the 2-loop level, taking into account various thresholds, and computes sparticle spectra including radiative corrections. The computation of the neutralino relic density was done by mean of the IsaReD code [71] and LFV rates were computed using full one-loop formulae from Ref. [37]. A graphical outline of our procedure is presented in Fig. 2.1, and details of the program are provided in Appendix B.

In the neutrino sector we employ the "top-down" approach in which $\mathbf{f}_\nu$ and $\mathbf{M}_N$ are inputs at the scale M_{GUT}. Physical neutrino masses and mixings are derived results which we require to be within the experimental bounds (1.98). We consider the two cases for the neutrino Yukawa unification parameter, $R_{\nu u} = 1$ and $R_{\nu u} = 3$, which were introduced earlier. For each case we consider scenarios with large and small neutrino mixings using Eqs. (2.6) and (2.9) to set the neutrino Yukawa matrix at M_{GUT}. This also restricts Majorana masses to be below that scale, *i.e.* $max(M_{N_i}) \lesssim M_{GUT}$.

In the quark sector we choose a basis at the weak scale in which CKM rotation is entirely in the up-quark sector: we set the fermion rotation matrices (1.109) to be $\mathbf{V_{u_L}} = \mathbf{V_{u_R}} = \mathbf{V}_{CKM}$ and $\mathbf{V_{d_L}} = \mathbf{V_{d_R}} = \mathbb{1}$. Note that this does not mean that $\mathbf{f}_d$ remains diagonal at all scales – off-diagonal terms will be generated at higher scales due to RGE effects. Similarly, for charged

leptons we set $\mathbf{V_{e_L}} = \mathbf{V_{e_R}} = \mathbb{1}$ at M_Z.

Regarding the SUSY sector we work in the well-studied scenario with mSUGRA-like boundary conditions, specified by the parameter set

$$m_0,\ m_{1/2},\ A_0,\ \tan\beta,\ sgn(\mu) \tag{2.12}$$

where GUT-scale boundary conditions are universal and defined by Eq.(1.121). Instead of scanning over the full parameter space, which would be exceedingly computationally intensive, we study specific points for each DM-allowed region. Throughout this work we take $\mu > 0$ as suggested by measurements of the muon anomalous magnetic moment [72, 73, 74] and set the pole mass of the top quark $m_t = 171$ GeV in accord with Tevatron data [75].

For the DM relic density, we consider the conceptually simplest scenario in which the DM is comprised only of the lightest neutralino $\widetilde{Z}_1$, which is thermally produced in the standard ΛCDM cosmology. We first calculate the neutralino Relic Density (RD) and LFV rates in our framwork *with* SUSY-seesaw using points from Table 2.1 that have WMAP-allowed values in the mSUGRA framework *without* seesaw – a procedure commonly used in the literature. Then, if the RD turns out to be too high, as it is frequently the case, we find new points consistent with the WMAP range (2.1) by adjusting SSB parameters, and then calculate the corresponding LFV rates.

2.3 Code description

Our code, which we refer to here as Isajet-M, is ISAJET 7.78[70] modified to include the neutrino sector and to handle all couplings and SSB parameters in full matrix form at the 2-loop level. Couplings and parameters can also be complex, allowing for the study of CP-violation.

Isajet-M takes as input the specification of a SUSY-breaking model and its GUT-scale parameters, a specification of the neutrino mass model (e.g., GUT-scale neutrino Yukawas and right-handed Majorana mass matrix), and known Standard Model parameters: fermion masses, the Z-boson pole mass $M_{\rm Z}$, the fine-structure constant $\alpha^{\overline{MS}}(M_{\rm Z})$, the strong coupling constant

parameter	Value	parameter	Value
M_Z	91.1876	m_t	171
$1/\alpha^{\overline{MS}}(M_Z)$	127.918	$m_b - m_c$	3.42
$\alpha_s^{\overline{MS}}(M_Z)$	0.1176	$m_e \times 10^3$	0.511
$\sin^2\theta_W(M_Z)$	0.23122	m_μ	0.10566
$m_u(2\,\text{GeV})$	0.003	m_τ	1.77699
$m_d(2\,\text{GeV})$	0.006	$\sin\theta_{12}^{CKM}$	0.22715
$m_s(2\,\text{GeV})$	0.095	$\sin\theta_{23}^{CKM}$	0.04161
$m_c(m_c)^{\overline{MS}}$	1.25	$\sin\theta_{13}^{CKM}$	0.003682
$m_b(m_b)^{\overline{MS}}$	4.20	δ^{CKM}	1.0884

Table 2.2: SM input parameters [12] for ISAJET-M. All masses are in GeV units and angular quantities are in radians.

$\alpha_s^{\overline{MS}}(M_Z)$, and the CKM angles in the "standard parameterization." These values are summarized in Table 2.2.

It solves the renormalization group equations for the given theory and returns as output the SUSY spectrum, Higgs masses, and the decay widths and branching ratios for the sparticles. Optionally, Isajet-M will also calculate and return:

- the neutralino relic density $\Omega_{\widetilde{Z}_1}h^2$ in the standard cosmological model,
- dark matter direct detection rates, i.e. neutralino cross-section-velocity products,
- SUSY contributions to the anomalous magnetic moment of the muon $\Delta a_\mu \equiv (g-2)_\mu/2$,
- the $b \to s\,\gamma$ branching fraction,
- the $B_s \to \ell\ell$ branching fraction,
- the rate for $\mu \to e$ conversion in nuclei,
- and branching fractions for $\ell_i \to 3\ell_j\,\gamma$.

These computations are done, respectively, by IsaReD [71], IsaReS [76], IsaAMU [74], IsaBSG [77], IsaBMM [78], and codes from the IsaTools package.

For the evolution of gauge and Yukawa couplings, Isajet-M uses a multiscale effective theory approach proposed in Ref. [79], where heavy degrees of freedom are integrated out at each

particle threshold. There is an unpublished erratum correcting mistakes in the printed formulae of Ref. [79]; we list the corrected Yukawa 1-loop RGEs in Appendix A. In the second-loop RGE terms we change from MSSM formulae [80] to SM expressions [20, 81] at a single scale, $Q = M_{SUSY} \equiv \sqrt{m_{\tilde{t}_L} m_{\tilde{t}_R}}$, The introduced error is expected to be of the 3-loop order and thus can be neglected with our precision.

This "step beta-function approach" produces continuous matching conditions across thresholds. However, decoupling of a heavy particle also introduces finite shifts in RGE parameters [82]; a similar effect has long been known in QCD, where the decoupling of heavy quarks leads to shifts in the running masses of the light quarks [83]. Expressions for shifts induced by decoupling of each individual sparticle depend on the ordering of sparticle spectrum and are not yet known for the general case. Therefore, we implement these sparticle-induced finite shifts (to all three generations) collectively at a common scale $Q = M_{SUSY}$ in the basis where Yukawa matrices are diagonal; we use 1-loop expressions of Ref. [84] without logarithmic terms that has already been resummed by the RGEs evolution. For the top Yukawa coupling additional 2-loop SUSY-QCD corrections are included according to Ref. [85]. These finite threshold corrections are particularly important for GUT theories since they change ratios of Yukawa couplings from those at the weak scale, as was recently emphasized in Ref. [86]. This multiscale approach is a generalization of the one used by the standard ISAJET, as is described in detail in Ref. [87], and is preferred to single-scale decoupling when sparticle hierarchy is large (as appears, for example, in the HB/FP region [59] of mSUGRA)

For the SSB parameters we use 2-loop RGEs from Ref. [80] with the following conversion between notations: $\mathbf{f}_\bullet \equiv \mathbf{Y}_\bullet{}^T$, $\mathbf{a}_\bullet \equiv -\mathbf{h}_\bullet{}^T$, $b \equiv -B$. Unlike the gauge and Yukawa couplings, where beta-functions change at every threshold, the SSB beta-functions remain those of the MSSM all the way down to M_Z. We do not take into account threshold effects from the appearance of new couplings in the region of broken supersymmetry introduced in Ref. [19, 20].

The evolution of neutrino sector parameters also uses the multiscale approach that is mandatory to obtain correct values in the neutrino sector in the case of hierarchical RHNs [88]; Isajet-M's approach is identical to that used in the code REAP [89]. Above the scale of the

heaviest RHN we have a full MSSM+RHN setup, where the MSSM RGEs are extended to include full 2-loop equations for $\mathbf{f}_\nu$, $\mathbf{a}_\nu$, $\mathbf{m}^2_{\tilde{\nu}_\mathbf{R}}$ and $\mathbf{M}_N$ [39, 51]. We also take into account additional contributions to RGEs of ordinary MSSM parameters due to the RHN superfields up to 2-loop order [39, 90, 89, 51]. For large neutrino Yukawa couplings these additional RGE terms cause changes to the MSSM sparticle spectrum that can have significant effect on experimental rates [62, 18].

The main driver routine for Isajet-M is the program `SUGRUN` . `SUGRUN` takes user input to select the model and boundary conditions as well as various auxiliary settings controlling the functionality of Isajet-M. It then calls the routine `SUGRA`, which solves the RGEs, and (if desired) `SSMSSM`, `ISARED`, `ISARES`, `ISABSG`, `ISAAMU`, `ISABMM`, `ISALLG`, `ISAMNE`, and `ISAL3L`, which calculate decay widths and branching ratios for SUSY particles as well as the various rare decays and processes mentioned above. This information is returned to the user and written to output files in text or Les Houches Accord format.

The core of Isajet-M's RGE-solving is the routine `SUGRA`. It is responsible for the solution of the RGEs themselves once all the boundary conditions have been set up. Isajet-M proceeds in an iterative fashion, running up from the weak scale (M_Z) to the GUT scale (M_{GUT}) and back down again in each iteration. This continues until all basic parameters have converged to within a specified tolerance (by default, 0.3% for all parameters save the rapidly-varying μ and B, for which it is only 5%.) The stepsize is decreased by 20% each iteration. Isajet-M will also halt if the specified maximum number of iterations has been reached, or until an exception is found at the specified point. Exceptions include

- non-perturbative Yukawa couplings,
- failure of gauge couplings to unify within 10^{19} GeV,
- failure of parameters to converge within the maximum number of iterations,
- igutst
- tachyonic particles,

- a non-neutralino LSP,
- and negative Higgs mass(es) squared.

An exception also occurs when there is no radiative electroweak symmetry breaking, but this is not checked until the final iteration. When any of these conditions are found, the NOGOOD variable is set, which effectively throws an exception and returns execution up the calling stack to SUGRA.

The first iteration is handled specially inside SUGRA; further iterations are handled by subroutine SUGRGE. Before the first iteration, the SUSY spectrum is not yet known, so we guess M_{SUSY} and the Higgs vev at $M_{\rm Z}$; for later iterations these are replaced by their values during the previous iteration.

Before we can begin the main sequence of iterations, we must obtain running masses and gauge couplings at $M_{\rm Z}$ in the $\overline{DR}$ scheme (Isajet-M does its RGE evolution in $\overline{DR}$) from the SM inputs. To this end, SUGRA calls the routine SMSET. SMSET first runs the couplings $\alpha^{\overline{MS}}$ and $\alpha_s^{\overline{MS}}$ from $M_{\rm Z}$ to 2 GeV using 2-loop QCD$\times$QED RGEs supplemented with a third QCD loop[91, 92]. During this evolution fermions are stepwise decoupled at the scales of their running mass, and finite threshold corrections at the two-loop level are applied[93]. The running lepton masses in $\overline{MS}$ are obtained from their $\overline{MS}$ pole masses using 1-loop equations from[91],

$$m_l^{\overline{MS}}(Q)=m_l\left[1-\frac{\alpha^{\overline{MS}}(Q)}{\pi}\left(1+\frac{3}{4}\ln\frac{Q^2}{m_l^2}\right)\right], \tag{2.13}$$

after which the fermion masses (save for the top) and gauge couplings are run back up to $M_{\rm Z}$. They are then converted from $\overline{MS}$ into $\overline{DR}$ according to [94, 95] (corrections are neglected for the light fermions e,μ,u,d,s.)

$$\begin{aligned}
m_b^{\overline{DR}}(M_Z) &= m_b^{\overline{MS}}(M_Z)\left(1-\frac{\alpha_s}{3\pi}-\frac{29\alpha_s^2}{72\pi^2}+\frac{3g_2^2}{128\pi^2}+\frac{13g_1^2}{1920\pi^2}\right)_{\overline{MS}}\\
m_c^{\overline{DR}}(M_Z) &= m_c^{\overline{MS}}(M_Z)\left(1-\frac{\alpha_s}{3\pi}-\frac{29\alpha_s^2}{72\pi^2}+\frac{3g_2^2}{128\pi^2}+\frac{g_1^2}{1920\pi^2}\right)_{\overline{MS}}\\
m_\tau^{\overline{DR}}(M_Z) &= m_\tau^{\overline{MS}}(M_Z)\left(1+\frac{3g_2^2}{128\pi^2}-\frac{9g_1^2}{640\pi^2}\right)_{\overline{MS}}
\end{aligned} \tag{2.14}$$

For the top quark, we obtain its running mass at m_t using the 2-loop QCD expression from [85]:

$$m_t^{\overline{DR}}(m_t) = m_t \left[1 + \frac{5}{3}\frac{\alpha_s(m_t)}{\pi} + \left(\frac{\alpha_s(m_t)}{\pi}\right)^2 \Sigma_t^{2loop}\right] \tag{2.15}$$

where Σ_t^{2loop} is the 2-loop piece. Note that we activate the top quark at the scale of its mass, so we have the 5-flavor scheme below $Q = m_t$ and the full 6 flavors above it.

These $\overline{DR}$ masses are then substituted into Eq.(1.109) to calculate the Yukawa matrices at M_Z in the gauge eigenbasis, which are saved and used as the Z-scale boundary conditions for subsequent iterations. By default, CKM mixing is placed entirely in the up quark sector and the charged leptons are diagonal, i.e. $V_{d_L} = V_{d_R} = V_{e_L} = V_{e_R} = 1$, but other mixing patterns can be specified. Alternatively, either the unmixed or dominant third-family approximations can be used if full treatment of the quark sector is not desired.

At this point the main process of iterating is begun. Within each iteration, several steps take place. The actual evolution is accomplished via a fourth-order Runge-Kutta integrator routine `CRKSTP`; the RGEs themselves are in the routine `CSURG157`. The RGEs are two-loop $\overline{DR}$ beta functions from Ref. [80], with the following conversion in notation: $\mathbf{f}_\bullet \equiv \mathbf{Y}_\bullet{}^T$, $\mathbf{a}_\bullet \equiv -\mathbf{h}_\bullet{}^T$, $b \equiv -B$. The complete RGEs used can be found in Appendix A.

All the SM parameters are set to their Z-scale calculated values, then run up towards M_{GUT}. At m_{top} the top quark Yukawa is activated; its $\overline{DR}$ running mass is obtained from its pole mass via the 2-loop QCD expression [85]. At the SUSY scale (calculated to be $\sqrt{m_{\tilde{t}_L} m_{\tilde{t}_R}}$) we implement sparticle threshold corrections. Sparticles are activated and decoupled automatically in the RGEs, each individually at its mass as calculated in the previous iteration. As we pass the frozen-out mass of each right-handed neutrino, we activate these neutrinos (and deactivate the corresponding effective mass operator κ) in the routine `ZRHNACT`.

`ZRHNACT` and its inverse function `ZRHNDEC` switch the running parameters and hence RGEs in use. Below the scale of each RHN, the RGEs used are those of the MSSM plus additional equations for the coupling κ of the dimension-5 effective neutrino operator (1.102) that are included at 2-loop level [89]. Above each scale, the relevant rows and columns of the $\mathbf{f}_\nu$ and $\mathbf{M}_N$

matrices are present. The functions use the tree-level matching conditions from Eq.(1.103), neglecting small finite threshold corrections. Note that the expression (1.103) is valid only in the basis where $\mathbf{M}_N$ is diagonal at the threshold, which is different from the original basis at M_{GUT} due to RGE effects.

The GUT scale $M_{\rm GUT}$ is defined to be the scale at which the SU(2) and U(1) gauge couplings unify, i.e. where $g_1 = g_2$ with $g_1 = \sqrt{5/3}\, g'$ the hypercharge coupling in the GUT-scale normalization. By default we do not impose an exact unification of the strong coupling ($g_3 = g_1 = g_2$) at $M_{\rm GUT}$, assuming that the resulting few percent discrepancy comes from the GUT-scale threshold corrections [5].

When this is reached, we store all the GUT-scale running values and re-impose the GUT scale boundary conditions determined by the SUSY-breaking model and the right-handed neutrino inputs. We then run back down to the Z scale, applying the preceding operations in reverse. The right-handed neutrinos' masses are decoupled at their running mass, and replaced by the dimension-5 effective mass operator. Sparticle threshold corrections are applied at the SUSY scale and the top quark is decoupled at its scale. Once we reach the Z-scale, Z-scale running values for this iteration are saved, and the SUSY mass spectrum and neutrino mass and mixing parameters are calculated. The renormalization group improved 1-loop corrected Higgs potential is calculated and minimized. The obtained mass spectrum is used in the next iteration to appropriately take into account the sparticle threshold effects on the RGEs evolution.

Note that on each downward run, the position of the RHN thresholds M_{N_k} are determined by the eigenvalues of the RGE-evolving Majorana mass matrix $\mathbf{M}_N$ at those scales. Decoupling of the $k-$th RHN by `ZRHNDEC` also involves rotating to the basis where $\mathbf{M}_N$ is diagonal, and then removing the corresponding columns of $\mathbf{f}_\nu$ and $\mathbf{a}_\nu$ as well as the $k-$th row and column of $\mathbf{m}^{\mathbf{2}}_{\tilde{\nu}_{\mathbf{R}}}$ and $\mathbf{M}_N$.

The minimization of the RGE-improved Higgs potential is done by routine `SSMSPEC` using the tadpole method[96]. The dominant contributions are those from the third-generation sfermions; the contributions from charginos, neutralinos, and Higgs bosons are also included. By doing this calculation at the scale M_{SUSY} we effectively account for the leading 2-loop corrections. As

the tadpole graphs entering into computations of μ and B depend strongly on the parameters μ and B themselves, we must employ an iterative procedure. Calculations of μ, B, and their tadpole corrections are iterated until they converge to a consistent values with a precision of at least 0.1%. Typically this requires 3-4 iterations.

In the computation of sparticle masses we use SSB parameters extracted at their respective mass scales. Then SSB matrices are assembled and rotated to the SCKM basis as shown in Eq. (1.111). The resultant matrices are plugged into the sfermion mass-squared matrices (1.110). Instead of diagonalizing the full 6×6 matrices (1.110), we diagonalize three 2×2 submatrices, therefore neglecting the intragenerational mixings, which are required to be small by experimental limits on flavor changing neutral current processes [63]. For the finite corrections, the full expressions of Ref. [84] for 1-loop self-energies are used.

2.4 Results

2.4.1 Large mixing

We begin by considering the $R_{\nu u} = 1$ case. Numerically we found that the GUT-scale Majorana mass matrix,

$$\mathbf{M}_N = diag\left(4.75 \times 10^{-6}, 4.75 \times 10^{-5}, 1\right) \cdot 1.398 \times 10^{14}\,\text{GeV}, \tag{2.16}$$

produces the spectrum $m_{\nu_1} \sim 10^{-5}$ eV, $m_{\nu_2} \simeq \sqrt{\Delta m^2_{21}} \simeq 8 \times 10^{-3}$ eV and $m_{\nu_3} \simeq \sqrt{\Delta m^2_{31}} \simeq 5 \times 10^{-2}$ eV that is in accord with experimental limits (1.98). We chose the mass of the lightest RHN to be far above M_{SUSY} to prevent the unwanted mixing in sneutrino sector (see discussion for Eq.(1.113)). Equation (2.16) is in good agreement with our estimate (2.8), up to a factor of ~ 2 reduction of up-quark Yukawa couplings (see for example Ref. [81]) due to the RGE effects. This is because $\mathbf{f}_\nu$, $\mathbf{M}_N$, and the spectrum of light neutrinos are hierarchical and as such experience very little change in RGE evolution [89].

In the Harrison-Scott parameterization (2.7), which we use for the mixing in the neutrino

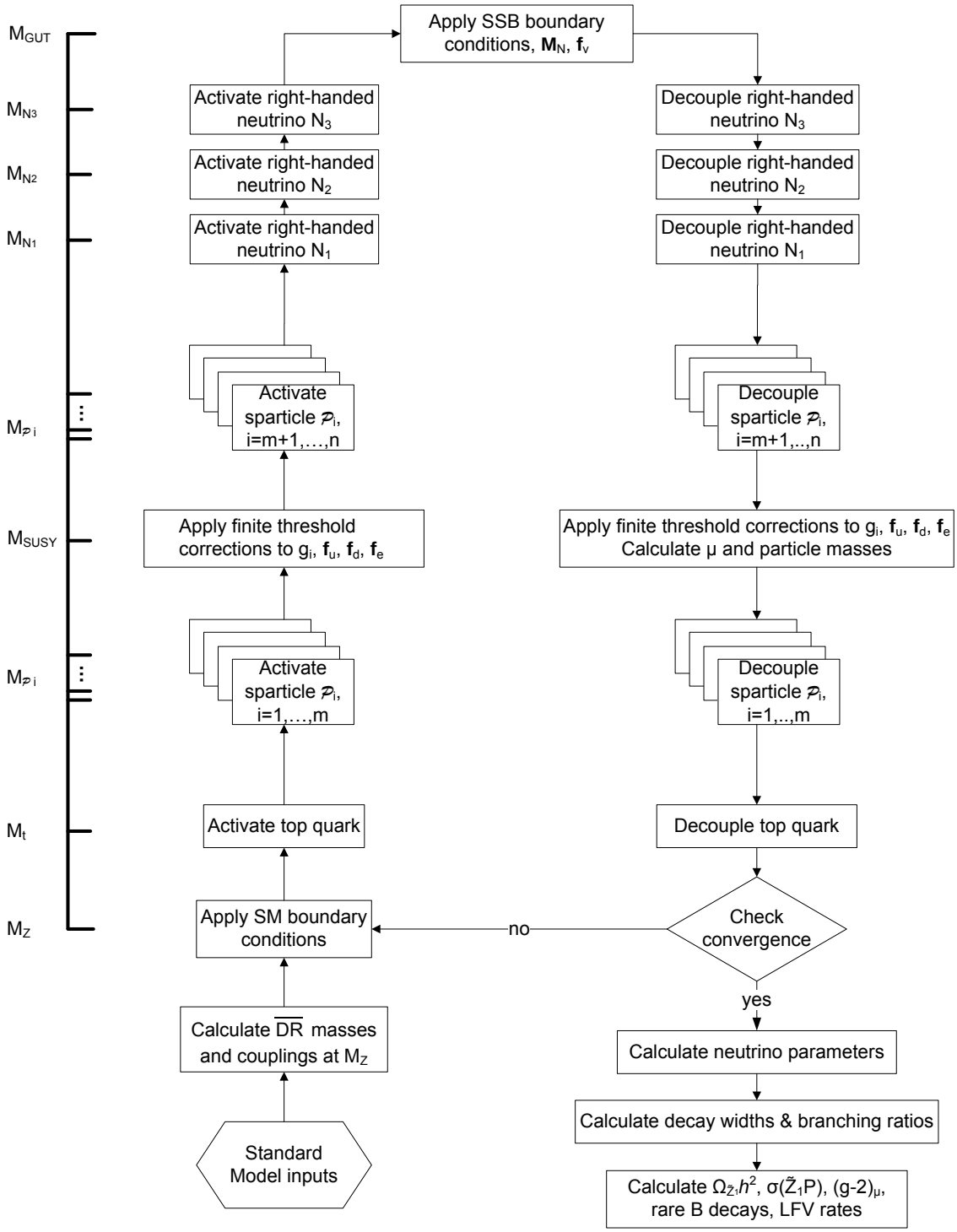

Figure 2.1: Code flowchart. $\mathcal{P}_i$ represent sparticles and Higgses arranged in the ascending order of their masses. See Appendix B for the details.

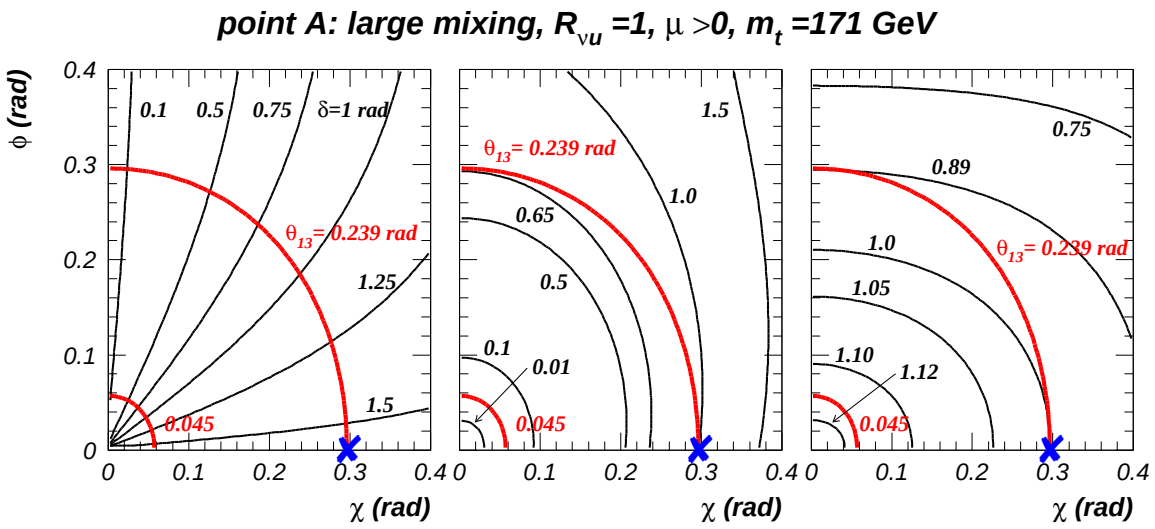

Figure 2.2: Dependence of the weak-scale Dirac phase (left), $BR(\mu \to e\gamma)$ (middle) and $BR(\tau \to \mu\gamma)$ (right) on GUT-scale values of the Harrison-Scott parameters for the benchmark point A with Yukawa unification parameter $R_{\nu u} = 1$. The contours for LFV branching ratios represent enhancement factors with respect to the point with $\delta = \pi/2$, namely $(\phi,\, \chi) = (0,\, 0.294)$, that is marked by the blue cross. All angles are in radians. The thick red lines are iso-θ_{13} contours for $\theta_{13} = 0.239$ (at the CHOOZ bound [97]; see Eq. 1.98) and for the ultimate 90% C.L. reach of the Daya Bay experiment $\theta_{13} = 0.045$. The contours remains essentially unchanged for all other points with large mixing and for $R_{\nu u} = 3$.

Yukawa matrix at the GUT scale, the Dirac phase δ and mixing angles are a function of ϕ and χ. The Dirac phase $\delta = \pi/2$ for $\phi = 0$ – see the left frame of Fig. 2.2. It is know that LFV rates depend on the value of the unknown Dirac phase [43]. In addition, most LFV rates are very sensitive to the value of θ_{13} [48] for which only an upper bound exists. To quantify these dependences, in the middle frame of Fig. 2.2 we show the branching ratio for $\mu \to e\gamma$ as function of Harrison-Scott parameters. We present them as enhancement factors relative to the rates at $\{\phi, \chi\} = \{0, 0.294\}$ for which $\theta_{13} = 0.239$ (i.e. $\sin^2\theta_{13} = 0.056$) and $\delta = \pi/2$. We see that with θ_{13} fixed, varying δ changes the branching ratio by up to $\sim 35\%$. The dependence on θ_{13} is stronger and more complex: rates change by about two orders of magnitude for θ_{13} ranging from 0.239 down to 0.045 (or $\sin^2 2\theta_{13} = 0.008$), with the latter being the ultimate reach of the Daya Bay experiment [98]. Closer to $\phi = \chi = 0$, rates change much faster and drop by several more orders of magnitude. The rates for the other θ_{13}-dependent LFV processes follow the same pattern as expected from Eqs. (1.126) and (1.127). On the other hand, rates for $\tau \to \mu\gamma$ and $\tau \to 3\mu$ are relatively independent of θ_{13} [48]. In the right frame of Fig. 2.2 we show enhancement factor contours for $\tau \to \mu\gamma$. We see that rates change with θ_{13} by only $\sim 13\%$: this variation is an artifact of the paramterization (2.7), in which $\sin^2\theta_{12} = 0.33/\cos^2\theta_{13}$. Also the variation due to δ is smaller – only up to $\sim 10\%$. We numerically confirmed that $\tau \to 3\mu$ rates behave similarly, as expected from Eq. (1.126).

In figures 2.3, 2.4, 2.5, and 2.6, we show the LFV rates along with current experimental bounds (horizontal dashed lines) and projected future sensitivities (dash-dotted lines). To account for the abovementioned dependences on θ_{13} and δ, we show rates for large values of $\{\phi, \chi\} = \{0, 0.294\}$ (for which $\sin^2\theta_{13} = 0.056$ and $\delta = \pi/2$) as diagonally hatched bars and for $\phi = \chi = 0$ (resulting in $\sin^2\theta_{13} = 0$) as solid bars. We also present rates for $\{\phi, \chi\} = \{0, 0.022\,\text{rad}\}$ (giving $\sin^2\theta_{13} = 0.002$) as cross-hatched bars to indicate the upper limit on the rates if the Daya Bay [98] and Double Chooz [99] experiments produce a null result.

In the bulk [55, 56] and the stau-coannihilation [57, 71] regions, neutralino RD is within the WMAP range due to $\widetilde{Z}_1$ interactions with the the lighter stau $\tilde{\tau}_1$. Under universal boundary conditions $\tilde{\tau}_1$ is a dominantly right-handed state and as such remains unaffected by the neutrino

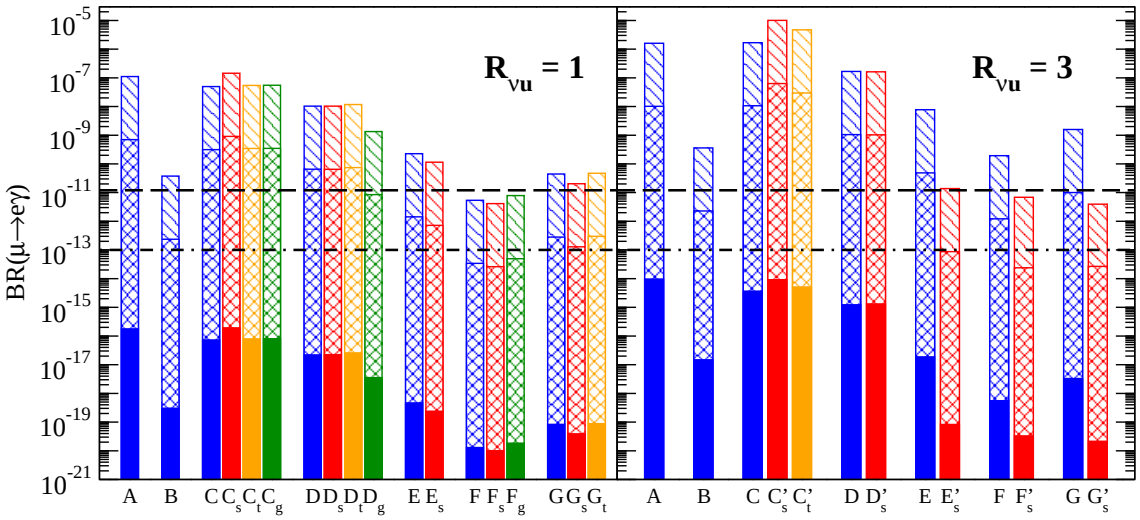

Figure 2.3: Radiative LFV decay rates in the large mixing case for two values of $R_{\nu u}$ (c.f. Eqs. (1.122) and (1.125)). The heights of the solid bars show rates for exact tri-bimaximal mixing $\chi = \phi = 0$ at the GUT scale. Diagonally hatched bars represent $\{\phi,\, \chi\} = \{0,\, 0.294\}$ yielding the maximum allowed θ_{13} and $\delta = \pi/2$. Cross-hatched bars represent $\{\phi,\, \chi\} = \{0,\, 0.022\}$ which has $\delta = \pi/2$ and $\theta_{13} \simeq 0.045$ that is the ultimate reach of the Daya Bay experiment. Dashed lines represent the current bound and dash-dotted lines the projected sensitivity listed in Table 1.3. The letters denote various benchmark points presented in Tables 2.1,2.3 and 2.4. Points C through G have RD above the WMAP bound. The corresponding WMAP-consistent points indicated by subscripts s,t, and g are obtained by adjusting m_0, A_0, and $m_{1/2}$, respectively.

Yukawa coupling[3]. Therefore, the use of mSUGRA values (points A and B) in models with RHNs still produces the correct RD. At point A in the $R_{\nu u} = 1$ case, $BR(\mu \to e\gamma)$ changes from 1.77×10^{-16} for $\phi = \chi = 0$ to 8.57×10^{-8} for $\{\phi,\, \chi\} = \{0,\, 0.294\}$; intermediate allowed ϕ, χ values produce rates between these. For $\tau \to \mu\gamma$ and $\tau \to 3\mu$ dependence on ϕ and χ parameters is reversed: larger ϕ and χ produce smaller rates. For example, at point A in the $R_{\nu u} = 1$ case, the $\tau \to \mu\gamma$ branching fraction is 2.09×10^{-7} for $\phi = \chi = 0$ and 1.77×10^{-7} for $\{\phi,\, \chi\} = \{0,\, 0.294\}$. We see that $\tau \to \mu\gamma$ and $\tau \to 3\mu$ are excellent probes of LFV: the current experimental bound of $\tau \to \mu\gamma$ rules out the bulk region for all values of ϕ and χ.

In the stop-coannihilation region [58] the picture is radically different. A naive use of input parameters for point C gives a neutralino relic density $\Omega_{\widetilde{Z}_1} h^2 = 0.34$, well above the WMAP

[3]Detailed discussion of neutrino Yukawa coupling effects on the SUSY spectrum and DM observables can be found in Refs. [18].

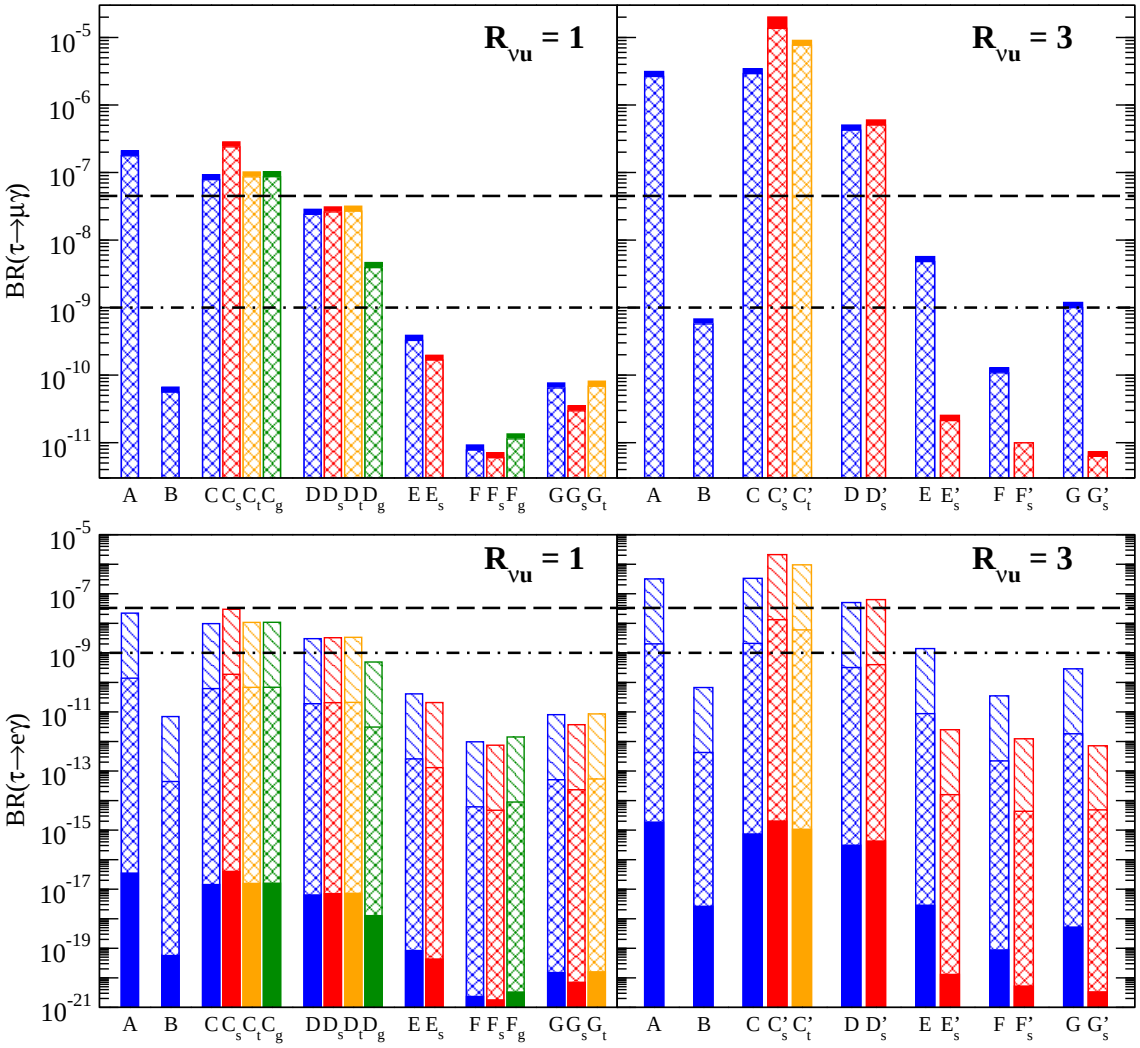

Figure 2.4: Similar to Fig. 2.3 for τ radiative LFV decays. For $\tau \to \mu\gamma$, the $\{\phi, \chi\} = \{0, 0.022\}$ case is not shown as it produces rates very close to those for $\{\phi, \chi\} = \{0, 0.294\}$ (cross-hatched).

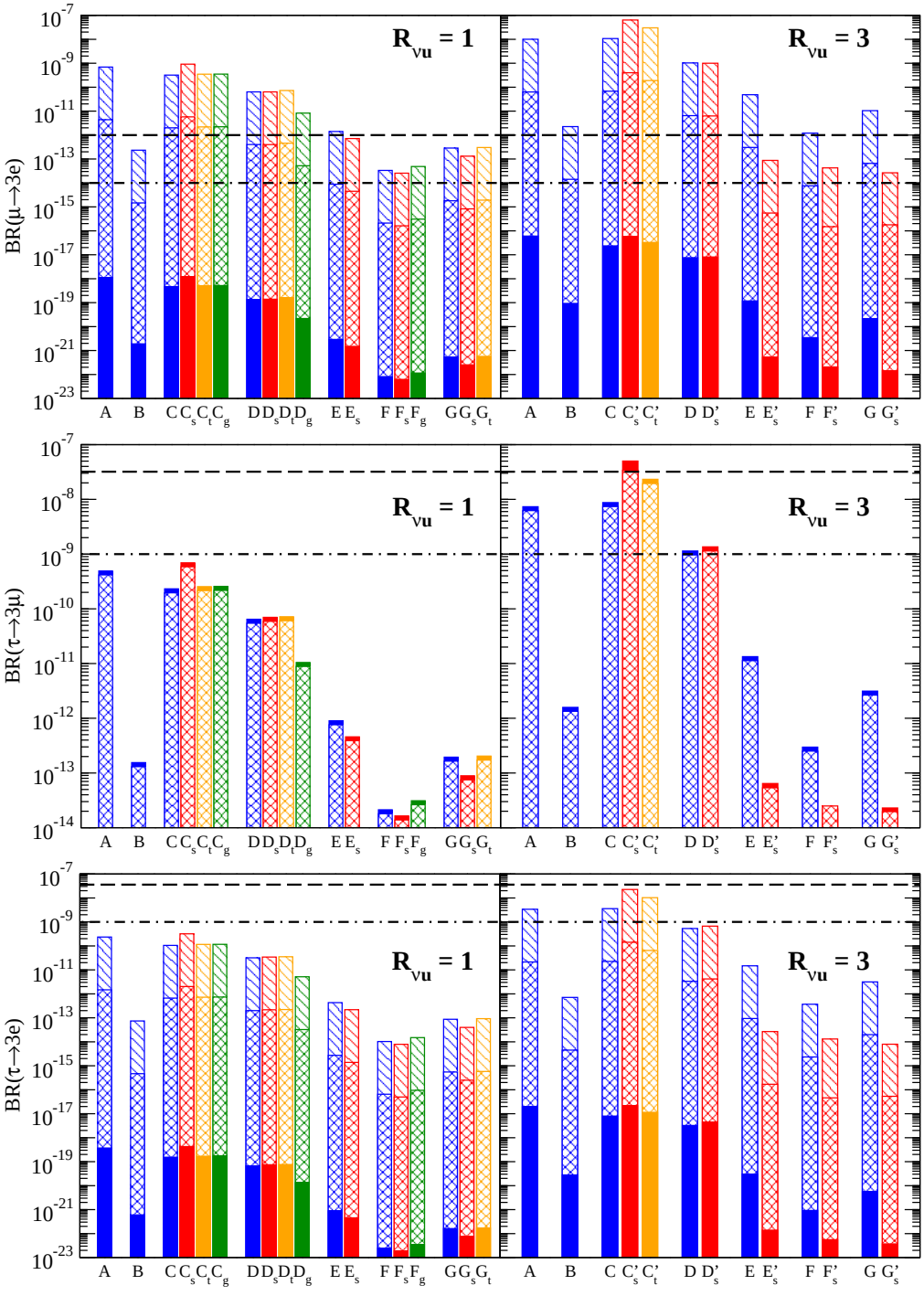

Figure 2.5: Similar to Fig. 2.3 for trilepton LFV decays.

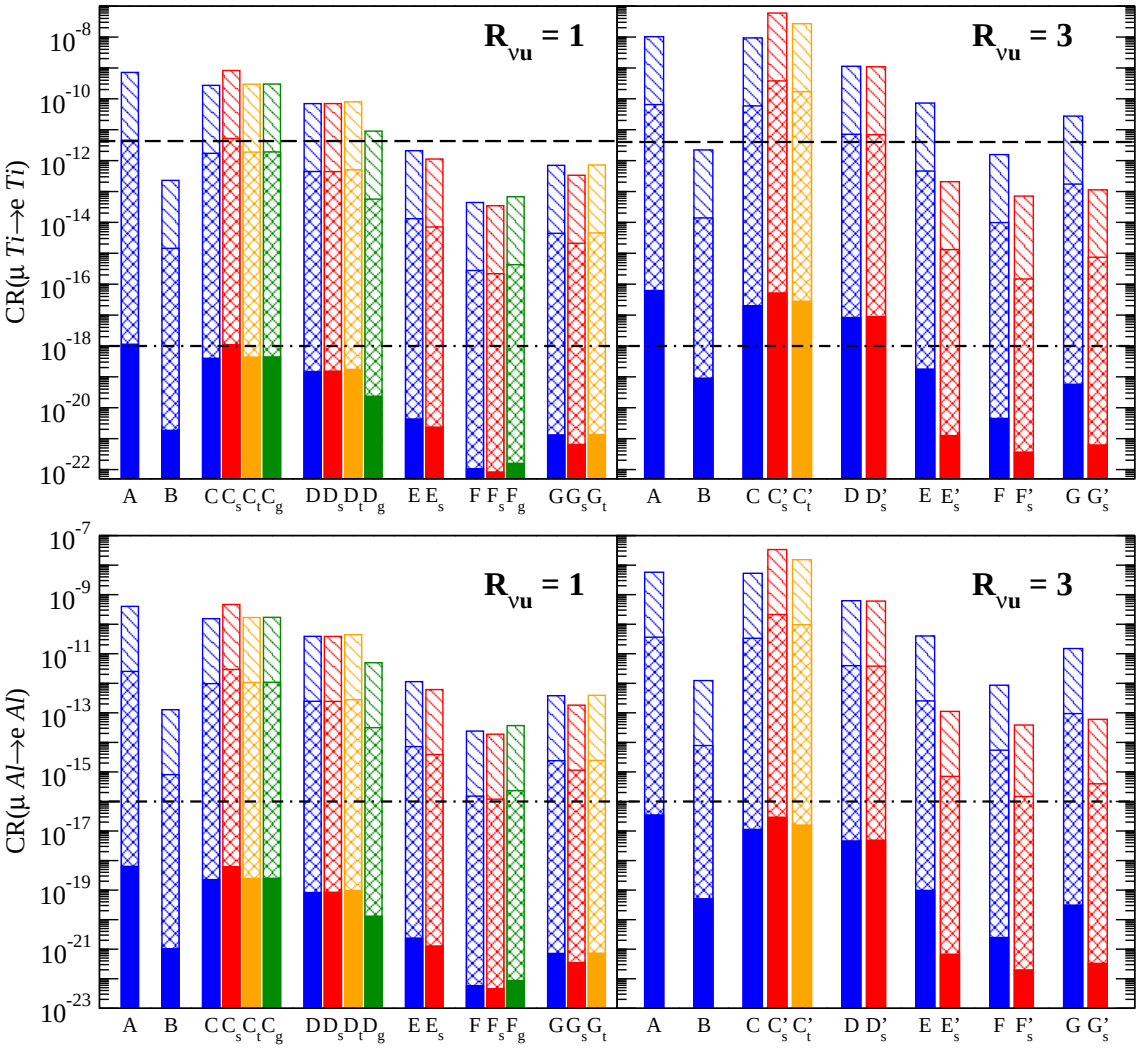

Figure 2.6: Similar to Fig. 2.3 for LFV $\mu \rightarrow e$ conversion rates in titanium (top frame) and aluminum (bottom frame) targets.

bound. This is because $\tilde{t}_1$ is pushed to a higher mass causing stop-coannihilation to cease. To restore the stop-coannihilation mechanism and bring $\Omega_{\widetilde{Z}_1} h^2$ down to the WMAP range, one can counteract the effect of $\mathbf{f}_\nu$ by adjusting SSB parameters. Adjusting the common scalar mass parameter m_0, with the rest of the SSB parameters fixed, can lower the stop mass back to the desired mass range leading to new WMAP-consistent point that we denote[4] C_s with parameter values shown in Table 2.3. Increasing m_0 also makes sleptons lighter and increases their mixing, as can be seen from Eqs.(1.122) and (1.125), leading to a factor of ~ 2.8 increase in LFV rates as compared to point C. The stop mass can also be lowered by dialing the trilinear A-term, resulting in another modified point C_t. The rates increase with respect to values at point C by only about 10%. Alternatively, one can raise $\widetilde{Z}_1$ mass closer to that of the $\tilde{t}_1$ by adjusting the common gaugino mass parameter $m_{1/2}$ to produce correct RD at the point C_g. Since the required increase is small, rates again grow only by $\sim 10\%$.

Point	m_0	$m_{1/2}$	A_0	$\tan\beta$	Region
C_s	**94**	300	-1095	5	$\tilde{t}$-coan.
C_t	150	300	**-1120**	5	$\tilde{t}$-coan.
C_g	150	**294**	-1095	5	$\tilde{t}$-coan.
D_s	**440**	450	0	51	A-funnel
D_t	500	450	**150**	51	A-funnel
D_g	500	**724**	0	51	A-funnel
E_s	**1722**	300	0	10	HB/FP
F_s	**3607**	1000	0	10	HB/FP
F_g	3143	**806.5**	0	10	HB/FP
G_s	**2435**	130	-2000	10	h-funnel
G_t	2000	130	**-1680**	10	h-funnel

Table 2.3: Modified benchmark points for mSUGRA-seesaw in the case of large mixing with $R_{\nu u} = 1$ obtained from their counterparts in Table 2.1 by adjusting the parameter highlighted in boldface to produce the RD dictated by WMAP. All dimensionful parameters are in GeV. For all points $\mu > 0$ and $m_t = 171$ GeV.

In the A-funnel region [56, 60], $\mathbf{f}_\nu$ pushes the mass of the CP-odd Higgs boson A up and away from the resonance, resulting in a larger RD of 0.144 for point D. This can be reduced

[4]Hereafter we use subscripts s, t, and g to denote points obtained from those in Table 2.1 by adjusting the value of one the model parameters: *s*calar mass m_0, *t*rilinear coupling A_0, or *g*augino mass $m_{1/2}$, respectively. Single and double primes are used to further distinguish modified points in the large mixing with $R_{\nu u} = 3$ and the small mixing with $R_{\nu u} = 1$ scenarios.

by decreasing the scalar mass parameter (point D_s) or by increasing the value of the trilinear A-term (point D_t), which lowers the A mass back to the resonance regime. In both cases LFV rates increase by about 8%. Increasing the gaugino mass parameter can increase the $\widetilde{Z}_1$ mass to the resonance value $m_{\widetilde{Z}_1} = 0.5 m_A$. But the A mass also grows with $m_{1/2}$, although slower than the neutralino mass, so a large dialing is required, resulting in point D_g. This large change in $m_{1/2}$ increases the masses of charginos circulating in the loop resulting in about an order of magnitude drop of LFV rates.

In the lower part of the HB/FP region [59], at point E the RD is two orders of magnitude above the WMAP range. This is due to an increased value of μ from the $\mathbf{f}_\nu$ effect, which can be counteracted by increasing m_0, resulting in the new WMAP-allowed point E_s. The heavier sfermion spectrum causes LFV rates to decrease by about a factor of two. Adjustment of the trilinear parameter can somewhat lower μ [2], but not enough to get back into the HB/FP regime. It would be possible to reduce the RD by lowering $m_{1/2}$ to 189 GeV, but at this value the chargino mass falls below the LEP2 bound of 103.5 GeV [100].

In the upper portion of the HB/FP region, the neutrino Yukawa couplings have an extremely large effect – the RD at point F becomes 12.3. Similarly to point E, the RD can be lowered by increasing the scalar mass parameter. In this part of the HB/FP region the chargino mass is sufficiently high that $m_{1/2}$ can be lowered without violating the LEP2 chargino bound, resulting in a WMAP-allowed value at point F_g. Since charginos become lighter with this adjustment, LFV rates increase by about 40%.

In the light Higgs resonance region [56, 61], the neutrino Yukawa coupling also destabilizes the $\widetilde{Z}_1$ annihilation mechanism producing too large a RD at point G. Although neither the $\widetilde{Z}_1$ nor h masses are moved away from the desired regime $2m_{\widetilde{Z}_1} = m_h$, the resonance mechanism ceases to function because $\widetilde{Z}_1$ becomes bino-like and can no longer couple to the Higgs. The neutralino-higgs coupling can be restored by lowering μ by increasing the scalar mass. This decreases LFV rates by about 20%. The desired value of the neutralino-higgs coupling can also be achieved by adjustment of the trilinear parameter resulting in point G_t. In this case, the LFV rates increase only marginally compared to point G.

For $R_{\nu u} = 3$ case, we found that experimental limits (1.98) are satisfied for a GUT-scale Majorana mass matrix of the form

$$\mathbf{M}_N = diag\left(4.5 \times 10^{-6}, 4.5 \times 10^{-5}, 1\right) \cdot 1.3 \times 10^{15}\,\text{GeV}, \tag{2.17}$$

which we use in subsequent computations. This is a simple rescaling of Eq.(2.16) as expected from the seesaw formula. We have numerically verify that that dependence of the neutrino mixing parameters and LFV rates follow the same pattern shown in Fig. 2.2. Thus, rates on Figs. 2.3-2.6 are presented for the same choice of ϕ and χ discussed earlier.

As for $R_{\nu u} = 1$, the RD in points A and B remains unaffected by the presence of additional neutrino Yukawa couplings. However, the very large neutrino Yukawa generates large off-diagonal terms in the slepton mass matrix, as can be seen from Eq.(1.122), which boost LFV rates by more than an order of magnitude as compared to the $R_{\nu u} = 1$ case. Nevertheless, this is still not enough to rule out point B for the whole range of χ and ϕ values.

At point C, the RD is too large: the $\tilde{t}_1$ mass is pushed further away from the $\widetilde{Z}_1$ due to larger neutrino Yukawa effects. Thus restoration of the stop coannihilation mechanism requires larger adjustments of scalar mass and trilinear coupling parameters, leading to new WMAP-consistent points C'_s and C'_t listed in Table 2.4. Unlike the $R_{\nu u} = 1$ case, adjustment of $m_{1/2}$ cannot restore the stop-coannihilation: effects of $\mathbf{f}_\nu$ make $m_{\tilde{\tau}_1} < m_{\tilde{t}_1}$ and the RD is lowered to the WMAP range at $m_{1/2} = 725$ GeV by the stau-coannihilation mechanism. Increasing $m_{1/2}$ further makes $\tilde{\tau}_1$ the LSP before the stop-coannihilation regime can be reached.

In the A-funnel, larger neutrino Yukawas push m_A away from the resonance resulting in $\Omega_{\widetilde{Z}_1} h^2 = 0.33$ at point D. Lowering the scalar mass parameter can bring the A mass back into the resonance regime at point D'_s. The RD can also be lowered by either adjusting A_0 to -692 GeV or raising $m_{1/2}$ to 745 GeV. However, either of these bring the $\tilde{\tau}_1$ mass close to the $\widetilde{Z}_1$ mass and activate the stau-coannihilation mechanism; further dialing of either parameter makes $\tilde{\tau}_1$ the LSP.

In the HB/FP point E, μ is pushed by neutrino Yukawa couplings to very large values re-

Point	m_0	$m_{1/2}$	A_0	$\tan\beta$	Region
C'_s	**96**	300	-1095	5	$\tilde{t}$-coan.
C'_t	150	300	**-1197**	5	$\tilde{t}$-coan.
D'_s	**355**	450	0	51	A-funnel
E'_s	**6061.5**	300	0	10	HB/FP
F'_s	**7434**	1000	0	10	HB/FP
G'_s	**6530**	130	-2000	10	h-funnel

Table 2.4: Modified benchmark points for mSUGRA-seesaw in the case of large mixing with $R_{\nu u} = 3$ obtained from their counterparts in Table 2.1 by adjusting the parameter highlighted in boldface to produce the RD dictated by WMAP. All dimensionful parameters are in GeV. For all points $\mu > 0$ and $m_t = 171$ GeV.

sulting in large RD, $\Omega_{\widetilde{Z}_1} h^2 = 25$. To compensate, one needs to dial the scalar mass parameter to very high values (point E'_s). At such a large m_0, sleptons become very heavy causing LFV rates to drop by about two orders of magnitude. Consequently, rates for LFV muon decay and $\mu - e$ conversion fall below current limits for all χ and ϕ values. For this point, μ is so large that the HB/FP regime cannot be recovered by adjusting A_0 or $m_{1/2}$.

Similarly, for point F we get an extremly high relic density $\Omega_{\widetilde{Z}_1} h^2 = 72$ that can be compensated by a very large scalar mass at point F'_s. That will lower the LFV rates by a factor of ~ 15 so that muon LFV rates are below experimental bounds for all allowed mixing angles. As in the lower part of the HB/FP region, dialing A_0 or $m_{1/2}$ cannot bring $\Omega_{\widetilde{Z}_1} h^2$ back in accord with WMAP.

In the h-resonance point G, μ is pushed so high that $\widetilde{Z}_1$ becomes a pure bino state unable to couple to the Higgs boson. This can be compensated only by significantly increasing the scalar mass, yielding a new WMAP-consistent point G'_s with LFV rates that are smaller by two orders of magnitude.

2.4.2 Small mixing

For the case of small mixing, we set $\mathbf{f}_\nu(M_{GUT})$ according to Eq. (2.9) and choose the neutrino spectrum to be $m_{\nu_1} = 6 \times 10^{-4}$ eV, $m_{\nu_2} = 8 \times 10^{-3}$ eV and $m_{\nu_3} = 5 \times 10^{-2}$ eV. Our choice for m_{ν_1} is constrained by the fact that we need $M_{N_1} \gg M_{SUSY}$ for our approximation to

remain valid. In this scenario LFV rates do not depend on variations of neutrino mixing angles: Eq. (2.9) fixes the neutrino Yukawa matrix completely and perturbations of the structure of $\mathbf{M}_N$ do not produce significant changes in RGE evolution, as can be seen from Eq. (1.122).

For $R_{\nu u} = 1$, the full RGE evolution with our code yields the following eigenvalues of the Majorana mass matrix:

$$M_{N_1} \simeq 8 \times 10^4 \,\text{GeV}, \; M_{N_2} \simeq 3.5 \times 10^9 \,\text{GeV}, \; M_{N_3} \simeq 2.5 \times 10^{15} \,\text{GeV}. \tag{2.18}$$

This would appear to be in conflict with thermal leptogenesis, which requires the lightest Majorana mass to be heavier than about 10^9 GeV [101]. Nevertheless, successful leptogenesis is possible through the decay of the next-to-lightest RHN [102]. Also notice that M_{N_3} is closer to M_{GUT} than it was in the case of large mixing. This, combined with small mixing in $\mathbf{f}_\nu$, leads to LFV rates that are several orders of magnitude smaller, putting them all significantly below current experimental bounds, as shown in Figs. 2.7, 2.8 and 2.9.

As discussed in Section 2.4.1, the use of mSUGRA values at points A and B still produces the correct RD. For example, at point A we have $BR(\mu \to e\gamma) = 1.1 \times 10^{-13}$ which is barely above the reach of the future MEG experiment. In the A-funnel, neutrino Yukawa couplings do affect the annihilation mechanism, but the effect is small and the RD remains within the WMAP range. For the other regions, adjustment of SSB parameters is necessary; the modified points are listed in Table 2.5.

Even a decoupling scale as high as $M_{N_3} \sim 10^{15}$ GeV is enough to destabilize the stop-coannihilation mechanism, resulting in too large a RD for point C. Lowering the scalar mass parameter decreases the $\tilde{t}_1$ mass to the desired RD value at point C_s'', leading to a $\sim 50\%$ increase in LFV rates. The stop coannihilation mechanism can also be restored by adjusting the trilinear A-term (point C_t'') or the gaugino mass (point C_g''). In both cases LFV rates increase only slightly from those for point C. At all points $\mu \to e\gamma$ rates are slightly below the MEG reach, so this region will only be probed by $\mu \to e$ conversion experiments.

At point E, the RD is also too high. For the reasons discussed in section 2.4.1, only ad-

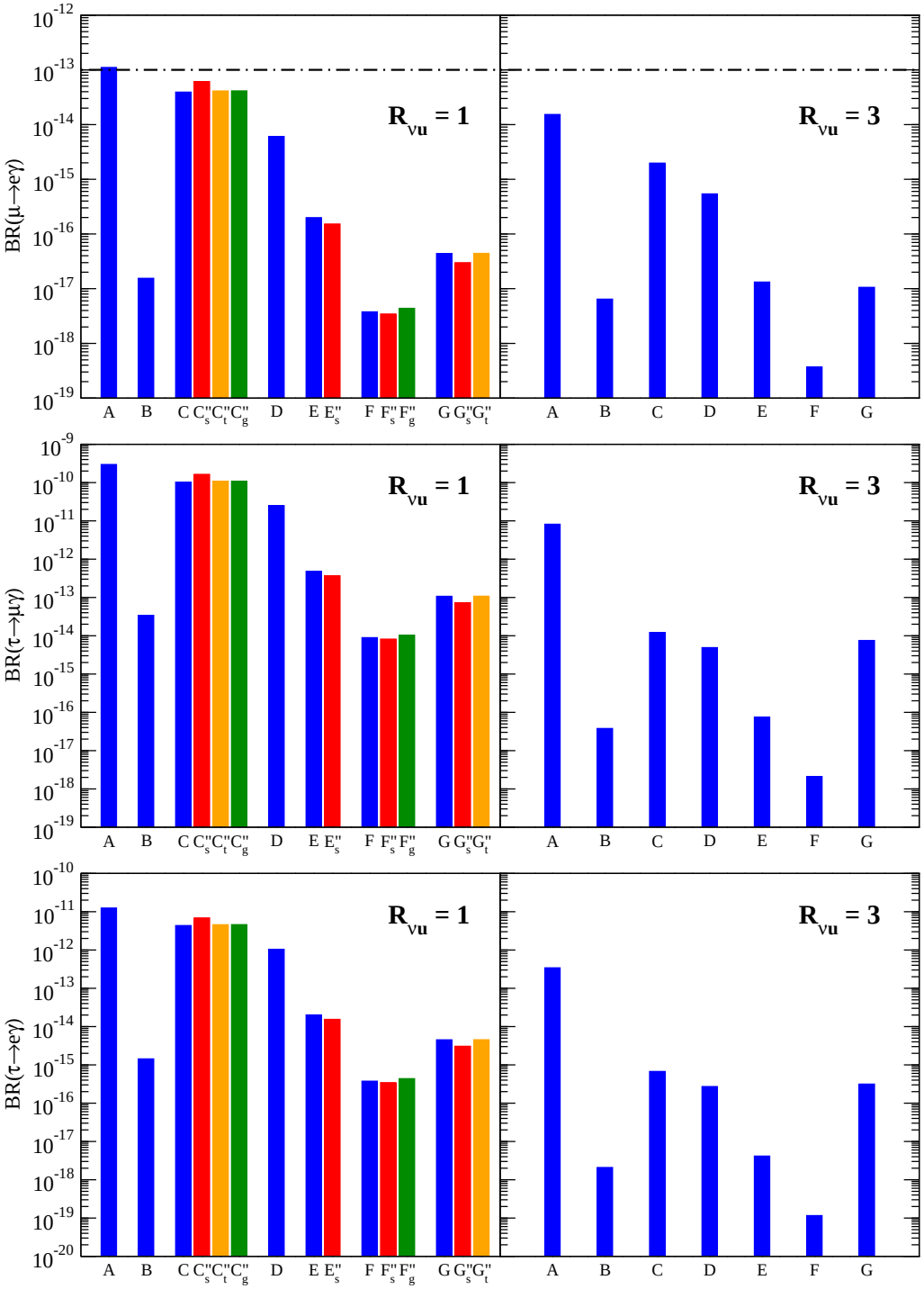

Figure 2.7: Radiative LFV decay rates for the small mixing case for benchmark points presented in Tables 2.1 and 2.5. All rates are below current experimental bounds. Dash-dotted lines represent the projected future sensitivity listed in Table 1.3.

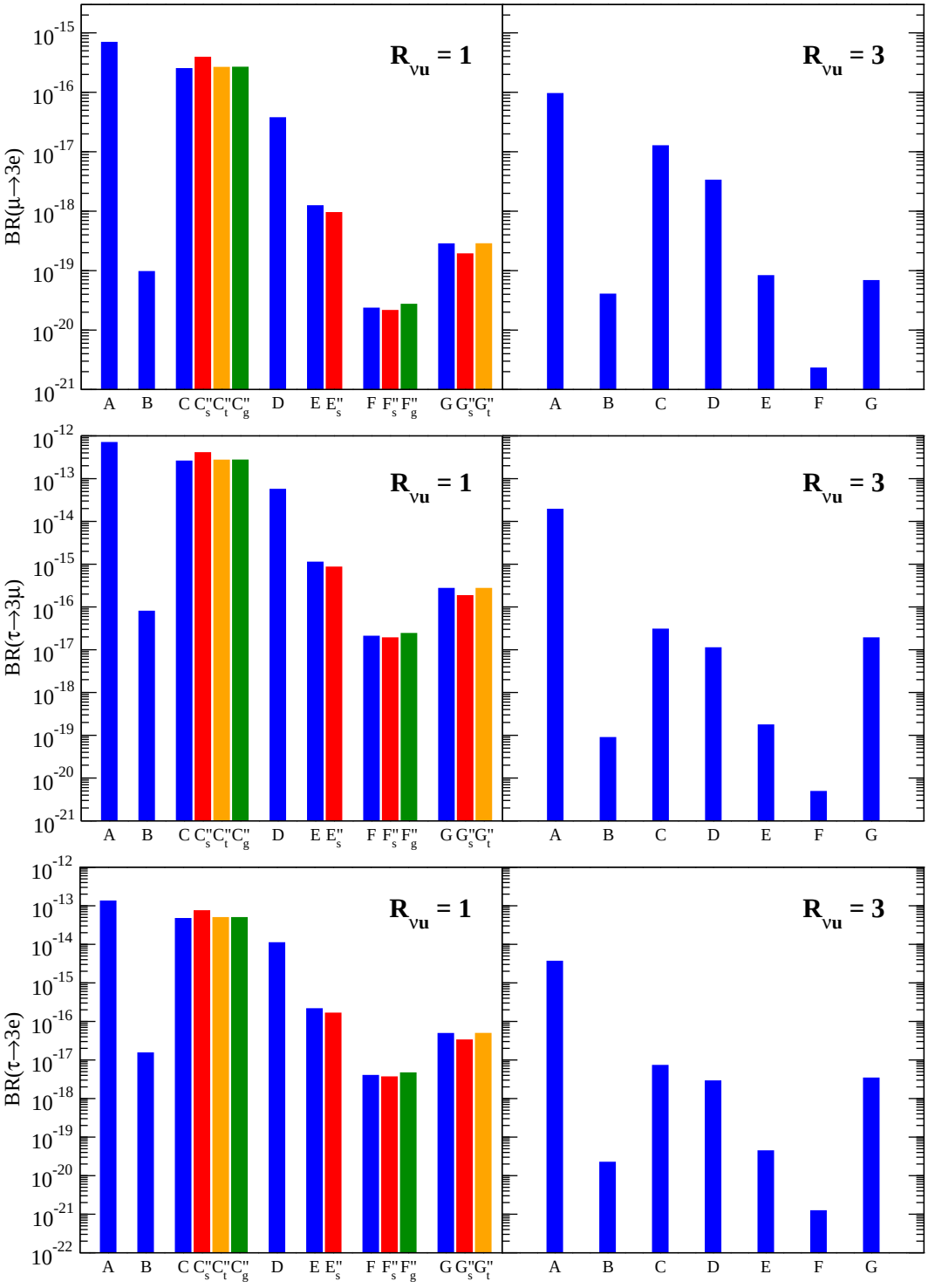

Figure 2.8: Similar to Fig. 2.7 for trilepton LFV decays.

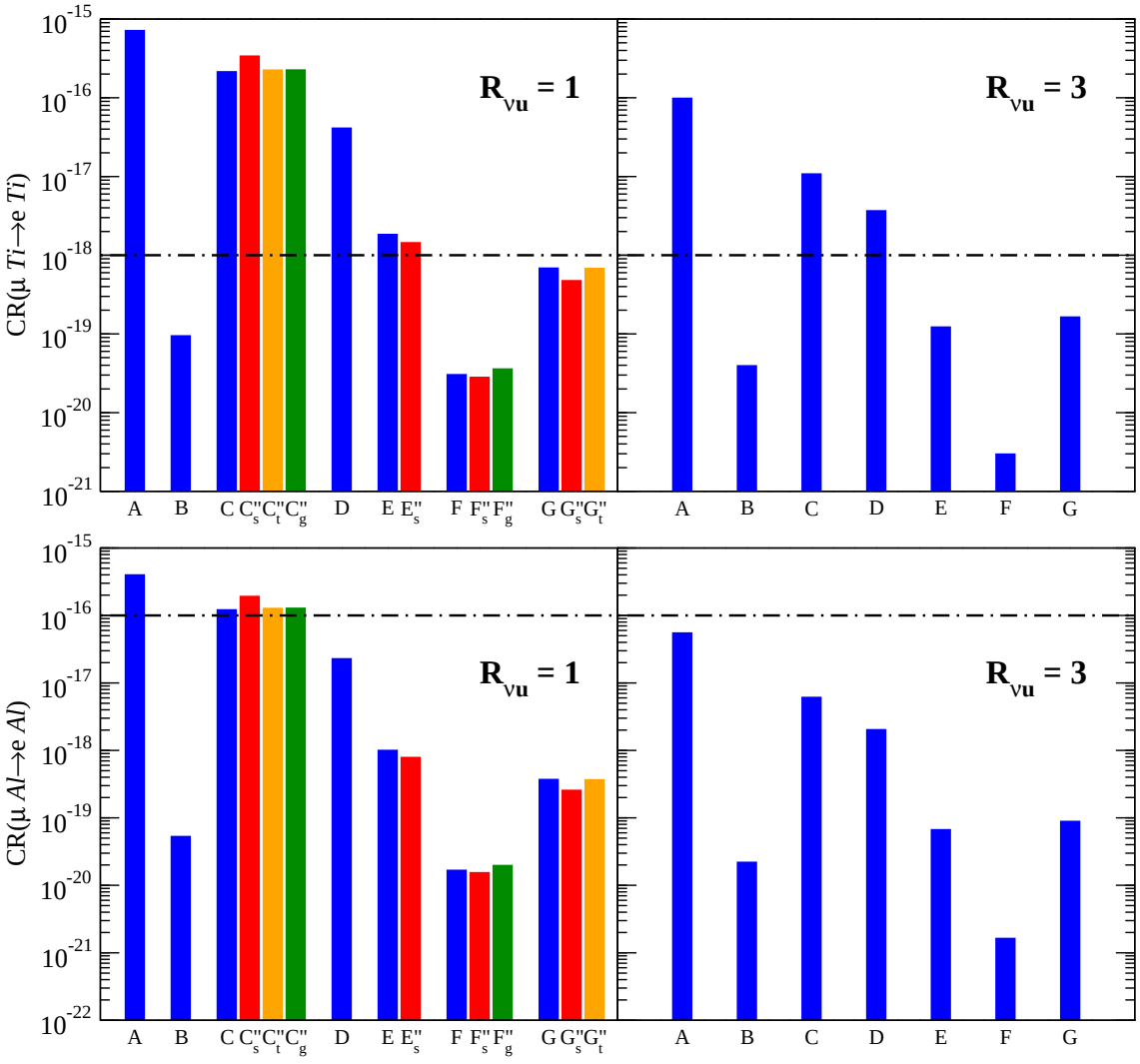

Figure 2.9: Similar to Fig. 2.7 for LFV conversion rates for titanium (top frame) and aluminum (bottom frame) targets.

Point	m_0	$m_{1/2}$	A_0	$\tan\beta$	Region
C_s''	**126**	300	-1095	5	$\tilde{t}$-coan.
C_t''	150	300	**-1106**	5	$\tilde{t}$-coan.
C_g''	150	**297**	-1095	5	$\tilde{t}$-coan.
E_s''	**1505**	300	0	10	HB/FP
F_s''	**3300**	1000	0	10	HB/FP
F_g''	3143	**943**	0	10	HB/FP
G_s''	**2205**	130	-2000	10	h-funnel
G_t''	2000	130	**-1895**	10	h-funnel

Table 2.5: Modified benchmark points for mSUGRA-seesaw in case of the small mixing with $R_{\nu u} = 1$ obtained form their counterparts in Table 2.1 by adjusting one parameter highlighted in boldface. to produce RD in the WMAP range (2.1). All dimensionful parameters are in GeV units. For all points $\mu > 0$ and $m_t = 171$ GeV.

justment of m_0 is possible, leading to consistency with WMAP range for the values at point E_s''. Since the required shift is not as significant as in the large mixing case, the LFV rates drop by only $\sim 30\%$.

In the upper part of the HB/FP region at point D, the RD exceeds the WMAP value by two orders of magnitude. The desired higgsino content of $\widetilde{Z}_1$ can be restored by adjusting the scalar or gaugino mass parameters, giving points F_s'' and F_g'' respectively. As a result, the LFV rates change by about 10% with respect to those at point D.

At point F, the higgsino content of $\widetilde{Z}_1$ is diminished by neutrino Yukawa RGE effects resulting in too high a RD. The h-resonance mechanism can be restored by adjusting the scalar mass (point G_s'') or the trilinear A-term (point G_t''). These adjustments change the LFV rates by approximately a factor of two with respect to the prediction for point F.

For $R_{\nu u} = 3$, we find the eigenvalues of the Majorana mass matrix to be

$$M_{N_1} \simeq 7 \times 10^5 \,\text{GeV},\ M_{N_2} \simeq 3 \times 10^{10} \,\text{GeV},\ M_{N_3} \simeq 2.2 \times 10^{16} \,\text{GeV}. \tag{2.19}$$

The heaviest Majorana mass value is very close to $M_{GUT} \simeq 2.3 \times 10^{16}$ GeV. Because of this, the effect of $\mathbf{f}_\nu$ on RD is negligible and WMAP-consistent values are obtained for the mSUGRA points in Table 2.1. From the resultant LFV rates on Figs.2.7-2.9, we see that the larger neutrino Yukawa coupling produces LFV rates that are smaller by almost an order of magnitude. This is

the opposite of what we saw in the large mixing scenarios where $R_{\nu u} = 3$ rates were more than an order of magnitude greater that their $R_{\nu u} = 1$ cousins. This is also a direct consequence of the proximity of M_{N_3} to M_{GUT}: the largest neutrino Yukawa decouples almost immediately and off-diagonal elements in the slepton doublet matrix are generated by the much smaller Yukawas of the first and second generations.

2.5 Discussion

We have perfomed a detailed study of LFV rates at the RD-allowed benchmark points, and demonstrated that the interconnection between the neutrino sector and neutralino dark matter is very important for predictions of the LFV rates. Proper consideration of these effects change LFV rates by factors of a few to up to two orders of magnitude. We emphasize that although we used $SO(10)$ models to set the structure of the neutrino Yukawa matrix at the GUT scale, our results are generic; they will hold in any type-I SUSY-seesaw scenario with large neutrino Yukawa couplings.

The results in section 2.4 imply the following observations about models with universal (or mSUGRA-like) SSB boundary conditions stipulated at the GUT scale:

- The small mixing scenario is completely consistent with present experimental bounds on LFV. Upcoming $\mu \to e\gamma$ experiments will probe only a very small corner of parameter space where both m_0 and $m_{1/2}$ are small and $R_{\nu u} = 1$. Future $\mu \to e$ conversion experiments, although suppressed by a factor $\sim Z\alpha/\pi$ with respect to $\mu \to e\gamma$, have better prospects due to the very well defined experimental signal. The PRIME experiment [36] will be able to probe the entire bulk and stop-coannihilation regions as well as a significant portion of the A-funnel region, while the Mu2e experiment [32] will only be able to probe the bulk and stop-coannihilation regions for $R_{\nu u} = 1$.

- Contrary to naive expectations, in the small mixing case, LFV rates are expected to be about an order of magnitude *smaller* for $R_{\nu u} = 3$ than for $R_{\nu u} = 1$. Such small rates will only be probed by PRIME $\mu - e$ conversion experiment with a Ti target.

- Future $\mu \to e\gamma$ measurements will not rule out large mixing scenarios for any values of ϕ and χ in the mixing matrix of Eq. (2.7) because of the high sensitivy of this channel to the value of θ_{13}. On the other hand, if θ_{13} is close to the CHOOZ bound, only the HB/FP and h-funnel regions are consistent with current limits.

- The $\tau \to \mu\gamma$ channel is an excellent probe as it is not sensitive to θ_{13}. Current experimental limits exclude the bulk region and the stop-coannihilation regions. For large $R_{\nu u}$, part of the A-funnel region is also excluded. Future experiments at Super Flavor factories [34] should be able to probe the A-funnel region almost entirely.

- Trilepton decays are weaker probes due to a factor $\sim \alpha$ suppression of the rates as compared to the two body modes. Nevertheless, current data rule out large θ_{13} close to the CHOOZ bound for some regions of SUSY parameter space.

- $\mu \to e$ conversion in nuclei is the best probe of LFV. Future experiments will have sensitivity to almost the entire parameter space. In the large mixing case, the $\mu \to e$ conversion searches are highly complementary to collider ones: they can probe large parts of the HB/FP region which cannot be probed at the LHC.

The upcoming Daya Bay and Double Chooz and Daya Bay experiments will soon be able to probe θ_{13} independently of the Dirac phase down to $\sin^2\theta_{13} = 0.0020$. A signal of nonzero θ_{13} will significantly reduce uncertainties in the predictions of LFV rates if the observed neutrino mixing arises dominantly from $\mathbf{f}_\nu$ as in the large mixing case. The θ_{13}-dependent LFV rates will be within about two orders of magnitude of the maximal value shown in Figs. 2.3-2.9 thus further constraining model parameter space with current LFV data. For instance, current $\mu \to e\gamma$ bound rules out a significant portion of the A-funnel for the case of large mixing and either value of $R_{\nu u}$. With future $\mu \to e\gamma$ measurements we will be able tell if the type-I SUSY-seesaw can be realized in the stau-coannihilation region with large f_ν mixing regardless of $R_{\nu u}$; see point B in Fig. 2.3.

If the LHC finds signals of SUSY, then GUTs become very appealing. It may become possible to combine the knowledge of the sparticle spectrum from the LHC with results from LFV

experiments to determine the value of $R_{\nu u}$, or to extract some information about the mixing pattern in the neutrino Yukawas. For example, if SUSY is found to be realized in the bulk region (point A), then a type-I SUSY-seesaw can only exist if the mixing in $\mathbf{f}_\nu$ is small. Then measurements from the PRIME experiment could be used to identify $R_{\nu u}$. The situation becomes even more favorable if θ_{13} is known. For example, if SUSY is found to be consistent with the A-funnel region, then with the value of θ_{13} in hand, PRIME measurements will be able to test if the type-I SUSY-seesaw is operative, for all mixing patterns and $R_{\nu u}$ values.

2.6 Conclusions

Previous work by collaborators [18] demonstrated that large neutrino Yukawa couplings can significantly affect the neutralino relic density. This effect can be counteracted by the adjustment of SSB parameters, with concomitant changes in the low-energy phenomenology. In this work, we studied LFV processes in the type-I SUSY-seesaw properly taking into account neutrino Yukawa effects on the neutralino RD. For simplicity, we considered a scenario with flavor-blind universal (or mSUGRA-like) boundary conditions defined at the GUT scale. In the neutrino sector we utilized the "top-down" approach in which neutrino Yukawa and Majorana mass matrices are inputs at M_{GUT}. We considered two cases for neutrino-up quark unification parameter $R_{\nu u}$ (see Eq. 2.5) that are inspired by $SO(10)$ models. For each scenario we examined two extreme cases for the mixing in the neutrino Yukawa matrix. We found that the common practice of using WMAP allowed points of mSUGRA in models with RHNs overestimates the LFV rates in most regions of parameter space.

In the $R_{\nu u} = 1$ case we found that the neutrino-neutralino interplay can result in significant changes in LFV predictions. The rates can change by a factor of up to 5 in the WMAP-allowed regions compared to naive estimates. These effects are most prominent in regions with a large scalar mass parameter m_0 such as the HP/FP and h-funnel regions. If the mixing in the neutrino Yukawa matrix is small, then all LFV rates are below current experimental bounds. In the future, this case can be probed to some extent by the MEG experiment and by the PRIME and Mu2e

conversion experiments.

The case of a very large unification parameter $R_{\nu u} = 3$, contrary to common lore, is not ruled out by current bounds on LFV processes even if the mixing in the neutrino Yukawa matrix is large. In the large mixing case a proper treatment of neutralino-neutrino interplay leads to LFV rates to be smaller by about two order of magnitude than naively expected. As a result, many rates fall below current limits. Surprisingly, we found that if mixing in the neutrino Yukawa matrix is small, then for $R_{\nu u} = 3$, the LFV rates that are an order of magnitude smaller than for $R_{\nu u} = 1$. If this scenario is realized, then only the future PRIME experiment will have sensitivity to some regions of the parameter space.

Appendices

Appendix A

Yukawa RGEs

The following are the 1-loop RGEs for MSSM Yukawa coupling matrices with sparticle/higgs thresholds from Ref. [79] with corrections from their unpublished erratum implemented.

$$
\begin{aligned}
(4\pi)^2\frac{d(\mathbf{f}_u^{\mathrm{T}})_{ij}}{dt} &= \frac{3}{2}\left(s^2\theta_h + c^2\theta_H\right)(\mathbf{f}_u^{\mathrm{T}}\mathbf{f}_u^*\mathbf{f}_u^{\mathrm{T}})_{ij} + \frac{1}{2}\left(c^2\theta_{\tilde{h}} + s^2\theta_{\tilde{h}}\right)\sum_{k=1}^{N_{\tilde{d}}}(\mathbf{f}_d^{\mathrm{T}})_{ik}(\mathbf{f}_d^*)_{kl}(\mathbf{f}_u^{\mathrm{T}})_{lj} \qquad \text{(A.1)}\\
&+\frac{1}{2}\left(s^2\theta_{\tilde{h}} + c^2\theta_{\tilde{h}}\right)\left[2(\mathbf{f}_u^{\mathrm{T}})_{il}\sum_{k=1}^{N_{\tilde{Q}}}(\mathbf{f}_u^*)_{lk}(\mathbf{f}_u^{\mathrm{T}})_{kj} + \sum_{k=1}^{N_{\tilde{u}}}(\mathbf{f}_u^{\mathrm{T}})_{ik}(\mathbf{f}_u^*)_{kl}(\mathbf{f}_u^{\mathrm{T}})_{lj}\right]\\
&+\frac{1}{2}\left(c^2\theta_h + s^2\theta_H - 4c^2(\theta_h - \theta_H)\right)(\mathbf{f}_d^{\mathrm{T}}\mathbf{f}_d^*\mathbf{f}_u^{\mathrm{T}})_{ij}\\
&+(\mathbf{f}_u^{\mathrm{T}})_{ij}\left[(s^2\theta_h + c^2)\,\mathrm{Tr}\{3\mathbf{f}_u^*\mathbf{f}_u^{\mathrm{T}}\} + c^2(\theta_h - 1)\,\mathrm{Tr}\{3\mathbf{f}_d^*\mathbf{f}_d^{\mathrm{T}} + \mathbf{f}_e^*\mathbf{f}_e^{\mathrm{T}}\}\right]\\
&-(\mathbf{f}_u^{\mathrm{T}})_{ij}\left[\frac{3}{5}g_1^2\left\{\frac{17}{12} + \frac{3}{4}\theta_{\tilde{h}} - \left(\frac{1}{36}\theta_{\tilde{Q}_j} + \frac{4}{9}\theta_{\tilde{u}_i} + \frac{1}{4}\theta_{\tilde{h}}\right)\theta_{\tilde{B}}\right\}\right.\\
&\qquad\left. +g_2^2\left\{\frac{9}{4} + \frac{9}{4}\theta_{\tilde{h}} - \frac{3}{4}\left(\theta_{\tilde{Q}_j} + \theta_{\tilde{h}}\right)\theta_{\tilde{W}}\right\} + g_3^2\left\{8 - \frac{4}{3}\left(\theta_{\tilde{Q}_j} + \theta_{\tilde{u}_i}\right)\theta_{\tilde{g}}\right\}\right],
\end{aligned}
$$

$$
\begin{aligned}
(4\pi)^2\frac{d(\mathbf{f}_d^{\mathrm{T}})_{ij}}{dt} &= \frac{3}{2}\left(c^2\theta_h + s^2\theta_H\right)(\mathbf{f}_d^{\mathrm{T}}\mathbf{f}_d^*\mathbf{f}_d^{\mathrm{T}})_{ij} + \frac{1}{2}\left(s^2\theta_{\tilde{h}} + c^2\theta_{\tilde{h}}\right)\sum_{k=1}^{N_{\tilde{u}}}(\mathbf{f}_u^{\mathrm{T}})_{ik}(\mathbf{f}_u^*)_{kl}(\mathbf{f}_d^{\mathrm{T}})_{lj} \qquad \text{(A.2)}\\
&+\frac{1}{2}\left(c^2\theta_{\tilde{h}} + s^2\theta_{\tilde{h}}\right)\left[2(\mathbf{f}_d^{\mathrm{T}})_{il}\sum_{k=1}^{N_{\tilde{Q}}}(\mathbf{f}_d^*)_{lk}(\mathbf{f}_d^{\mathrm{T}})_{kj} + \sum_{k=1}^{N_{\tilde{d}}}(\mathbf{f}_d^{\mathrm{T}})_{ik}(\mathbf{f}_d^*)_{kl}(\mathbf{f}_d^{\mathrm{T}})_{lj}\right]\\
&+\frac{1}{2}\left(s^2\theta_h + c^2\theta_H - 4s^2(\theta_h - \theta_H)\right)(\mathbf{f}_u^{\mathrm{T}}\mathbf{f}_u^*\mathbf{f}_d^{\mathrm{T}})_{ij}\\
&+(\mathbf{f}_d^{\mathrm{T}})_{ij}\left[s^2(\theta_h - 1)\,\mathrm{Tr}\{3\mathbf{f}_u^*\mathbf{f}_u^{\mathrm{T}}\} + (c^2\theta_h + s^2)\,\mathrm{Tr}\{3\mathbf{f}_d^*\mathbf{f}_d^{\mathrm{T}} + \mathbf{f}_e^*\mathbf{f}_e^{\mathrm{T}}\}\right]\\
&-(\mathbf{f}_d^{\mathrm{T}})_{ij}\left[\frac{3}{5}g_1^2\left\{\frac{5}{12} + \frac{3}{4}\theta_{\tilde{h}} - \left(\frac{1}{36}\theta_{\tilde{Q}_j} + \frac{1}{9}\theta_{\tilde{d}_i} + \frac{1}{4}\theta_{\tilde{h}}\right)\theta_{\tilde{B}}\right\}\right.\\
&\qquad\left. +g_2^2\left\{\frac{9}{4} + \frac{9}{4}\theta_{\tilde{h}} - \frac{3}{4}\left(\theta_{\tilde{Q}_j} + \theta_{\tilde{h}}\right)\theta_{\tilde{W}}\right\} + g_3^2\left\{8 - \frac{4}{3}\left(\theta_{\tilde{Q}_j} + \theta_{\tilde{d}_i}\right)\theta_{\tilde{g}}\right\}\right],
\end{aligned}
$$

$$
\begin{aligned}
(4\pi)^2 \frac{d(\mathbf{f}_e^{\mathrm{T}})_{ij}}{dt} &= \frac{3}{2}\left(c^2\theta_h + s^2\theta_H\right)(\mathbf{f}_e^{\mathrm{T}}\mathbf{f}_e^{*}\mathbf{f}_e^{\mathrm{T}})_{ij} \\
&+\frac{1}{2}\left(c^2\theta_{\tilde{h}} + s^2\theta_{\tilde{h}}\right)\left[2(\mathbf{f}_e^{\mathrm{T}})_{il}\sum_{k=1}^{N_{\tilde{L}}}(\mathbf{f}_e^{*})_{lk}(\mathbf{f}_e^{\mathrm{T}})_{kj} + \sum_{k=1}^{N_{\tilde{e}}}(\mathbf{f}_e^{\mathrm{T}})_{ik}(\mathbf{f}_e^{*})_{kl}(\mathbf{f}_e^{\mathrm{T}})_{lj}\right] \\
&+(\mathbf{f}_e^{\mathrm{T}})_{ij}\left[s^2(\theta_h - 1)\,\mathrm{Tr}\{3\mathbf{f}_u^{*}\mathbf{f}_u^{\mathrm{T}}\} + (c^2\theta_h + s^2)\,\mathrm{Tr}\{3\mathbf{f}_d^{*}\mathbf{f}_d^{\mathrm{T}} + \mathbf{f}_e^{*}\mathbf{f}_e^{\mathrm{T}}\}\right] \\
&-(\mathbf{f}_e^{\mathrm{T}})_{ij}\left[\frac{3}{5}g_1^2\left\{\frac{15}{4} + \frac{3}{4}\theta_{\tilde{h}} - \left(\frac{1}{4}\theta_{\tilde{L}_j} + \theta_{\tilde{e}_i} + \frac{1}{4}\theta_{\tilde{h}}\right)\theta_{\tilde{B}}\right\}\right. \\
&\qquad\left.+g_2^2\left\{\frac{9}{4} + \frac{9}{4}\theta_{\tilde{h}} - \frac{3}{4}\left(\theta_{\tilde{L}_j} + \theta_{\tilde{h}}\right)\theta_{\tilde{W}}\right\}\right],
\end{aligned}
\tag{A.3}
$$

where $s = \sin\alpha$, $c = \cos\alpha$, α is Higgs mixing angle and the various $\theta_{\mathcal{P}}$'s are equal to zero below the mass threshold of the respective particle and equal to one above it. The contributions from neutrino Yukawa couplings can be found in Refs. [39, 51].

Appendix B

Detailed code description

Here we give descriptions of the major routines in Isajet-M. (The reader is referred to the schematic description of the code in Sec. (2.3) for an understanding of the basic layout.) First we summarize the contents of the important *common blocks* (global variables), and then outline the behavior of many Isajet-M procedures. High-level pseudocode is presented for the most important ones; for other major routines we describe the input and output parameters and give a overview of their behavior. For minor subroutines we provide a brief description of their effects. Only those routines that were significantly altered in Isajet-M or are important to understanding the flow of the code are described here.

All floating-point variables are double precision (REAL*8) unless otherwise noted. Complex variables are also double-precision unless otherwise noted.

B.1 Common blocks

Isajet makes extensive use of many common blocks to share information among its components and their various routines. Isajet-M modifies and extends a number of preexisting Isajet blocks as well as using several of its own. The contents of the most important of these are listed below.

/SSPAR/

Contains output mass and mixing parameters for most SUSY particles (at M_{SUSY}).

AMGLSS = gluino mass
AMULSS = up-left squark mass
AMELSS = left-selectron mass
AMERSS = right-slepton mass
AMNiSS = sneutrino mass for generation i
TWOM1 = Higgsino mass = $-mu$
RV2V1 = ratio v_2/v_1 of vevs
AMfLSS,AMfRSS = left,right stop/sbottom/stau masses for f=T,B,L
AMf1SS,AMf2SS = light,heavy stop/sbottom/stau masses for f=T,B,L
AMZiSS = signed mass of Z_i
ZMIXSS = Z_i mixing matrix
AMWiSS = signed W_i mass
GAMMAL,GAMMAR = W_i left, right mixing angles
AMHL,AMHH,AMHA = neutral Higgs h, H, A masses
AMHC = charged Higgs H^+ mass
ALFAH = Higgs mixing angle
AAf = stop/sbottom/stau trilinear term for f=T,B,L
THETAf = stop/sbottom/stau mixing angle for f=T,B,L
AMGVSS = gravitino mass
MTQ = top mass at MSUSY
MBQ = bottom mass at MSUSY
MLQ = tau mass at MSUSY
FBMA = b-Yukawa at m_A scale
VUQ = H_u vev at MSUSY
VDQ = H_d vev at MSUSY
SGNM3 = sign of gaugino mass M_3

/SSSM/

Standard Model experimental input parameters. Set by SMSET at the beginning of the main program.

AMUP,...,AMTP = quark pole masses
AMBMB = b-quark running mass in MSbar at mb scale
AME,AMMU,AMTAU = lepton pole masses
AMW,AMZ = W,Z pole masses
GAMW,GAMZ = W,Z widths
ALFAEM,ALFA3 = SM couplings in MSbar at Z scale
SN2THW = $\sin^2\theta_w$ in MSbar
ALQCD4 = 4-flavor lambda QCD
AS12,AS13,AS23 = sin of quark mixing angles
DELCKM = CKM phase

/SSNU/

Stores parameters in the neutrino sector.

```
AMNUi               = neutrino masses in eV
ATH12,ATH13,ATH23   = neutrino mixing angles in rad
DM2SOL              = solar mass^2 difference in eV
DM2ATM              = atmospheric mass^2 difference in eV
MNULIT              = mass of the lightest neutrino in eV
APHDIR              = Dirac phase
APHI1,APHI2         = Majorana phases
APHE,APHMU,APHTAU   = unphysical phases in e,mu,tau
EPSNU               = ratio of f_nu to f_u yukawas at MGUT
TBCHI,TBPHI         = parameters for tri-bimaximal mixing matrix at MGUT
FTRHLD              = Majorana mass threshold factors
LND5ON              = logical flag to take into account evolution
                      of dim-5 effective neutrino operator
IRHN                = integer flag on f_nu approach
                      =0 = no RH neutrinos
                      =1 = bottom-up
                      =2 = top-down with f_nu ~ f_u at MGUT
                      =3 = top-down with tri-bimaximal f_nu(MGUT)
                      =7 = top-down with custom f_nu(MGUT)
SMQHCPL             = SM quartic Higgs coupling at MZ
```

/MSSDEC/

Stores the decoupling scales of the sfermions & RHNs.

```
MSQDEC(i)  = i-th generation of squark doublet
MSLDEC(i)  = i-th generation of slepton doublet
MSUDEC(i)  = i-th generation of up squark singlet
MSDDEC(i)  = i-th generation of down squark singlet
MSEDEC(i)  = i-th generation of charged lepton singlet
MRNDEC(i)  = i-th generation of RH neutrino
MSHDEC     = higgsino
MHHDEC     = heavy higgses
MSGDEC     = gluino
MSBDEC     = bino
MSWDEC     = wino
```

/FROT/

Stores the complex fermion rotation matrices at $M_{\rm Z}$ and M_{SUSY}, in the normal convention $m \sim V_R \, \mathbf{f}^{\rm T} V_L^\dagger$.

```
VER,VEL          = charged lepton rotation matrices at MZ
VUR,VUL,VDR,VDL  = up and down quark rotation matrices at MZ
VxxQ             = corresponding fermion rotation matrices at MSUSY
```

/YUKQ/

FUQ(3),FDQ(3),FLQ(3) contain the diagonalized lepton Yukawa couplings at M_{SUSY}.

/FROTPAR/

The integer switches controlling fermion rotation behavior in Isajet-M. These are used to select the desired mixing scheme in the quark and lepton sectors, and to choose whether to keep track of complex phases in those sectors.

```
Fermion rotation scheme selection:
IQROT    quark mixing scheme parameter
         =0 - dominant 3rd family
         =1 - unmixed
         =2 - CKM mixing in up quarks (f_u ~ CKM^T m_u CKM^*,   f_d ~ m_d)
         =3 - CKM mixing in down quarks (f_u ~ m_u,   f_d ~ CKM^* m_d CKM^T)
         =4 - CKM mixing in left up quarks (f_u ~ CKM^T m_u,   f_d ~ m_d)
         =5 - CKM mixing in left down quarks (f_u ~ m_u,   f_d ~ CKM^* m_d)
         =6 - custom rotation scheme
ILROT    charged lepton mixing scheme parameter
         =0 - dominant 3rd family
         =1 - unmixed
         =6 - custom rotation scheme
Switches for phases [0=off, 1=on]:
IQPHASE  for quark sector
ILPHASE  for charged lepton sector
INPHASE  for RH neutrino sector
```

/NRDCPL/

/NRDCPL/NRrot(3,3,i) stores the complex rotation matrix for the ith RHN at its decoupling scale. It is used by NRACTIV and NRDECOP when changing basis at each RHN's activation/deactivation.

/SUGCOUPL/

Stores SM couplings in $\overline{DR}$ at $M_{\rm Z}$.

```
DASMZ      = alpha_strong
YEMZ(3,3)  = complex charged leptons Yukawa matrix
YUMZ(3,3)  = complex up quarks Yukawa matrix
YDMZ(3,3)  = complex down quarks Yukawa matrix
KAMZ(3,3)  = complex matrix of dim-5 effective neutrino operator kappa
```

/SUPSSB/

The 3×3 complex SSB sfermion matrices in the super-CKM basis.

```
sM2Qu  = squark doublet mass^2 rotated in parallel with left up quarks
sM2Qd  = squark doublet mass^2 rotated in parallel with left down quarks
sM2U   = up-squark singlet mass^2 rotated in parallel with right up quarks
sM2D   = down-squark singlet mass^2 rotated in parallel with right down quarks
sM2L   = charged slepton doublet mass^2
sM2E   = charged slepton singlet mass^2
sTU    = up squark trilinear coupling
sTD    = down squark trilinear coupling
sTE    = charged slepton trilinear coupling
```

/SUGMG/

The frozen-out couplings and masses from the RGEs at M_{GUT}.

```
  Couplings:
  GSS( 1)  = g_1      GSS( 2)  = g_2       GSS( 3)  = g_3
  GSS( 4)  = y_tau    GSS( 5)  = y_b       GSS( 6)  = y_t
  GSS( 7)  = M_1      GSS( 8)  = M_2       GSS( 9)  = M_3
  GSS(10)  = A_tau    GSS(11)  = A_b       GSS(12)  = A_t
  GSS(13)  = M_hd^2   GSS(14)  = M_hu^2    GSS(15)  = M_er^2
  GSS(16)  = M_el^2   GSS(17)  = M_dnr^2   GSS(18)  = M_upr^2
  GSS(19)  = M_upl^2  GSS(20)  = M_taur^2  GSS(21)  = M_taul^2
  GSS(22)  = M_btr^2  GSS(23)  = M_tpr^2   GSS(24)  = M_tpl^2
  GSS(25)  = mu       GSS(26)  = B         GSS(27)  = Y_N
  GSS(28)  = M_nr     GSS(29)  = A_n       GSS(30)  = vdq
  GSS(31)  = vuq      GSS(32)  = M_dnl^2   GSS(33)  = M_btl^2
  Masses:
  MSS( 1)  = glss     MSS( 2)  = upl       MSS( 3)  = upr
  MSS( 4)  = dnl      MSS( 5)  = dnr       MSS( 6)  = stl
  MSS( 7)  = str      MSS( 8)  = chl       MSS( 9)  = chr
  MSS(10)  = b1       MSS(11)  = b2        MSS(12)  = t1
  MSS(13)  = t2       MSS(14)  = nuel      MSS(15)  = numl
  MSS(16)  = nutl     MSS(17)  = el-       MSS(18)  = er-
  MSS(19)  = mul-     MSS(20)  = mur-      MSS(21)  = tau1
  MSS(22)  = tau2     MSS(23)  = z1ss      MSS(24)  = z2ss
  MSS(25)  = z3ss     MSS(26)  = z4ss      MSS(27)  = w1ss
  MSS(28)  = w2ss     MSS(29)  = hl0       MSS(30)  = hh0
  MSS(31)  = ha0      MSS(32)  = h+
  Unification:
  MGUTSS   = M_GUT    GGUTSS   = g_GUT     AGUTSS   = alpha_GUT
                      G3GUTSS  = g3_GUT    A3GUTSS  = alpha3_GUT
```

/SUGXIN/

Contains the inputs (model parameters) to the main routine SUGRA. Not all of these are relevant at the same time, since they describe several different SUSY-breaking models. In the current work, only the mSUGRA parameters are used. Note the /SUGXIN/XNRIN array is used only by legacy Isajet; Isajet-M uses the /SUGXIN/XRHNIN array instead.

Also contains the /SUGXIN/XISAIN array, which contains MSSM mass, coupling, etc. *outputs*, for use by Isajet routines to calculate physical masses and decays. We will not list this array; see the Isajet documentation[70] for details.

```
XSUGIN(1)      = M_0           XSUGIN(2)  = M_(1/2)  XSUGIN(3)  = A_0
XSUGIN(4)      = tan(beta)     XSUGIN(5)  = sgn(mu)  XSUGIN(6)  = M_t
XSUGIN(7)      = SUG BC scale
XGMIN(1)       = LAM           XGMIN(2)   = M_MES    XGMIN(3)   = XN5
XGMIN(4)       = tan(beta)     XGMIN(5)   = sgn(mu)  XGMIN(6)   = M_t
XGMIN(7)       = CGRAV         XGMIN(8)   = RSL      XGMIN(9)   = DEL_HD
XGMIN(10)      = DEL_HU        XGMIN(11)  = DY       XGMIN(12)  = N5_1
XGMIN(13)      = N5_2          XGMIN(14)  = N5_3
XNRIN(1)       = M_N3          XNRIN(2)   = M_MAJ    XNRIN(3)   = ANSS
XNRIN(4)       = M_N3SS
XISAIN         = MSSMi inputs in natural order
XRHNIN(1-9)    = M_RHN - RH neutrino mass matrix at M_GUT
XRHNIN(10-18)  = neutrino Yukawa matrix at M_GUT
XRHNIN(19)     = A_RHN - soft trilinear coupling of RHN at M_GUT
XRHNIN(20)     = m_RHN1 - first and second generation RHN SSB masses
XRHNIN(21)     = m_RHN3 - third generation RHN SSB mass
```

G(157)

While not a common block, this array is used often throughout Isajet-M. This is the array of running parameters, i.e. those parameters which are evolved according to their RGEs. For reference its elements are listed below. Functions expecting this array as an argument typically use the variable name X(157). Note that this array uses a Yukawa convention differing from our normal convention (the convention used elsewhere in Isajet-M.) To translate between them one must transpose Yukawas and SSB trilinears, i.e. $\mathbf{Y} = \mathbf{f}^{\mathrm{T}}$ and $\mathbf{t} = \mathbf{a}^{\mathrm{T}}$.

Note that some legacy Isajet routines use a smaller set of parameters, a 32-element array G(32).

G(1)	= g_1	G(61)	= μ
G(2)	= g_2	G(62)	= $B\mu$
G(3)	= g_3	G(63)	= $m^2_{H_u}$
G(4)	= Y_u(1,1)	G(64)	= $m^2_{H_d}$
G(5)	= Y_u(1,2)	G(65)-G(73)	= $\mathbf{m}^2_Q$
G(6)	= Y_u(1,3)	G(74)-G(82)	= $\mathbf{m}^2_L$
...	...	G(83)-G(91)	= $\mathbf{m}^2_U$
G(12)	= Y_u(3,3)	G(92)-G(100)	= $\mathbf{m}^2_D$
G(13)-G(21)	= $\mathbf{Y}_d$	G(101)-G(109)	= $\mathbf{m}^2_E$
G(22)-G(30)	= $\mathbf{Y}_e$	G(110)	= v_u
G(31)	= M_1	G(111)	= v_d
G(32)	= M_2	G(112)-G(120)	= $\mathbf{Y}_\nu$
G(33)	= M_3	G(121)-G(129)	= $\mathbf{M}_N$
G(34)-G(42)	= $\mathbf{t}_u$ (trilinear)	G(130)-G(138)	= $\mathbf{t}_\nu$
G(43)-G(51)	= $\mathbf{t}_d$	G(139)-G(147)	= $\mathbf{m}^2_{\tilde{\nu}_R}$
G(52)-G(60)	= $\mathbf{t}_e$	G(148)-G(156)	= κ

G(157) = λ (SM quartic higgs coupling)

B.2 Functions

A number of the functions below come in multiple versions, usually two. Typically one version is the "full" version, taking complex parameters and acting on the full set of parameters or matrices; the other is a simplified version acting only on real parameters or on the smaller legacy Isajet parameter set.

B.2.1 Main program routines

SUGRUN

The main program. Reads the input parameters, calls SUGRA to solve the RGEs, then calls various routines to calculate and print desired masses, decay rates, branching ratios, etc..

```
query user:
    input FNAME < output filename
    input IQROT < quark rotation scheme at \mz
        if custom scheme, input VUL, VUR, VDL, VDR matrices
    input IQPHASE < quark phases flag
    input ILROT < lepron rotation scheme at \mz
        if custom scheme, input VEL, VER matrices
    input IMODEL < choice of model (6 for Isajet-M extensions)
        if SUGRA, input MO, MHF, AO, TANB, SGNMU, MT
        input INPHASE < neutrino phases flag
        input IRHN < neutrino input scheme
            if fn-fu unification, input EPSNU < proportionality constant
            if tribimaximal scheme, input CHI, PHI < angles
```

```
            if custom scheme, input XRHNIN < fn matrix
         input XRHN < M_RHN
         input INUSUG < non-universal sneutrino SSB term flag
         input XRHNIN(19-21) < A_nu, M_NRSS1, M_NRSS3
         set LND50N=true (dim-5 effective neutrino mass operator flag)
      input IRED, IRES, IAMU, IBSG, IBLL, ILLG, IMNE, IL3L < Isatools
         calculation flags

   call SUGRA
   if ITACHY, output error message
   if NOGOOD or MHPNEG, output error message and stop
   print model parameters and results
   CALL SSMSSM (calc masses & decay results)
   CALL SUGPRT (print masses)
   CALL SSTEST (test for exp. problems with model)
   print error messages if problems found
   if flags set,
       CALL ISAAMU (muon g − 2)
       CALL ISABSG (b → sγ)
       CALL ISARES (dark matter cross-sections)
       CALL ISARED (relic density)
       CALL ISALLG (ℓ → ℓγ)
       CALL ISAMNE (μ → e conversion)
       CALL ISABMM (B → 2τ, B_s → 2μ)
       CALL ISAL3L (l → 3l)
   CALL SSPRT (print modes)
   if flag set, CALL ISALHA, ISALHD (print LHA format output)
```

SUGRA(M0,MHF,A0,TANB,SGNMU,MT,IMODEL)

M0	- m_0, common scalar mass at GUT scale
MHF	- $m_{1/2}$, common gaugino mass at GUT scale
A0	- A_0, trilinear soft breaking parameter at GUT scale
TANB	- $\tan(\beta)$, ratio of Higgs vevs
SGNMU	- ± 1, sign of Higgsino mass term
MT	- $m_{\rm top}$, mass of top quark
IMODEL	- model specifier, e.g. 6 for mSUGRA+neutrinos

The main driver routine. Sets up running Z-scale parameters, does a preliminary run up to M_{GUT} with guessed SUSY spectrum, applies GUT-scale boundary conditions, runs back down. It then iteratively solves the RGEs, calling SUGRGE to run up and down in each iteration.

```
Save input params in /SUGXIN/
Initialize SM parameters in /SSSM/
Compute some gauge mediated threshold functions (THRF, THRG, XLM)
```

Guess $M_{SUSY} = \sqrt{m_0^2 + m_{1/2}^2}$ for the first run
Set the Higgs vev at \mz using the Pierce prescription[84].
Convert from \MSb to \DRb (variables xxMZ)
Calculate $\alpha_s(m_{top})$, $m_{top}(m_{top})$ (ASMT, MTMT) using 2-loop QCD corrections
Guess RHN masses for the first run
Call FEROT to calculate fermion rotation matrices
Call YUKCON to calculate initial Yukawa matrices in gauge eigenbasis

Run up towards M_{GUT}. Until g1-g2 unification is found:
    At m_{top}, activate top quark using TOPACTY

    Evolve RGEs up by $\Delta \log Q \sim (\log M_{GUT} - \log M_Z)/NSTEP$

    Check for non-perturbative Yukawas
    Fail if maximum scale is reached (default 10^19 GeV)

At unification (GUT) scale:
    Save GUT-scale values in common blocks e.g. /SUGMG/
    Set unknown μ, B=0 for first run
    Set GUT-scale boundary conditions via BCGUT
    Guess sfermion decoupling scales (=MSUSY)
    Guess sfermion MSUSY rotation matrices (=same as at MZ)
    Check for tachyonic sleptons
    Switch off any already-decoupled neutrinos with ZRHNDEC

Run back down to Z scale:
    Evolve RGEs down by $\Delta \log Q = (\log M_{GUT} - \log M_Z)/NSTEP$
    At m_{top}, decouple top quark using ZYUKD / ZAYUKD
    Check for non-perturbative Yukawas
    Call SUGFRZ to freeze out particles at their proper scales
    At SUSY scale (Q=HIGFRZ), add sparticle threshold corrections
    Decouple RHNs at their running scales using ZRHNDEC

Save MZ scale values
Create traditional Isajet outputs with GF2GO
Calculate SUSY mass spectrum using SSMSPEC
Calculate neutrino masses and mixing angles using NUXTR

Iterate entire process:
    Call SUGRGE to run up to MGUT and back down again
    Increase NSTEP by ~20%, up to 30x original level
    Calc maximum % variation DEL in major parameters
    Check for fatal errors (NOGOOD != 0)
Until major parameters converge to <DELLIM or MXITER iterations reached

```
Check for proper radiative EWSB
Transfer final values to /SUGXIN/, /BSG/ for mass/BR/rate calculations
```

SUGRGE(M0,MHF,A0,TANB,SGNMU,MT,G,G0,GF,NSTEP,IMODEL,BADMU, IQROT,ILROT)

- `M0` - m_0, common scalar mass at GUT scale
- `MHF` - $m_{1/2}$, common gaugino mass at GUT scale
- `A0` - A_0, trilinear soft breaking parameter at GUT scale
- `TANB` - $\tan(\beta)$, ratio of Higgs vevs
- `SGNMU` - ± 1, sign of Higgsino mass term
- `MT` - $m_{\rm top}$, mass of t quark
- `G(157)` - current running values of parameters
- `G0(31)` - 'diagonal-only' frozen-out parameters for use by traditional Isajet routines
- `GF(157)` - 'frozen-out' values of parameters (e.g. SSB params at M_{SUSY})
- `NSTEP` - number of steps to use running from $M_{\rm Z}$to M_{GUT}
- `IMODEL` - model specifier, e.g. 6 for mSUGRA+neutrinos
- `BADMU` - flag for $\mu^2 < 0$ (unused)
- `IQROT` - quark rotation scheme (same as in /FROTPAR/)
- `ILROT` - lepton rotation scheme (same as in /FROTPAR/)

The main iteration routine. Makes one complete run of the RGEs from $M_{\rm Z}$ to M_{GUT} and back down, setting the boundary conditions at each end.

```
Recalculate m_top at m_top in DR-bar with 2-loop QCD corrections
Compute some necessary SUSY self-energies and gauge-mediated threshold
   functions

Impose Z-scale boundary conditions
Set sparticle activation scales to values from last iteration

Run up towards M_GUT. Until g1-g2 unification is found:
   At m_top, activate top quark using TOPACTY
   At SUSY scale (Q=HIGFRZ), add sparticle threshold corrections
   Call ZHRNACT to activate RHNs at their scales

   Evolve RGEs up by Δ log Q ~ (log M_GUT − log M_Z)/NSTEP

   Check for nonperturbative Yukawas
   Fail if maximum scale is reached (default 10^19 GeV)

At unification (GUT) scale:
   Switch on any un-activated neutrinos with ZRHNACT
   Save GUT-scale values in common blocks e.g. /SUGMG/
```

```
    Set GUT-scale boundary conditions via BCGUT
    Check for tachyonic sleptons
    Switch off any already-decoupled neutrinos with ZRHNDEC

Run back down to Z scale:
    Evolve RGEs down by Δ log Q = (log M_GUT − log M_Z)/NSTEP
    At m_top, decouple top quark using ZYUKD / ZAYUKD
    Check for non-perturbative Yukawas
    Call SUGFRZ to freeze out particles at their proper scales
    At SUSY scale (Q=HIGFRZ), add sparticle threshold corrections
    Decouple RHNs at their running scales using ZRHNDEC

Save MZ scale values
Create traditional Isajet outputs with GF2GO
Calculate SUSY mass spectrum using SSMSPEC
Calculate neutrino masses and mixing angles using NUXTR
```

B.2.2 General RGE routines

`CRKSTP(N,H,X,Y,SUB,W)`

`N`	-	Number of differential equations.
`H`	-	Stepsize to advance solution (real.)
`X`	-	Position of current solution (real.)
`Y(N)`	-	Input/output: solution of the differential equations (complex array.)
`SUB`	-	A subroutine containing the differential equations.
`W(N,3)`	-	Working space array (complex.)

A complex version of Isajet's 5th-order Runge-Kutta integrator routine `DRKSTP`. Given a set of N differential equations and a solution Y at X, advances the solution Y to the point X+H using a fifth-order Runge-Kutta method. The differential equations are specified by passing in a subroutine `SUB(XX,YY,FF)`, which should set the array FF(N) to the derivatives of the Y's evaluated at the point X=XX and Y=YY. Symbolically, that is, for a set of differential equations $d\mathbf{Y}/dX = \mathbf{f}(X,\mathbf{Y})$, `SUB(XX,YY,FF)` should set $\mathbf{FF} = \mathbf{f}(\mathrm{XX},\mathbf{YY})$.

`QCDQED(T,GX,FX)`

`T`	-	The log of the scale Q at which the RGEs are to be evaluated: $T \equiv \log(Q/M_{GUT})$.
`GX(10)`	-	Real array containing the values of all running parameters at the scale $Q = M_{GUT}\exp(T)$.
`FX(10)`	-	On output, this array is filled the right-hand side of the RGEs: $dGX_i/dT = FX_i(G)$.

The RGE β functions for 2-loop QCD+QED with an extra 3rd QCD loop for g_3 and the quark masses. This is the analog of `CSURG157` and `RGE157` above, although with far fewer parameters.

CSURG157(T,G,F)

- `T` - The log of the scale Q at which the RGEs are to be evaluated: $T \equiv \log(Q/M_{GUT})$.
- `G(157)` - The array containing the values of all running parameters at the scale $Q = M_{GUT}\exp(T)$.
- `F(157)` - On output, this array is filled the right-hand side of the RGEs: $dG_i/dT = F_i(G)$.

This subroutine contains the full set of ISAJET-M's complex-valued RGEs. Given a log-scale T and the values of the running parameters $G_i(T)$, it computes the β functions and returns these in the F array ($F_i(G) \equiv \beta(G)$.) It is normally called by an integration routine such as `CRKSTP`.

Note: the convention used for Yukawa couplings is different in this subroutine than in the rest of the code. Here, the fermion masses are taken to be proportional to the Yukawas ($m \sim Y$); whereas elsewhere, the masses are taken to be proportional to transposed Yukawas ($m \sim f^{\rm T}$). Therefore when accessing the array G(157) from other functions, care must be taken to transpose Yukawa and trilinear couplings.

CSURG32(T,GY,FY)

- `T` - The log of the scale Q at which the RGEs are to be evaluated: $T \equiv \log(Q/M_{GUT})$.
- `G(157)` - The array containing the values of a limited set of running parameters at the scale $Q = M_{GUT}\exp(T)$.
- `F(157)` - On output, this array is filled the right-hand side of the 32 RGEs: $dG_i/dT = F_i(G)$.

This subroutine is identical to CSURG157, except that it contains only a subset of 32 of the complex-valued β functions.

RGE157(T,G,F)

This subroutine is identical to `CSURG157` above, with one difference: it operates on all real-valued variables and contains real-valued RGEs. It is currently used only by `ISABSG` to calculate the $b \to s\,\gamma$ branching ratio.

SMset(MEMZ,MMUMZ,MTAMZ,MUPMZ,MCMZ,MDMZ,MSMZ,MBMZ)

Initialize the Standard Model parameters and obtain running masses and couplings in $\overline{MS}$ at $M_{\rm Z}$. Outputs are returned throught the passed parameters and through the block `/SSSM/`.

SUGINIT(INUHM)

Initializes the SUSY masses and mixings for the first RGE iteration. These values are crude guesses only; they are replaced by calculated values once the mass spectrum is obtained after

the first iteration. Sparticle masses are set to M_{SUSY} and mixings to zero. The set values all reside in the common blocks /SSPAR/, /SUGMG/, /FROT/, and /SUGPAS/. INUHM is a flag indicating non-universal Higgs masses.

TOPACTY(IQROT,FTMT,GY)

IQROT	-	Quark rotation scheme.
FTMT	-	Top quark Yukawa element ($m_{\rm top}/v_u$)
GY(32)	-	Reduced array of running quantities (complex).

Activates the top quark, according to the scheme specified by IQROT (see /FROT/ above.) For the schemes with nontrivial quark mixing (IQROT$\geq$2), this is done by first rotating to the basis where $\mathbf{f}_u$ is diagonal, setting the $3,3$ element to the value FTMT, and then rotating back to the original basis. Currently this routine is only used in the first run; later routines use ZYUKD/ZAYUKD to do the rotations directly.

TACTIV(IQROT,FTMT,G)

IQROT	-	Quark rotation scheme.
FTMT	-	Top quark Yukawa element ($m_{\rm top}/v_u$)
G(157)	-	Array of running quantities (real).

Activates the top quark, according to the scheme specified by IQROT (see /FROT/ above.) This is the real-valued version of TOPACTY, and functions similarly.

BCGUT(X,IMODEL)

Called by SUGRA and SUGRGE to set the GUT-scale boundary conditions in the matrix of running parameters X(157). IMODEL is not currently used by Isajet-M. Reference: [103].

BSGGUT(YUGUT,YDGUT,YEGUT,YNGUT,G,IMODEL,M0,MHF,A0)

The real-valued version of BCGUT. Sets the GUT-scale boundary conditions in the running array G according to BSG common blocks and the passed-in Yukawa and SUGRA parameters.

SUGFRZ(Q,G,GF,IGF,IQROT,ILROT)

Q	-	Energy scale at current step.
G(157)	-	Input array of running quantities.
GF(157)	-	Output array of "frozen-out" quantities.
IGF(157)	-	Output array of "frozen-out" flags.
IQROT	-	Flag indicating the quark mixing scheme to use (see above.)
ILROT	-	Flag indicating the lepton mixing scheme to use.

Freezes out final soft SUSY-breaking and other parameters during the downward RG evolution. When the scale Q drops below the relevant scale for a parameter, that parameter is copied into the GF array and the relevant entry in the IGF array is set to 1. SSBMFRZ is called to freeze out the SSB mass-squared terms. A number of parameters are extracted at intermediate scales for special purposes, such as the b-quark Yukawa at m_A for calculating Higgs decays. These parameters are stored in /SUGPAS/.

SSBMFRZ(G,INIT,Q,GF,IGF,DEC)

Freezes out the SSB mass-squared matrix MSQ of a decoupled sfermion. The mass-squared matrix MSQ is obtained from G(INIT)-G(INIT+9) and diagonalized. When the running mass falls below the current scale, the relevant entry is added to the frozen-out mass matrix in GF(INIT)-GF(INIT+9) by rotating that matrix to the basis where the matrix MSQ is diagonal, adding in the diagonal element to be frozen, and rotating it back.

GF2G0(GF,G0,IQROT,ILROT)

Translates frozen-out RGE matrices to traditional diagonal-only ISAJET RGE parameters. Yukawas are rotated from the weak eigenstate to the mass eigenstate basis. SSB matrices are rotated to the basis where all Yukawas are diagonal, i.e. to the super-CKM basis. Note: M_Q^2 is rotated differently in up- and down- squark mass matrices.

SUGPRT(IMODEL,IPRT)

IMODEL	-	Model type: 1=SUGRA 2=GMSB 7=AMSB
IPRT	-	Printout type: 1=print logo and input parameters 2=print results and MSSMi equivalent inputs

Prints the inputs to and results from the main program SUGRA.

B.2.3 Neutrino sector routines

NRDECOP(G,Q,QOLD,GF,IGF,FTRHLD,MRNDEC)

G(157)	-	Array of running quantities (real).
Q	-	Energy scale at current step.
QOLD	-	Energy scale at last step.
GF(157)	-	Array of "frozen-out" quantities.
IGF(157)	-	Flags indicating quantities have been frozen-out.
FTRHLD(3)	-	Majorana mass decoupling threshold factors.
MRNDEC(3)	-	=FTRHLD*mass. Scale at which RHNs decouple.

Checks whether to decouple each right-handed neutrino, and does so if necessary. The current (running) masses of the RHNs are used, along with the specified threshold factors (default 1.0), to determine whether a decoupling threshold has been crossed in the current step. If so, the RHN is decoupled by 1) rotating into the basis where the RHN mass matrix is diagonal, 2) removing the relevant entry from its mass matrix, and the corresponding row from the Yukawa and and trilinear coupling matrices, and 3) adding appropriate entries to the effective mass operator κ using the matching conditions. The basis change is stored in `/NRDCPL/NRrot`, and the decoupled entries are saved in GF, with IGF updated to indicate their status.

NRACTIV(G,GF,L)

`G(157)`	-	Array of running quantities (real).
`GF(157)`	-	Array of "frozen-out" quantities.
`L`	-	RHN to activate.

Activate the L-th right-handed neutrino. This is the opposite of routine `NRDECOP`. Nearly the same set of operations is followed in reverse: the relevant frozen-out entries are recovered from GF, the contributions to κ from the neutrino are removed, and the relevant entries in the mass matrix, Yukawa and trilinear couplings are restored. The saved basis information is then used to rotate back into the pre-decoupling basis.

ZRHNDEC(G,Q,QOLD,GF,IGF,FTRHLD,MRNDEC)

`G(157)`	-	Array of running quantities (complex).
`Q`	-	Energy scale at current step.
`QOLD`	-	Energy scale at last step.
`GF(157)`	-	Array of "frozen-out" quantities.
`IGF(157)`	-	Flags indicating quantities have been frozen-out.
`FTRHLD(3)`	-	Majorana mass decoupling threshold factors.
`MRNDEC(3)`	-	=FTRHLD*mass. Scale at which RHNs decouple.

Checks whether to decouple each right-handed neutrino, and does so if necessary. The current (running) masses of the RHNs are used, along with the specified threshold factors (default 1.0), to determine whether a decoupling threshold has been crossed in the current step. If so, the RHN is decoupled by 1) rotating into the basis where the RHN mass matrix is diagonal, 2) removing the relevant entry from its mass matrix, and the corresponding row from the Yukawa and and trilinear coupling matrices, and 3) adding appropriate entries to the effective mass operator κ using the matching conditions. The basis change is stored in `/NRDCPL/NRrot`, and the decoupled entries are saved in GF, with IGF updated to indicate their status.

ZRHNACT(G,Q,QOLD,GF,MRNDEC)

`G(157)`	-	Array of running quantities (complex).
`Q`	-	Energy scale at current step.
`QOLD`	-	Energy scale at last step.
`GF(157)`	-	Array of "frozen-out" quantities.

MRNDEC(3) - =FTRHLD*mass. Scale at which RHNs decouple.

Activate each right-handed neutrino if necessary. This is the opposite of routine ZRHNDEC. Nearly the same set of operations is followed in reverse: the relevant frozen-out entries are recovered from GF, the contributions to κ from the neutrino are removed, and the relevant entries in the mass matrix, Yukawa and trilinear couplings are restored. The saved basis information is then used to rotate back into the pre-decoupling basis.

NUXTR(VUP,G,WNU,MNS,TH12,TH13,TH23,DELTA,DELTAE,DELTAU, DELTAT,PHI1,PHI2)

VUP - Up-type Higgs vev.
G(157) - Array of running quantities.
MNS - Output: MNS matrix.
TH12,23,13 - Output: mixing angles.
DELTA - Output: Dirac phase.
DELTAE,U,T - Output: unphysical Dirac (lepton) phases.
PHI1,2 - Output: Majorana phases.

Calculates the light neutrino masses, mixing angles, and phases from the parameters given in the running array G(157). This routine works both above and below the RHN decoupling scales; it uses the appropriate combination of seesaw formula and effective mass operator κ.

NUXTR proceeds by first rotating to the basis in which the charged leptons are diagonal. Then the seesaw formula contributions are combined with those from κ to obtain the effective mass matrix MN_ROT. The squared mass matric MSQR is computed, and its eigenvalues and eigenvectors are found with ZGEEV. The eigenvectors are sorted appropriately, and the missing (unphysical) phases added in, to obtain a final MNS matrix. The mixing parameters are then extracted.

FEROT(IQROT,ILROT,IQPHASE,ILPHASE)

IQROT - Flag indicating the quark mixing scheme to use:
0=dominant 3rd-family approximation (unmixed),
1=diagonal (unmixed),
2=CKM mixing in up quarks $\left(\mathbf{f}_u \sim \mathrm{CKM}^{\mathrm{T}}\,\mathbf{m}_u\,\mathrm{CKM}^*, \quad \mathbf{f}_d \sim \mathbf{m}_d\right)$,
3=CKM mixing in down quarks $\left(\mathbf{f}_u \sim \mathbf{m}_u, \quad \mathbf{f}_d \sim \mathrm{CKM}^*\,\mathbf{m}_d\,\mathrm{CKM}^{\mathrm{T}}\right)$,
4=CKM mixing in left up quarks $\left(\mathbf{f}_u \sim \mathrm{CKM}^{\mathrm{T}}\mathbf{m}_u, \quad \mathbf{f}_d \sim \mathbf{m}_d\right)$,
5=CKM mixing in left down quarks $(\mathbf{f}_u \sim \mathbf{m}_u, \quad \mathbf{f}_d \sim \mathrm{CKM}^*\mathbf{m}_d)$,
6=custom scheme.
ILROT - Flag indicating the lepton mixing scheme to use:
0=dominant 3rd-family approximation (unmixed)
1=unmixed
6=custom rotation scheme
IQPHASE - Flag activating complex phases in the quark sector.
ILPHASE - Flag activating complex phases in the lepton sector.

/SSSM/ - Input: mixing angles.
/FROT/ - Output: calculated rotation matrices VER,VEL, VUR, VUL, VDR,VDL, all at M_Z.

Constructs the fermion rotation matrices given a set of mixing angles and a mixing scheme. The convention used is:

$$\mathbf{m} \sim \mathbf{V_R}\ \mathbf{Y}^{\mathrm{T}}\ \mathbf{V_L}^{\dagger}. \tag{B.1}$$

Isajet-M allows a choice of a variety of mixing schemes, specified by the flags IQROT and ILROT. Quark mixing can be placed entirely in either the up quark or down quark sector, it can be placed symmetrically, or it can be placed according to some other specified scheme.

YUKCON(ME,MMU,MTAU,MUP,MC,MT,MD,MS,MB,VU,VD,YU,YD,YE, IQROT,ILROT)

ME - Electron mass.
MMU - Electron mass.
MTAU - Tau mass.
MUP - Up quark mass.
MC - Charm quark mass.
MT - Top quark mass.
MD - Down quark mass.
MS - Strange quark mass.
MB - Bottom quark mass.
VU - Up-type Higgs vev.
VD - Down-type Higgs vev.
YU - Up-type Yukawa matrix in weak eigenbasis $\mathbf{f}_u$ (output.)
YD - Down-type Yukawa matrix in weak eigenbasis $\mathbf{f}_d$ (output.)
YE - Lepton Yukawa matrix in weak eigenbasis $\mathbf{f}_e$ (output.)
IQROT - Flag indicating the quark mixing scheme (see above.)
ILROT - Flag indicating the lepton mixing scheme (see above.)

Constructs the Yukawa coupling matrices YU, YD, YE ($\mathbf{f}_u$,$\mathbf{f}_d$,$\mathbf{f}_e$) in the weak eigenbasis given the fermion masses and mixings. The mixings are given as input in the common block /FROT/. The convention here is our usual $\mathbf{m} \sim \mathbf{f}^{\mathrm{T}}$.

ZYUKM2W(Y,VL,xY,VR)

Rotates the Yukawa matrix from the mass to weak eigenbasis. Given the mass-basis Yukawa xY, computes $Y \sim \mathrm{VL}^{\mathrm{T}}\,\mathrm{xY}\,\mathrm{VR}^{*}$.

YUKDIAG(G,INIT,YDIAG,VL,VR)

G(157) - Array containing values of running parameters.
INIT - Index i of G(i) where desired Yukawa matrix $\mathbf{f}$ begins.
YDIAG(3,3) - Output: Diagonal Yukawa matrix.

VL(3,3) - Output: left rotation matrix.
VR(3,3) - Output: right rotation matrix.

Assembles a Yukawa matrix in the weak eigenbasis from the RGE running vector G(i) and diagonalizes it, returning the diagonalized matrix YDIAG and the left and right rotation matrices VL, VR. The convention used is $Y_{\rm DIAG} = V_{\rm L}^* \, Y \, V_{\rm R}^{\rm T}$. Note that the Yukawas here are our usual $\mathbf{f}$'s despite the different notation, so $\mathbf{m} \sim \mathbf{Y}^{\rm T}$. This convention differs from that used in SURG157 and its variants.

AYUKDIAG(G,INIT,YDIAG,VL,VR)

G(157) - Output: Array containing values of running parameters.
INIT - Index i of G(i) where desired Yukawa matrix is to be placed.
YDIAG(3,3) - Diagonal Yukawa matrix.
VL(3,3) - Left rotation matrix.
VR(3,3) - Right rotation matrix.

The inverse of YUKDIAG. Takes a diagonal Yukawa matrix and rotation matrices, rotates the Yukawa matrix to the weak eigenbasis, and stores it in the desired elements of G(i). The convention used is $Y_{\rm DIAG} = V_{\rm L}^* \, Y \, V_{\rm R}^{\rm T}$. Note that the Yukawas here are our usual $\mathbf{f}$'s despite the different notation, so $\mathbf{m} \sim \mathbf{Y}^{\rm T}$. This convention differs from that used in SURG157 and its variants.

ZYUKD(G,INIT,YDIAG,VL,VR)

G(157) - Array containing values of running parameters.
INIT - Index i of G(i) where desired Yukawa matrix begins.
YDIAG(3,3) - Output: Diagonal Yukawa matrix.
VL(3,3) - Output: left rotation matrix.
VR(3,3) - Output: right rotation matrix.

Complex version of YUKDIAG. Assembles a Yukawa matrix in the weak eigenbasis from the RGE running vector G(i) and diagonalizes it, returning the diagonalized matrix YDIAG and the left and right rotation matrices VL, VR. The convention used is $Y_{\rm DIAG} = V_{\rm L}^* \, Y \, V_{\rm R}^{\rm T}$.

Note that the convention used for Yukawas here is the normal Isajet one ($\mathbf{m} \sim \mathbf{Y}^{\rm T}$), which differs from that used in SURG157 and its variants.

ZAYUKD(G,INIT,YDIAG,VL,VR)

G(157) - Output: Array containing values of running parameters.
INIT - Index i of G(i) where desired Yukawa matrix is to be placed.
YDIAG(3,3) - Diagonal Yukawa matrix.
VL(3,3) - Left rotation matrix.
VR(3,3) - Right rotation matrix.

The inverse of ZYUKDIAG, and the complex version of ZYUKD. Takes a diagonal Yukawa matrix and rotation matrices, rotates the Yukawa matrix to the weak eigenbasis, and stores it

in the desired elements of G(i). The convention used is $Y_{\rm DIAG} = V_{\rm L}^* \; Y \; V_{\rm R}^{\rm T}$. Note that the convention used for Yukawas here is the normal Isajet one ($\mathbf{m} \sim \mathbf{Y}^{\rm T}$), which differs from that used in SURG157 and its variants.

B.2.4 Mass and LFV calculation routines

SSMSPEC(G0,IMODEL,BADMU)

Computes SUSY masses and mixing angles for the model IMODEL given the (reduced) array of real running parameters G0(32). This is an iterative calculation using the tadpole method[96]. A two-stage process is employed. At each iteration of the main process, we first iteratively call SUGEFF which solves for μ,B, and their tadpole corrections, in order to obtain μ within the desired accuracy DMUSLIM (0.1% default). (This is necessary as the corrections are very sensitive to the values of μ and B themselves.) Then these values are used by SUGMAS and SSMASS to calculate the sparticle masses and mixings. This process is repeated until the sparticle masses and mixings converge to the desired accuracy DMSSLIM (0.1% default.)

SUGEFF(G0,SIG1,SIG2)

Computes the Higgs mass shift due to the 1-loop effective potential.

SUGMAS(G0,ILOOP,IMODEL,SIGA)

Computes sparticle masses and mixings. First computes tree level sparticle mass matrices and outputs them to /MSS/ and /XISAIN/; then calls SSMASS to calculate sparticle mixings.

SSMASS(XMG,XM1,XM2,IALLOW,ILOOP,MHLNEG,MHCNEG,IMODEL)

Diagonalizes neutralino, chargino, and Higgs mass matrices; computes their mixings. Results are stored in /SSPAR/. Then SSMHN, SSMHC, and SSM1LP are called to calculate radiative corrections to Higgs and sparticle masses.

SSMHN(MHLNEG)

Calculates radiative corrections to neutral Higgs mass and scalar Higgs mixing angle; outputs them to /SSPAR/. MHLNEG indicates an unexpected negative mass-squared value.

SSMHC(MHCNEG)

Calculates radiative corrections to charged Higgs mass and scalar Higgs mixing angle; outputs them to /SSPAR/. MHCNEG indicates a negative mass-squared value.

SSM1LP(M1,M2,IALLOW)

Calculates radiative corrections to sparticle masses.

ISA2LFV(IPRT)

IPRT - Flag indicating verbosity of output.
0=no output, 4=max output.

Interface from Isajet-M (ISASUGRA) to the LFV subroutines below. Transfers the parameters from Isajet-M output blocks into the Isajet LFV routines' common blocks, making the necessary changes to account for different conventions. Results are taken from blocks /SSSM/, /SUGMG/, /MSSDEC/, /SUGXIN/, /SUPSSB/, and /SSPAR/ and entered into the blocks /LFV/, /LFVFLAG/, /LFVSM/, /LFVSUGP/, and /LFVSS/. See the Isajet documentation for the structure of these common blocks.

SUG2BSG()

Interface from Isajet-M (ISASUGRA) to ISABSG. Transfers (filled) SUGRA common blocks to BSG common blocks. Values are taken from the Isajet-M blocks /SSSM/, /SUGMG/, /SUGXIN/, /SUGPAS/, /SUGNU/, /SSNU/, /SSPAR/, and /FROT/; they are entered into the BSG blocks /BSG/, /BSGSM/, /GGN/, /GLNN/, /BSGDEC/, and /BSGSUG/. See the Isajet and ISABSG[77] documentation for the structure of these blocks.

ISAL3L(IPRT,BRM3E,BRT3M,BRT3E)

IPRT - Flag indicating verbosity of output.
0=no output, 4=max output.
BRM3E - $\mu \to 3e$ branching ratio (output).
BRT3M - $\tau \to 3\mu$ branching ratio (output).
BRT3E - $\tau \to 3e$ branching ratio (output).

Calculates branching ratios for LFV $l_i \to 3l_j$ decays, following Ref. [37].

ISALLG(IPRT,BRMEG,BRTMG,BRTEG)

IPRT - Flag indicating verbosity of output.
0=no output, 4=max output.
BRMEG - $\mu \to e\gamma$ branching ratio (output).
BRTMG - $\tau \to \mu\gamma$ branching ratio (output).
BRTEG - $\tau \to e\gamma$ branching ratio (output).

Calculates branching ratios for LFV $l_i \to l_j\gamma$ decays, following Ref. [37].

ISAMNE(INUCL,IPRT,CR)

INUCL - Flag indicating nucleus type:
1=Titanium
2=Gold
3=Aluminum

4=Lead

`IPRT` - Flag indicating verbosity of output.
0=no output, 4=max output

`CR` - ratio of $\mu \to e$ conversion rate to muon capture rate (output).

Calculates the rate for $\mu \to e$ conversion in nucleus INUCL, following Refs. [37, 44, 45, 46].

B.2.5 Mathematical and utility routines

`SVDCMP(A,M,N,U,W,V)`

`A(M,N)` - $M \times N$ input matrix. It is preserved by the computation.
`U(M,M)` - left orthogonal matrix.
`W(N)` - vector of singular elements.
`V(N,N)` - right orthogonal matrix.
`M,N` - number of rows, cols in A.

Calculates the singular value decomposition of real input matrix A, $A = UWV^{\mathsf{T}}$.

`ZSVD(A,MMAX,NMAX,M,N,P,NU,NV,S,U,V)`

`A(M,N)` - Complex $M \times N$ input matrix. It is destroyed during the computation.
`U(M,M)` - Complex left unitary matrix.
`S(N)` - vector of REAL diagonal values.
`V(N,N)` - Complex right unitary matrix.
`MMAX,NMAX` - leading dimension of A, U, V.
`M,N` - number of rows, cols in A.
`NU,NV` - number of columns of U, V to compute.

Calculates the singular value decomposition of complex input matrix A, $A = USV^*$. Reference: [104].

`ZMDIAG(A,W,U,V)`

Diagonalizes the 3x3 complex symmetric matrix A preserving the generation structure. The convention used is $U^\dagger A\, V = W$ (diagonal). The original matrix A is destroyed.

`MDIAG(A,W,Z)`

Diagonalizes the symmetrix 3x3 matrix A preserving the generation structure. The convention used is $Z^{\mathrm{T}} A\, Z = W$ (diagonal).

`EIGSYS(NM,N,AR,WR,ZR,IERR,WORK)`

Computes the eigenvalues and eigenvectors of the real symmetric NxN matrix AR, storing the eigenvalues in the vector WR, and the eigenvectors as columns in ZR. WORK is an N-element vector. The convention used is ZR^{T} AR ZR = diagonal. This is a double-precision adaptation of EISRS1 from CERNLIB. It uses subsidiary functions `TRDIAG` and `TQLEIG`.

`TQLEIG(NM,N,D,E,Z,IERR)`

Computes the eigenvalues and eigenvectors of a symmetric tridiagonal NxN matrix using the QL-algorithm. This is a double-precision adaptation of TQL2 from CERNLIB.

`TRDIAG(NM,N,A,D,E,Z)`

Reduces the real symmetric N$\times$N matrix A to symmetric tridiagonal form. This is a double-precision adaptation of TRED2 from CERNLIB.

`ZSORTEIG(N,W,Z)`

Given an array of N real eigenvalues W, and an N$\times$N complex matrix Z with eigenvectors as columns, reorders the eigenvalues into ascending order, ordering the eigenvectors accordingly.

`COLSWAP(MAT,M,N)`

Swaps the M,N columns of the 3×3 complex matrix MAT.

`MAT2VEC(G,INIT,MAT,IORD)`

Stores the 3×3 matrix MAT in the linear array G (from G(INIT)-G(INIT+9)), in either row-wise or column-wise order according to IORD=+1,-1 respectively.

`VEC2MAT(G,INIT,MAT,IORD)`

Extracts the 3×3 matrix MAT from the array G (from G(INIT)-G(INIT+9)), in either row-wise or column-wise order according to IORD.

`ZMAT2VEC(G,INIT,MAT,IORD)`

Stores the 3×3 complex matrix MAT in the linear array G (from G(INIT)-G(INIT+9)), in either row-wise or column-wise order according to IORD.

`ZVEC2MAT(G,INIT,MAT,IORD)`

Extracts the 3×3 complex matrix MAT from the linear array G (from G(INIT)-G(INIT+9)), in either row-wise or column-wise order according to IORD.

`MPROD`*n*`(Y,A,B,...)`

Stores the product of the *n* 3×3 real matrices A,B,... in Y.

MPROD*n*X(X,I,A,B,...)

Stores the product of the *n* 3×3 real matrices A,B,... in X(I), the Ith submatrix of the $250 \times 3 \times 3$ real auxiliary matrix X.

ZMPROD*n*(Y,A,B,...)

Complex version of MPROD*n*(Y,A,B,...)

ZMPROD*n*X(X,I,A,B,...)

Complex version of MPROD*n*(X,I,A,B,...)

MREADIN(M,IMCMPLX)

Prompts for and reads in a 3×3 complex matrix M(3,3) from standard input, row-wise. If the flag IMCMPLX is set, then the imaginary parts of the matrix elements are also read in; if not, they are set to zero.

MRHNRIN(XRHNIN,IMCMPLX)

Prompts for and reads in the right-handed neutrino Majorana mass matrix. IMCMPLX is a flag indicating the matrix should be complex; XRHNIN is the array in which the matrix will be stored (elements XRHNIN(1)-XRHNIN(9).)

SYMMATIN(M,IMCMPLX)

Asks for and reads in the 3×3 complex symmetric matrix M from standard input. The upper-triangular portion only should be entered, row-wise. IMCMPLX is a flag determining whether the imaginary part should be read in as well.

YNURIN(XRHNIN,IMCMPLX)

Reads in the neutrino Yukawa from standard input and stores it in /SUGXIN/XRHNIN.

NANCHECK(NOGOOD)

Checks mass spectra and mixing angles for NaN values; if found, replaces them with zeros, returns the proper NOGOOD=17 error codetitle, and prints an error message.

Bibliography

[1] H. Baer and X. Tata, *Weak Scale Supersymmetry: From Superfields to Scattering Events*, (Cambridge University Press, 2006).

[2] M. Drees, R. Godbole and P. Roy, *Theory and phenomenology of sparticles: An account of four-dimensional N=1 supersymmetry in high energy physics*, (World Scientific,2004); S. P. Martin, arXiv:hep-ph/9709356.

[3] Rudolf Haag, Jan T. Lopuszanski, and Martin Sohnius. All Possible Generators of Supersymmetries of the s Matrix. Nucl. Phys. B **88**, 257 (1975).

[4] M. T. Grisaru, W. Siegel and M. Roček, Nucl. Phys. B **159**, 429 (1979); N. Seiberg, Phys. Lett. B **318**, 469 (1993).

[5] J. Hisano, H. Murayama and T. Yanagida, Nucl. Phys. B **402**, 46 (1993) [arXiv:hep-ph/9207279]; Y. Yamada, Z. Phys. C **60**, 83 (1993).

[6] L. Girardello and M. T. Grisaru, Nucl. Phys. B **194**, 65 (1982).

[7] H.P. Nilles, *Supersymmetry, Supergravity and Particle Physics*, *Phys. Rept.* 110, 1 (1984).

[8] S. Ferrara et al., Phys. Rev. D **15**, 1013 (1977).

[9] E. Cremmer, S. Ferrara, L. Girardello, and Antoine Van Proeyen, Nucl. Phys. B **212**, 413 (1983).

[10] E. Fermi, Ricerca Scientifica **4 (II)**, 491 (1933), in E. Fermi, *Note e Memorie Vol. I*, E. Segrè et al. eds., (Accademia Nazionale dei Lincei and University of Chicago Press, 1962).

[11] C. L. Cowan, Jr., F. Reines, F. B. Harrison, H. W. Kruse and A. D. McGuire, Science **124**, 103 (1956).

[12] C. Amsler *et al.* [Particle Data Group], Phys. Lett. B **667**, 1 (2008).

[13] For a review of neutrino oscillations, see V. Barger, D. Marfatia and K. Whisnant, *Int. J. Mod. Phys. E* **12**, 569 (2003) [arXiv:hep-ph/0308123] and references therein.

[14] T. Schwetz, M. Tortola and J. W. F. Valle, New J. Phys. **10**, 113011 (2008) [arXiv:0808.2016 [hep-ph]].

[15] H. Fritzsch and P. Minkowski, Phys. Lett. B **62**, 72 (1976); P. Minkowski, Phys. Lett. B **67**, 421 (1977); M. Gell-Mann, P. Ramond and R. Slansky, in *Supergravity: proceedings of the workshop*, Stony Brook, NY, (North-Holland, Amsterdam, 1979); T. Yanagida, KEK Report No.79-18, 1979; S. Glashow, in *Quarks and Leptons*, Cargese, France,(Plenum, New York, 1980); R. N. Mohapatra and G. Senjanovic, Phys. Rev. Lett. **44**, 912 (1980).

[16] C. S. Aulakh, A. Melfo, A. Rasin and G. Senjanovic, Phys. Lett. B **459**, 557 (1999) [arXiv:hep-ph/9902409].

[17] J. A. Casas, V. Di Clemente, A. Ibarra and M. Quiros, Phys. Rev. D **62**, 053005 (2000) [arXiv:hep-ph/9904295]; J. A. Casas, J. R. Espinosa and I. Hidalgo, JHEP **0411**, 057 (2004) [arXiv:hep-ph/0410298].

[18] V. Barger, D. Marfatia and A. Mustafayev, Phys. Lett. B **665**, 242 (2008) [arXiv:0804.3601 [hep-ph]]

[19] A. D. Box and X. Tata, Phys. Rev. D **77**, 055007 (2008) [arXiv:0712.2858 [hep-ph]] and "Threshold and Flavour Effects in the Renormalization Group Equations of the arXiv:0810.5765 [hep-ph].

[20] A. D. Box, arXiv:0811.2444 [hep-ph].

[21] L. J. Hall, V. A. Kostelecky and S. Raby, *Nucl. Phys.* **B 267** (1986) 415.

[22] Z. Maki, M. Nakagawa and S. Sakata, Prog. Theor. Phys. **28**, 870 (1962).

[23] N. Cabibo, *Phys. Rev. Lett.* **10** (1963) 531, M. Kobayashi and T. Maskawa, Prog. Theor. Phys. **49**, 652 (1973).

[24] S. L. Glashow, J. Iliopoulos and L. Maiani, Phys. Rev. D **2**, 1285 (1970).

[25] S. T. Petcov, Sov. J. Nucl. Phys. **25**, 340 (1977) (1977 ERRAT,25,698.1977 ERRAT,25,1336.1977); S. M. Bilenky, S. T. Petcov and B. Pontecorvo, Phys. Lett. B **67**, 309 (1977); T. P. Cheng and L. F. Li, Phys. Rev. Lett. **45**, 1908 (1980); B. W. Lee, S. Pakvasa, R. E. Shrock and H. Sugawara, Phys. Rev. Lett. **38**, 937 (1977) [Erratum-ibid. **38**, 1230 (1977)]; V. D. Barger and D. V. Nanopoulos, Nuovo Cim. A **44**, 303 (1978).

[26] M. L. Brooks *et al.* [MEGA Collaboration], Phys. Rev. Lett. **83**, 1521 (1999) [arXiv:hep-ex/9905013].

[27] K. Hayasaka *et al.* [Belle Collaboration], Phys. Lett. B **666**, 16 (2008) [arXiv:0705.0650 [hep-ex]].

[28] B. Aubert *et al.* [BABAR Collaboration], Phys. Rev. Lett. **96**, 041801 (2006).

[29] U. Bellgardt *et al.* [SINDRUM Collaboration], *Nucl. Phys.* **B 299** (1) 1988.

[30] Y. Miyazaki *et al.* [Belle Collaboration], Phys. Lett. B **660**, 154 (2008) [arXiv:0711.2189 [hep-ex]].

[31] C. Dohmen *et al.* [SINDRUM II Collaboration.], Phys. Lett. B **317**, 631 (1993).

[32] E.C. Dukes *et al.* [Mu2e Collaboration], "Proposal to Search for $\mu^- N \to e^- N$ with a Single Event Sensitivity Below 10^{-16} ", http://mu2e.fnal.gov/public/hep/index.shtml

[33] S. Ritt [MEG Collaboration], Nucl. Phys. Proc. Suppl. **162**, 279 (2006); T. Mori, Nucl. Phys. Proc. Suppl. **169**, 166 (2007).

[34] M. Bona *et al.*, arXiv:0709.0451 [hep-ex]; A. G. Akeroyd *et al.* [SuperKEKB Physics Working Group], arXiv:hep-ex/0406071.

[35] With no planned experiment we use theoretical estimates based on the PSI beam intensity from W. J. Marciano, T. Mori and J. M. Roney, Ann. Rev. Nucl. Part. Sci. **58**, 315 (2008).

[36] Y. Mori *et al.* [The PRIME Working Group], "An Experimental Search for the $\mu^- - e^-$ Conversion Process at an Ultimate Sensitivity of the Order of 10^{-18} with PRISM", LOI-25, http://www-ps.kek.jp/jhf-np/LOIlist/LOIlist.html

[37] J. Hisano, T. Moroi, K. Tobe, M. Yamaguchi and T. Yanagida, Phys. Lett. B **357**, 579 (1995) [arXiv:hep-ph/9501407]; J. Hisano, T. Moroi, K. Tobe and M. Yamaguchi, Phys. Rev. D **53**, 2442 (1996) [arXiv:hep-ph/9510309].

[38] J. Hisano and D. Nomura, Phys. Rev. D **59**, 116005 (1999) [arXiv:hep-ph/9810479].

[39] J. A. Casas and A. Ibarra, *Nucl. Phys.* **B 618** (2001) 171 [arXiv:hep-ph/0103065].

[40] S. T. Petcov, S. Profumo, Y. Takanishi and C. E. Yaguna, Nucl. Phys. B **676**, 453 (2004) [arXiv:hep-ph/0306195].

[41] K. S. Babu and C. Kolda, Phys. Rev. Lett. **89**, 241802 (2002) [arXiv:hep-ph/0206310]; A. Dedes, J. R. Ellis and M. Raidal, Phys. Lett. B **549**, 159 (2002) [arXiv:hep-ph/0209207]; R. Kitano, M. Koike, S. Komine and Y. Okada, Phys. Lett. B **575**, 300 (2003) [arXiv:hep-ph/0308021].

[42] See for example, A. Belyaev, S. Dar, I. Gogoladze, A. Mustafayev and Q. Shafi, arXiv:0712.1049 [hep-ph].

[43] E. Arganda and M. J. Herrero, Phys. Rev. D **73**, 055003 (2006) [arXiv:hep-ph/0510405]; E. Arganda, M. J. Herrero and A. M. Teixeira, JHEP **0710**, 104 (2007) [arXiv:0707.2955 [hep-ph]].

[44] H. C. Chiang, E. Oset, T. S. Kosmas, A. Faessler and J. D. Vergados, Nucl. Phys. A **559** (1993) 526.

[45] A. Czarnecki, W. J. Marciano and K. Melnikov, AIP Conf. Proc. **435**, 409 (1998) [arXiv:hep-ph/9801218]; R. Kitano, M. Koike and Y. Okada, Phys. Rev. D **66**, 096002 (2002) [Erratum-ibid. D **76**, 059902 (2007)] [arXiv:hep-ph/0203110].

[46] T. Suzuki, D. F. Measday and J. P. Roalsvig, Phys. Rev. C **35**, 2212 (1987).

[47] F. Deppisch, H. Pas, A. Redelbach, R. Ruckl and Y. Shimizu, Eur. Phys. J. C **28**, 365 (2003) [arXiv:hep-ph/0206122]; F. Deppisch, H. Pas, A. Redelbach and R. Ruckl, Phys. Rev. D **73**, 033004 (2006) [arXiv:hep-ph/0511062]; S. Antusch, E. Arganda, M. J. Herrero and A. M. Teixeira, Nucl. Phys. Proc. Suppl. **169**, 155 (2007) [arXiv:hep-ph/0610439]; A. Masiero, S. Profumo, S. K. Vempati and C. E. Yaguna, JHEP **0403**, 046 (2004) [arXiv:hep-ph/0401138]; A. Masiero, S. K. Vempati and O. Vives, New J. Phys. **6**, 202 (2004) [arXiv:hep-ph/0407325]; J. R. Ellis, J. Hisano, M. Raidal and Y. Shimizu, Phys. Rev. D **66**, 115013 (2002) [arXiv:hep-ph/0206110]; D. F. Carvalho, J. R. Ellis, M. E. Gomez and S. Lola, Phys. Lett. B **515**, 323 (2001) [arXiv:hep-ph/0103256]; S. T. Petcov, W. Rodejohann, T. Shindou and Y. Takanishi, Nucl. Phys. B **739**, 208 (2006) [arXiv:hep-ph/0510404]; S. T. Petcov, T. Shindou and Y. Takanishi, Nucl. Phys. B **738**, 219 (2006) [arXiv:hep-ph/0508243]; S. Antusch and S. F. King, Phys. Lett. B **659**, 640 (2008) [arXiv:0709.0666 [hep-ph]]; T. Blazek and S. F. King, Nucl. Phys. B **662**, 359 (2003) [arXiv:hep-ph/0211368]; A. Ibarra, T. Shindou and C. Simonetto, JHEP **0810**, 021 (2008) [arXiv:0809.0608 [hep-ph]]; M. C. Chen and K. T. Mahanthappa, Int. J. Mod. Phys. A **18**, 5819 (2003) [arXiv:hep-ph/0305088].

[48] S. Antusch, E. Arganda, M. J. Herrero and A. M. Teixeira, JHEP **0611**, 090 (2006) [arXiv:hep-ph/0607263].

[49] L. Calibbi, A. Faccia, A. Masiero and S. K. Vempati, Phys. Rev. D **74**, 116002 (2006) [arXiv:hep-ph/0605139].

[50] A. Masiero, S. K. Vempati and O. Vives, Nucl. Phys. B **649**, 189 (2003) [arXiv:hep-ph/0209303].

[51] A. Ibarra and C. Simonetto, JHEP **0804**, 102 (2008) [arXiv:0802.3858 [hep-ph]].

[52] For reviews, see *e.g.* C. Jungman, M. Kamionkowski and K. Griest,*Phys. Rept.* **267** (1996) 195; A. Lahanas, N. Mavromatos and D. Nanopoulos, *Int. J. Mod. Phys.* **D 12** (2003) 1529; M. Drees, arXiv:hep-ph/0410113; K. Olive, astro-ph/0503065 and "Dark matter and dark matter candidates," Adv. Space Res. **42**, 581 (2008).

[53] E. Komatsu *et al.*, arXiv:0803.0547 [astro-ph]; see also http://lambda.gsfc.nasa.gov/product/map/current/parameters.cfm

[54] A. Chamseddine, R. Arnowitt and P. Nath, *Phys. Rev. Lett.* **49** (1982) 970; R. Barbieri, S. Ferrara and C. Savoy, *Phys. Lett.* **B 119** (1982) 343; N. Ohta, *Prog. Theor. Phys.* **70** (1983) 542; L. J. Hall, J. Lykken and S. Weinberg, *Phys. Rev.* **D 27** (1983) 2359; for reviews, see H. P. Nilles, *Phys. Rept.* **110** (1984) 1, and P. Nath, arXiv:hep-ph/0307123.

[55] J. R. Ellis, J. S. Hagelin, D. V. Nanopoulos, K. A. Olive and M. Srednicki, *Nucl. Phys.* **B 238** (1984) 453; V. Barger and C. Kao, *Phys. Rev.* **D 57** (1998) 3131.

[56] H. Baer and M. Brhlik, "Cosmological relic density from minimal supergravity with implications for *Phys. Rev.* **D 53** (1996) 597.

[57] J. Ellis, T. Falk and K. Olive, *Phys. Lett.* **B 444** (1998) 367; J. Ellis, T. Falk, K. Olive and M. Srednicki, *Astropart. Phys.* **13** (2000) 181; M.E. Gómez, G. Lazarides and C. Pallis, *Phys. Rev.* **D 61** (2000) 123512 and *Phys. Lett.* **B 487** (2000) 313; A. Lahanas, D. V. Nanopoulos and V. Spanos, *Phys. Rev.* **D 62** (2000) 023515; R. Arnowitt, B. Dutta and Y. Santoso, *Nucl. Phys.* **B 606** (2001) 59.

[58] C. Böhm, A. Djouadi and M. Drees, *Phys. Rev.* **D 30** (2000) 035012; J. R. Ellis, K. A. Olive and Y. Santoso, *Astropart. Phys.* **18** (2003) 395; J. Edsjö, *et al.*, *JCAP* **0304** (2003) 001.

[59] K. L. Chan, U. Chattopadhyay and P. Nath, *Phys. Rev.* **D 58** (1998) 096004; J. Feng, K. Matchev and T. Moroi, *Phys. Rev. Lett.* **84** (2000) 2322 and *Phys. Rev.* **D 61** (2000) 075005; H. Baer, C. H. Chen, F. Paige and X. Tata, *Phys. Rev.* **D 52** (1995) 2746 and *Phys. Rev.* **D 53** (1996) 6241; H. Baer, C. H. Chen, M. Drees, F. Paige and X. Tata, *Phys. Rev.* **D 59** (1999) 055014.

[60] M. Drees and M. Nojiri, *Phys. Rev.* **D 47** (1993) 376; H. Baer and M. Brhlik, *Phys. Rev.* **D 57** (1998) 567; H. Baer, M. Brhlik, M. Diaz, J. Ferrandis, P. Mercadante, P. Quintana and X. Tata, *Phys. Rev.* **D 63** (2001) 015007; J. Ellis, T. Falk, G. Ganis, K. Olive and M. Srednicki, *Phys. Lett.* **B 510** (2001) 236; L. Roszkowski, R. Ruiz de Austri and T. Nihei, *J. High Energy Phys.* **0108** (024) 2001; A. Djouadi, M. Drees and J. L. Kneur, *J. High Energy Phys.* **0108** (2001) 055; A. Lahanas and V. Spanos, *Eur. Phys. J.* **C 23** (2002) 185.

[61] R. Arnowitt and P. Nath, *Phys. Rev. Lett.* **70** (1993) 3696; A. Djouadi, M. Drees and J. Kneur, *Phys. Lett.* **B 624** (2005) 60.

[62] H. Baer, C. Balazs, J. K. Mizukoshi and X. Tata, Phys. Rev. D **63**, 055011 (2001) [arXiv:hep-ph/0010068].

[63] M. Ciuchini, A. Masiero, P. Paradisi, L. Silvestrini, S. K. Vempati and O. Vives, Nucl. Phys. B **783**, 112 (2007) [arXiv:hep-ph/0702144].

[64] R. N. Mohapatra and A. Y. Smirnov, Ann. Rev. Nucl. Part. Sci. **56**, 569 (2006) [arXiv:hep-ph/0603118], C. H. Albright and M. C. Chen, Phys. Rev. D **74**, 113006 (2006) [arXiv:hep-ph/0608137].

[65] R. N. Mohapatra and B. Sakita, Phys. Rev. D **21**, 1062 (1980).

[66] P. F. Harrison, D. H. Perkins and W. G. Scott, Phys. Lett. B **530**, 167 (2002) [arXiv:hep-ph/0202074]; Z. z. Xing, Phys. Lett. B **533**, 85 (2002) [arXiv:hep-ph/0204049]; X. G. He and A. Zee, Phys. Lett. B **560**, 87 (2003) [arXiv:hep-ph/0301092]

[67] P. F. Harrison and W. G. Scott, Phys. Lett. B **535**, 163 (2002) [arXiv:hep-ph/0203209].

[68] C. H. Albright, Phys. Lett. B **599**, 285 (2004) [arXiv:hep-ph/0407155].

[69] C. H. Albright, arXiv:0905.0146 [hep-ph].

[70] ISAJET, by H. Baer, F. Paige, S. Protopopescu and X. Tata, arXiv:hep-ph/0312045.

[71] IsaRED, by H. Baer, C. Balazs and A. Belyaev, *J. High Energy Phys.* **0203** (2002) 042.

[72] G. W. Bennett *et al.* [Muon (g-2) Collaboration], arXiv:0811.1207 [hep-ex].

[73] A. Czarnecki and W. J. Marciano, Phys. Rev. D **64**, 013014 (2001); [arXiv:hep-ph/0102122]. S. Komine, T. Moroi and M. Yamaguchi, Phys. Lett. B **506**, 93 (2001) [arXiv:hep-ph/0102204].

[74] H. Baer, C. Balazs, J. Ferrandis and X. Tata, Phys. Rev. D **64**, 035004 (2001) [arXiv:hep-ph/0103280].

[75] [Tevatron Electroweak Working Group and CDF Collaboration and D0 Collab], arXiv:0903.2503 [hep-ex].

[76] H. Baer, C. Balazs, A. Belyaev and J. O'Farrill, JCAP **0309**, 007 (2003) [arXiv:hep-ph/0305191].

[77] H. Baer and M. Brhlik, Phys. Rev. D **55**, 3201 (1997) [arXiv:hep-ph/9610224]; H. Baer, M. Brhlik, D. Castano and X. Tata, Phys. Rev. D **58**, 015007 (1998) [arXiv:hep-ph/9712305].

[78] J. K. Mizukoshi, X. Tata and Y. Wang, Phys. Rev. D **66**, 115003 (2002) [arXiv:hep-ph/0208078].

[79] D. J. Castano, E. J. Piard and P. Ramond, Phys. Rev. D **49**, 4882 (1994) [arXiv:hep-ph/9308335].

[80] S. P. Martin and M. T. Vaughn, Phys. Rev. D **50**, 2282 (1994) [arXiv:hep-ph/9311340].

[81] V. D. Barger, M. S. Berger and P. Ohmann, Phys. Rev. D **47**, 1093 (1993) [arXiv:hep-ph/9209232].

[82] S. Weinberg, Phys. Lett. B **91**, 51 (1980); L. J. Hall, Nucl. Phys. B **178**, 75 (1981); B. A. Ovrut and H. J. Schnitzer, Phys. Lett. B **100**, 403 (1981); B. A. Ovrut and H. J. Schnitzer, Nucl. Phys. B **179**, 381 (1981).

[83] W. Wetzel, Nucl. Phys. B **196**, 259 (1982).

[84] D. M. Pierce, J. A. Bagger, K. T. Matchev and R. j. Zhang, Nucl. Phys. B **491**, 3 (1997) [arXiv:hep-ph/9606211].

[85] A. Bednyakov, A. Onishchenko, V. Velizhanin and O. Veretin, Eur. Phys. J. C **29**, 87 (2003) [arXiv:hep-ph/0210258].

[86] G. Ross and M. Serna, Phys. Lett. B **664**, 97 (2008) [arXiv:0704.1248 [hep-ph]].

[87] H. Baer, J. Ferrandis, S. Kraml and W. Porod, Phys. Rev. D **73**, 015010 (2006) [arXiv:hep-ph/0511123].

[88] S. Antusch, J. Kersten, M. Lindner and M. Ratz, Phys. Lett. B **538**, 87 (2002) [arXiv:hep-ph/0203233].

[89] S. Antusch, J. Kersten, M. Lindner, M. Ratz and M. A. Schmidt, JHEP **0503**, 024 (2005) [arXiv:hep-ph/0501272].

[90] J. A. Casas, J. R. Espinosa, A. Ibarra and I. Navarro, Phys. Rev. D **63**, 097302 (2001) [arXiv:hep-ph/0004166].

[91] H. Arason, D. J. Castano, B. Keszthelyi, S. Mikaelian, E. J. Piard, P. Ramond and B. D. Wright, Phys. Rev. D **46**, 3945 (1992).

[92] O. V. Tarasov, A. A. Vladimirov and A. Y. Zharkov, Phys. Lett. B **93**, 429 (1980); S. G. Gorishnii, A. L. Kataev and S. A. Larin, Sov. J. Nucl. Phys. **40**, 329 (1984) [Yad. Fiz. **40**, 517 (1984)].

[93] K. G. Chetyrkin, B. A. Kniehl and M. Steinhauser, Phys. Rev. Lett. **79**, 2184 (1997) [arXiv:hep-ph/9706430]; K. G. Chetyrkin, B. A. Kniehl and M. Steinhauser, Nucl. Phys. B **510**, 61 (1998) [arXiv:hep-ph/9708255].

[94] L. V. Avdeev and M. Y. Kalmykov, Nucl. Phys. B **502**, 419 (1997) [arXiv:hep-ph/9701308].

[95] S. P. Martin and M. T. Vaughn, Phys. Lett. B **318**, 331 (1993) [arXiv:hep-ph/9308222]

[96] P. H. Chankowski, S. Pokorski and J. Rosiek, Nucl. Phys. B **423**, 437 (1994) [arXiv:hep-ph/9303309]; V. D. Barger, M. S. Berger and P. Ohmann, Phys. Rev. D **49**, 4908 (1994) [arXiv:hep-ph/9311269].

[97] M. Apollonio *et al.* [CHOOZ Collaboration], Eur. Phys. J. C **27**, 331 (2003) [arXiv:hep-ex/0301017].

[98] X. Guo *et al.* [Daya-Bay Collaboration], arXiv:hep-ex/0701029.

[99] F. Ardellier *et al.* [Double Chooz Collaboration], arXiv:hep-ex/0606025.

[100] **LEP2 SUSY Working Group**, *Combined LEP chargino results, up to 208 GeV for large m0*, http://lepsusy.web.cern.ch/lepsusy/www/inos_moriond01/charginos_pub.html .

[101] G. F. Giudice, A. Notari, M. Raidal, A. Riotto and A. Strumia, Nucl. Phys. B **685**, 89 (2004) [arXiv:hep-ph/0310123]; A. Abada, S. Davidson, A. Ibarra, F. X. Josse-Michaux, M. Losada and A. Riotto, JHEP **0609**, 010 (2006) [arXiv:hep-ph/0605281].

[102] P. Di Bari and A. Riotto, Phys. Lett. B **671**, 462 (2009) [arXiv:0809.2285 [hep-ph]].

[103] P. F. Harrison and W. G. Scott, Phys. Lett. B **557**, 76 (2003) [arXiv:hep-ph/0302025].

[104] P. Businger and G. Golub. Communications of the ACM **12**, 564 (1969).